



1986

## Characterization and Modulation of Central Apnea Occurring During Cluster Breathing in the Cat

Linda Mae Oyer  
*Loyola University Chicago*

Follow this and additional works at: [https://ecommons.luc.edu/luc\\_diss](https://ecommons.luc.edu/luc_diss)



Part of the [Medicine and Health Sciences Commons](#)

---

### Recommended Citation

Oyer, Linda Mae, "Characterization and Modulation of Central Apnea Occurring During Cluster Breathing in the Cat" (1986). *Dissertations*. 2403.

[https://ecommons.luc.edu/luc\\_diss/2403](https://ecommons.luc.edu/luc_diss/2403)

This Dissertation is brought to you for free and open access by the Theses and Dissertations at Loyola eCommons. It has been accepted for inclusion in Dissertations by an authorized administrator of Loyola eCommons. For more information, please contact [ecommons@luc.edu](mailto:ecommons@luc.edu).



This work is licensed under a [Creative Commons Attribution-Noncommercial-No Derivative Works 3.0 License](#).  
Copyright © 1986 Linda Mae Oyer

CHARACTERIZATION AND MODULATION OF  
CENTRAL APNEA OCCURRING DURING  
CLUSTER BREATHING IN THE CAT

by

Linda Mae Oyer

**Library -- Loyola University Medical Center**

A Dissertation Submitted to the Faculty of the Graduate School  
of Loyola University of Chicago in Partial Fulfillment  
of the Requirements for the Degree of  
Doctor of Philosophy

January

1986

## ACKNOWLEDGEMENTS

I would like to thank the committee members: Dr. Melvin Lopata, Dr. Walter St. John, Dr. John Sharp, and Dr. Robert Wurster, for their time spent in reading and evaluating this dissertation. A very special thanks is due my advisor and friend, Dr. Charles Webber, for his guidance and patience in the completion of this study.

The programming talents of Mr. Daniel Bauman and Mr. Robert Carpenter are gratefully acknowledged. I would also like to thank Mr. Blaine Welman for his assistance in electronic design and construction.

My deepest appreciation goes to my family: Dad, Mom, Brenda, Jan and Cindy, for their love and concern which made this accomplishment possible.

## VITA

The author, Linda Mae Oyer, is the daughter of Richard Lee and Marilyn (Roth) Oyer. She was born June 18, 1958 in Peoria, Illinois.

Linda received her elementary and secondary education in the public school system of Gridley, Illinois. She was graduated from Gridley High School in May, 1976. In September, 1976, Linda entered Wheaton College in Wheaton, Illinois. In 1979, she was elected to membership in the Wheaton College Honor Society. She was graduated with High Honors, receiving the Bachelor of Science degree in Biology, in May, 1980.

In July, 1980, she entered the Department of Physiology, Loyola University of Chicago. She began working in the laboratory of Dr. Charles L. Webber, Jr. in 1981. While a graduate student, Linda was supported by a Basic Science Fellowship from 1980-1984. In 1984, she received the Schmitt Dissertation Fellowship. Linda was elected to student membership in the American Physiological Society in 1983.

In February, Linda will begin postdoctoral studies in the Department of Physiology at Dartmouth Medical School in Hanover, New Hampshire.

## PUBLICATIONS

1. OYER, L.M., S.B. Jones and D.S. Bruce. Effects of the beta-adrenergic blocker, propranolol, on the hamster (*Mesocricetus auratus*) rewarming from induced hypothermia. Cryobiology 19: 402-406, 1982.
2. Webber, C.L., Jr. and L.M. OYER. Afferent influences on respiratory instability and periodic breathing in cats. Proc. Int. Symp.: Central Neural Production of Periodic Respiratory Movements, pp. 117-118, 1982.
3. OYER, L.M. and C.L. Webber, Jr. Mechanoreceptor influence on Biot (cluster) breathing in cats. The Physiologist 25: 187, 1982.
4. OYER, L.M. and C.L. Webber, Jr. Destabilization of the respiratory pattern following bilateral pneumotoxic ablation. Fed. Proc. 43: 903, 1984.
5. OYER, L.M. and C.L. Webber, Jr. Prolongation of central apnea by positive end-expiratory pressure in cluster breathing. Fed. Proc. 44: 1584, 1985.
6. Webber, C.L., Jr. and L.M. OYER. Modification of the three power spectrum peaks in the phrenic neurogram by ablation of pontine nuclei. Fed. Proc. 44: 1584, 1985.
7. OYER, L.M. and C.L. Webber, Jr. Expiratory cell discharges in cluster breathing: effect of positive end-expiratory pressure. Fed. Proc.: in press.

## TABLE OF CONTENTS

	Page
ACKNOWLEDGEMENTS . . . . .	ii
VITA . . . . .	iii
PUBLICATIONS . . . . .	iv
TABLE OF CONTENTS . . . . .	v
LIST OF TABLES . . . . .	vii
LIST OF FIGURES . . . . .	viii

### Chapter

I. INTRODUCTION . . . . .	1
II. REVIEW OF THE RELATED LITERATURE . . . . .	2
A. Central Pattern Generation. . . . .	2
1. Anatomical organization of the CPG . . . . .	2
2. Neurophysiology of the CPG . . . . .	10
B. Afferent modulation of the CPG . . . . .	18
1. Modulation of inspiratory duration . . . . .	20
2. Modulation of expiratory duration . . . . .	21
C. Efferent outflows of the CPG . . . . .	24
1. Upper airway musculature . . . . .	24
2. Expiratory musculature . . . . .	28
D. Periodic breathing . . . . .	32
1. Types of periodic breathing . . . . .	33
2. Types of apnea . . . . .	35
III. SPECIFIC AIMS . . . . .	38
IV. METHODS. . . . .	40
A. Surgical procedures . . . . .	40
B. Methods of data acquisition . . . . .	50
1. Nerve recordings . . . . .	51
2. Artificial ventilation . . . . .	52
3. Extracellular recordings . . . . .	56
4. Recording of variables . . . . .	58
C. Experimental groups . . . . .	62
D. Statistical evaluation . . . . .	63

## TABLE OF CONTENTS (continued)

Chapter		Page
V.	RESULTS . . . . .	65
	A. Characteristics of the Biot pattern . . . . .	65
	B. Group I - Mechanoreceptor effects on Biot breathing . . . . .	68
	1. Multiple breath responses to PEEP. . . . .	71
	2. Single breath responses to PEEP. . . . .	78
	C. Group II - Responses of upper airway and abdominal motoneurons to PEEP . . . . .	85
	D. Group III - Respiratory cell discharges during Biot breathing. . . . .	97
	1. Inspiratory cell activity . . . . .	100
	2. Expiratory cell activity . . . . .	105
VI.	DISCUSSION. . . . .	114
	A. Characteristics of the Biot pattern . . . . .	114
	1. Factors predisposing to Biot breathing . . . . .	115
	2. Biot and eupneic breathing contrasted . . . . .	117
	B. Respiratory responses to PEEP . . . . .	118
	1. Multiple breath responses. . . . .	119
	2. Habituation to PEEP . . . . .	122
	3. Determination of $T_e$ by chemical and mechanical factors. . . . .	124
	C. Activities of upper airway and abdominal nerves . . . . .	128
	1. Abdominal nerve activity patterns . . . . .	128
	2. Recurrent laryngeal nerve patterns . . . . .	132
	D. Discharges of respiratory cells in Biot breathing . . . . .	134
	1. Inspiratory cell discharges . . . . .	134
	2. Expiratory cell discharges . . . . .	136
	E. Summary . . . . .	140
VII.	CONCLUSIONS . . . . .	144
VIII.	REFERENCES . . . . .	146

LIST OF TABLES

Table	Page
1. Respiratory and cardiovascular variables in eupnea and Biot breathing . . . . .	69
2. Alveolar gas tensions in response to single breath PEEP . . . . .	80
3. Carbon dioxide levels for CIHG nerve activity . . . . .	91
4. Alveolar gas tensions in response to multiple breath PEEP . . . . .	94
5. Respiratory variables for expiratory cell recordings . . . . .	113

## LIST OF FIGURES

Figure	Page
1. Experimental procedure for groups I and II. . . . .	45
2. Experimental procedure for group III. . . . .	46
3. No inflation test in eupnea and Biot breathing . . . . .	48
4. Effect of PRG lesions on breathing pattern. . . . .	49
5. Oscilloscope tracing of I/E gate. . . . .	53
6. Examples of tracheal pressure changes. . . . .	55
7. Oscilloscope tracing of spike-triggered pulses. . . . .	57
8. Representative polygraph tracings in eupnea and Biot breathing. . . . .	66
9. PRG lesion areas for group I . . . . .	70
10. Polygraph tracing of response to PEEP in eupnea. . . . .	72
11. Polygraph tracing of response to PEEP in Biot breathing. . . . .	73
12. Respiratory variables in response to PEEP . . . . .	75
13. Respiratory variables in response to PEEP (cont.) . . . . .	76
14. Polygraph tracing of response to single breath PEEP in eupnea . . . . .	77
15. Pooled response to single breath PEEP in eupnea and Biot breathing . . . . .	79
16. Polygraph tracing of response to single breath PEEP in Biot breathing . . . . .	81
17. Regression of $T_e$ versus PEEP in eupnea and Biot breathing . . . . .	83
18. Regression of $V_T$ versus PEEP in eupnea and Biot breathing . . . . .	84

LIST OF FIGURES (continued)

Figure	Page
19. PRG lesion areas for group II . . . . .	86
20. Polygraph tracing of variables for group II . . . . .	87
21. Oscilloscope tracing of nerves recorded in group II . . . . .	89
22. Expiratory duration and abdominal nerve activity in eupnea . . . . .	92
23. Polygraph tracings of abdominal nerve activity in response to PEEP in Biot breathing . . . . .	95
24. Expiratory duration and abdominal nerve activity in Biot breathing . . . . .	96
25. Regression of recurrent laryngeal nerve activity versus PEEP in eupnea and Biot breathing . . . . .	98
26. PRG lesion areas for group III . . . . .	99
27. Locations of respiratory cells recorded . . . . .	101
28. Polygraph tracings of integrated inspiratory cell discharges . . . . .	102
29. Polygraph tracing of integrated inspiratory cell discharge during central apnea in Biot breathing . . . . .	103
30. Discharge frequency profiles of inspiratory cells in response to withholding inflation . . . . .	104
31. Inspiratory cell characteristics . . . . .	106
32. Polygraph tracings of expiratory cell discharges . . . . .	107
33. Discharge frequency profiles of expiratory cells in response to PEEP . . . . .	109

## CHAPTER I

### INTRODUCTION

The respiratory control system is composed of three components. A central pattern generator rhythmically activates the efferent outflows of the system, the respiratory muscles. The output of the central pattern generator is adjusted in accordance with the afferent feedbacks from chemoreceptors and mechanoreceptors. The activities of these three components: the central pattern generator, the afferent feedbacks and the efferent outflows, have been extensively studied in eupnea. However, very few systematic studies of the activity of these three components in periodic breathing have been performed.

This study was designed to investigate the activity of each of these three components in a periodic pattern, Biot breathing, in the cat. The modulation of Biot breathing by mechanoreceptor feedback was determined by altering lung volume feedback with the application of positive end-expiratory pressure. Efferent outflows to upper airway, diaphragm and abdominal muscles were characterized in Biot breathing and in response to alteration of lung volume feedback. The activity of the central pattern generator was studied by extracellular recordings of respiratory related neurons in the medulla.

## CHAPTER II

### REVIEW OF THE RELATED LITERATURE

#### A. Central Pattern Generation

The mechanical act of breathing is governed by a central oscillator or pattern generator. The central pattern generator (CPG) for respiration adjusts its output, both frequency and volume, to meet the metabolic needs of the organism at the lowest possible energy cost. In order to characterize the CPG, it is necessary to describe the anatomical locations and physiological processes involved in the generation of the respiratory rhythm.

##### I. Anatomical Organization of the CPG

Marckwald (127) performed a series of transection experiments in the vagotomized rabbit. Prolonged inspiratory cramps resulted when the brain stem was transected immediately behind the posterior colliculi. Marckwald concluded that this transection had removed a center residing in the inferior colliculus which was inhibitory to inspiration.

In his classic experiments in the cat, Lumsden (126) found that section of the brain stem behind the posterior colliculi resulted in no appreciable change in either the rate or depth of respiration. When the vagi were subsequently sectioned, respiration was slowed and deepened but only to the extent that occurred when the nervous system was intact. A midpontine transection resulted in the development of prolonged inspiratory activity or apneusis, which, it was noted, was not dependent upon whether the vagi were cut or intact. Lumsden concluded that an "apneustic center" was located in

the lower pons from which originated the impulses causing apneusis. A "pneumotaxic center" in the upper pons periodically inhibited the activity of this apneustic center and so produced normal respiration. A gasping type of respiratory pattern followed pontomedullary transection, thus the presence of a "gasping center" in the medulla was postulated. Transection between medulla and spinal cord resulted in the cessation of all respiratory efforts.

Stella (175) extended the observations of Lumsden when he found that midpontine transection resulted in apneusis in the cat only when both vagus nerves were sectioned. This observation demonstrated the essential role of vagotomy in the development of apneusis and focused attention on the role of afferent feedback loops in the modification of the respiratory rhythm. However, afferent feedback is not essential in the generation of the respiratory rhythm as demonstrated by Wang and co-workers. In the decerebrate cat, rhythmic respiration persisted following section of the ninth, tenth, eleventh and twelfth cranial nerves, the spinal cord at  $C_6$  and the  $C_1-C_6$  dorsal roots (182). Other experiments confirmed that a rhythmic respiratory output could be generated by the isolated brain stem (101,167). Thus, it was concluded that the site of respiratory rhythmogenesis was located within the pons and medulla.

Recordings of single cells in the brain stem were first made by Gesell (92) who found neurons with respiratory discharge patterns within the medulla. Respiratory related units have consequently been localized in two areas: the pons and the medulla.

Respiratory related neuronal activity has been localized in the medulla to two anatomical areas. The ventrolateral part of the nucleus tractus solitarius (18) comprises the dorsal respiratory group (DRG) and the ventral respiratory group (VRG) consists of the nucleus ambiguus (3) and the nucleus retroambiguus (130).

The nucleus tractus solitarius (NTS) consists almost entirely of inspiratory cells (20,29,30,74) in a column situated 2.0 to 3.0 mm lateral to the midline, extending 2.0 to 3.0 mm rostral from the level of the obex and lying at a depth of 0.6 to 2.6 mm below the dorsal surface (125). The inspiratory neurons have been classified into two types of units designated  $R_{\alpha}$  and  $R_{\beta}$  on the basis of their response to lung inflation (19).  $R_{\alpha}$  cells are inhibited by lung inflation sufficient to terminate inspiration and  $R_{\beta}$  discharge increases in frequency in response to lung inflation. In addition to these inspiratory cells, a small number of expiratory cells (74) and P cells (respirator pump cells) have been located in the NTS (20).

Axons of the cells of the NTS cross in the medulla and project predominantly to the contralateral side of the spinal cord (159,180). Initially it was thought that only  $R_{\alpha}$  cells projected to the spinal cord (74) but more recent observations have demonstrated that both types of inspiratory cells have spinal axons (20,122). The  $R_{\alpha}$  and  $R_{\beta}$  neurons project monosynaptically to both the phrenic and intercostal motoneurons (124,133).

The NTS also has projections within the medulla mainly to the ipsilateral VRG inspiratory cells and NRA expiratory cells (132). Neurons in the NTS have been shown to project ipsilaterally to the parabrachial nuclei by anatomical (106,112) and electrophysiological (32) studies.

The VRG is composed of two cell columns: the nucleus ambiguus (NA) and the nucleus retroambiguus (NRA). Inspiratory cells are found in the rostral portions of the NA-NRA complex from -1.0 to 4.0 mm rostral and 3.0 to 4.5 mm lateral to the obex. Expiratory cells are found in three regions: the NA, the caudal portion of the NRA from 1.0 to 8.0 mm caudal and 3.0 to 4.5 mm lateral to the obex and the most rostral portions of the NRA in the vicinity of the retrofacial nucleus, referred to as the Botzinger complex (125).

The cells of the NA are laryngeal and pharyngeal motoneurons and send axons through the glossopharyngeal and vagus nerves (29,30). The firing patterns of inspiratory neurons in the NA show an increase in firing frequency as inspiration progresses while expiratory laryngeal neurons reach their peak frequency early in expiration and then decrease as expiration proceeds (30).

Axons of the majority of NRA cells cross the medulla rostral (inspiratory) and caudal (expiratory) to the obex and descend in the contralateral cord (130,131). Inspiratory cells of the rostral NRA project to the phrenic and intercostal motoneurons (82,159). Expiratory cells of the caudal NRA project to the thoracic and lumbar levels of the cord (131) and monosynaptically excite expiratory intercostal and abdominal motoneurons (113).

The inspiratory cells of the NRA can be further divided into two types. The "early-burst" inspiratory neurons reach their peak firing rate almost immediately after the onset of activity. The "late" inspiratory neurons show an augmenting firing pattern which reaches peak frequency late in the inspiratory phase (30,131). In contrast to expiratory NA cells, the

expiratory neurons of the NRA have an incrementing firing pattern with the peak frequency occurring late in the expiratory phase (30,131).

The early burst inspiratory cells have very rich arborizations to the contralateral NRA inspiratory and expiratory neurons. Axons of late inspiratory NRA cells arborize among NRA inspiratory cells bilaterally with some arborizations among contralateral NRA expiratory neurons. NRA expiratory cells have no medullary collaterals (132).

The Botzinger complex (BotC) has been the subject of intense interest because of the lack of demonstration of medullary collaterals from NRA expiratory cells. In contrast, evidence for axonal projections from the expiratory cells of the BotC is more extensive. Injection of horseradish peroxidase (HRP) into areas of the NTS displaying inspiratory cell activity resulted in labeling of neurons 2.0 to 4.0 mm rostral to the injection site in the vicinity of the retrofacial nucleus (108). Lipski and Merrill (123) demonstrated that BotC expiratory cells could be antidromically activated from the contralateral NTS. Spike-triggered averaging of the membrane potential of intracellularly recorded NTS inspiratory cells revealed that discharge of BotC neurons was followed by a hyperpolarizing shift in the NTS membrane potential (135). These data provide evidence for an inhibition of NTS inspiratory cells by expiratory BotC neurons. Preliminary observations (unpublished, cited in 132) suggest that BotC expiratory neurons may also provide the augmenting excitatory input for the expiratory cells of the NRA.

The areas of the rostral pons participating in respiratory control were determined to be in the dorsolateral portion of the tegmentum (141,150,177,178,182). Later this function was specifically localized to the

nucleus parabrachialis medialis (NPBM, 27) and the Kolliker-Fuse nucleus (K-F, 28). It has recently been suggested that the term, pontine respiratory group (PRG), be substituted for the cumbersome names of the pontine nuclei in which respiratory related cells have been recorded (78). The term, PRG will be used in this dissertation although it has not gained widespread acceptance as yet.

The anatomical connections of these nuclei are numerous. Ngai and Wang (141) postulated that pathways coursed through the ventrolateral pons between the pontine nuclei and the medulla. Further experiments with HRP and complementary studies with radioactive amino acids have demonstrated that the NTS, NA and NRA project bilaterally to the pontine nuclei with the densest projection being ipsilateral (106,112). Projections have also been demonstrated by antidromic stimulation (32). Efferent connections from the NPBM and K-F to NTS were not demonstrated (106). However, antidromic activation of a small number of NTS respiratory cells by stimulation within the pons has been reported (33). In a study on expiratory neurons of the caudal region of the NRA, Kalia (107) found a significant number of retrogradely labeled neurons in the NPBM and K-F on the ipsilateral side.

Extracellular recordings of pontine units have revealed both continuous and discontinuous types of neuronal firing patterns. Phasically discharging inspiratory neurons were found to predominate in the K-F (28,60,102) while the NPBM contained both inspiratory and expiratory neurons as well as phase-spanning neurons (28,60).

In recordings from vagotomized cat, many respiratory related neurons are found in the PRG (27,28). In contrast, when the vagus nerves are intact these neurons are difficult to find. When lung inflation is withheld, many

tonically firing neurons show respiratory related phasic activity (80). This observation led to the postulation that pulmonary stretch receptor input prevents the respiratory modulation of PRG neurons by presynaptic inhibition of medullary inspiratory cells projecting to the PRG (57). Even though pulmonary stretch receptor afferents modulate the activity of pontine respiratory units, the pons is not primarily involved in mediating the lung inflation and deflation reflexes since these reflexes persist, albeit altered, after destruction of the NPBM (76,81,115).

The discharge patterns of PRG neurons become phasically active in the intact animal in some instances. "Reticular arousal" may be one such example (59,103). The sleep-wake cycle also modulates PRG neuron activity. Recordings in chronically instrumented cats revealed that during quiet sleep both the mean discharge rate and variability in discharge rate of PRG neurons decreased. During REM sleep, the discharge rate and variability increased. These changes in neuronal firing paralleled the changes in respiratory frequency. Thus, it was concluded that the changes in respiratory pattern associated with sleep-waking states could be due to a state-dependent modulation of the influence exerted by PRG neurons on respiratory phase transitions (172).

Apneustic breathing in chronic cats with bilateral PRG lesions and vagotomy disappears after recovery from anesthetic. If the animals were reanesthetized apneustic breathing reappeared (160). Similarly, cats with chronic PRG lesions showed regular breathing patterns when awake but an increased tendency for the development of apneusis was observed in REM sleep (8).

These observations led to the conclusion that influences from the higher central nervous system have the potential to compensate for the losses of PRG and vagal reflex systems in the unanesthetized, awake animal (160).

From ablation or transection experiments, it is clear that the cells of the PRG participate in the production of a normal respiratory pattern. The classical function assigned to the PRG is one of inspiratory inhibition. The production of apneusis when the PRG is ablated in vagotomized animals supports this concept (41,101,126,141,150,165,175,177,178,182). Also, stimulation in the ventral regions of the PRG can elicit a premature termination of inspiration (27,55).

More recent studies have revealed that PRG neurons contribute an excitatory input to the postulated off-switching system. The volume threshold for inspiratory termination is increased after PRG lesion (24,75,81,115) such that inspiratory duration ( $T_i$ ) and tidal volume ( $V_T$ ) are significantly elevated (160,165). Similar elevations in the off-switch threshold could be produced by unilateral lesions when stimulation in the contralateral, intact NPBM was used to terminate inspiration (76). In contrast to its effect on inspiratory duration, cold block of the PRG increases the sensitivity of the Breuer-Hering expiratory reflex, resulting in even greater prolongation of  $T_e$  with lung inflation (24,115).

The PRG also plays an important role in the ventilatory response to hypercapnia. Following bilateral destruction of the PRG, the end-tidal  $CO_2$  levels were significantly elevated in cats breathing 100%  $O_2$  (166) and room air (184). Not only was resting ventilation depressed but frequency responses to hypoxic and hypercapnic stimuli were also diminished. In contrast, the tidal volume response to hypercapnia was unaltered while that to hypoxia

increased. The net result of these changes was that minute ventilation in response to hypercapnia was decreased while minute ventilation in response to hypoxia was maintained (161,166). St. John has concluded (161) that the PRG constitutes an integral component of the central chemoreceptor controller system.

The role of the PRG in eupneic breathing in the unanesthetized animal remains unclear. The studies cited here do, however, lend credence to the hypothesis that the PRG may act to "finely tune the pattern generator" (137).

## 2. Neurophysiology of the CPG

On the basis of stimulation experiments with sustained, high frequency stimulation, Pitts found that widespread areas of the medulla existed from which could be elicited two primary responses, inspiratory prolongation and expiratory prolongation (148). In another series of experiments in midpontile decerebrate cats with cold-blocked vagus nerves, it was found that stimulation of the inspiratory centers in the medulla was effective in increasing the magnitude of apneusis and that stimulation in the expiratory centers could convert apneustic respiration to a eupneic type pattern. Apneusis could also be inhibited by stimulation of the central end of a cut vagus nerve (149). Pitts concluded that rhythmic respiration occurred by either reciprocal inhibition of the inspiratory and expiratory half-centers or periodic interruption of the tonic inspiratory discharge of medullary respiratory centers by the pontine and vagal pneumotaxic mechanisms (148,149).

The hypothesis that apneusis was the inherent output of the medullary centers was disproved by several observations (41,101) in the dog and cat.

Apneusis did not persist until death but was interrupted periodically by normal breaths. The conclusion was drawn that apneusis was an epiphenomenon related to factors outside of the medulla and not the inherent pattern of the medullary respiratory cells.

Pontomedullary transection in the vagotomized cat was observed to convert apneustic breathing to either gasping or a more eupneic type of breathing. Wang and co-workers (182) concluded that since the tonic activity of the apneustic center in the pons was so powerful as to obliterate the rhythmic activity of the medullary centers, the apneustic center must be the site of respiratory rhythmogenesis. A model was proposed in which pneumotaxic mechanisms of the pons and vagus nerves acted to periodically inhibit the tonic inspiratory activity of the apneustic center. The medullary centers could generate respiratory rhythmicity under certain conditions but normally functioned only as the efferent pathway for central respiratory control (182).

Hering and Breuer in their classical studies (42,99) first demonstrated the relationship between lung volume and inspiratory duration. They observed that the "central nervous organ" for breathing movements was continually influenced by the prevailing state of lung distension, mediated by the vagus nerves. An indirect relationship between lung volume and the duration of inspiration was observed: as the lung volume increased inspiration was inhibited and expiration promoted.

Boyd and Maaske (40) found, via stimulation of the vagus nerve in the anesthetized dog, that the simulated volume feedback necessary to terminate inspiration declined as the stimulus was delivered later in inspiration. They defined the inhibitory threshold as the number of afferent volleys needed to

produce a premature termination of inspiration. It was observed that the "inhibitory threshold" declined as vagal stimulation commenced later in inspiration. Larabee and Hodes (117) similarly noted that the threshold number of stimulations of the superior laryngeal nerve in the cat necessary to terminate inspiration declined progressively throughout the inspiratory phase of respiration. They postulated that a "central state" developed progressively during inspiration and when it reached a critical level, inspiration was terminated. Artificial stimulation added to this naturally occurring central state. Thus the progressive decline in threshold for termination of inspiration was due to the gradual development of the "central state".

The initial observations of Hering and Breuer were repeated and extended in both man and cat by Clark and von Euler (54). The relationship between inspiratory duration and tidal volume was observed in spontaneous breathing and during rebreathing from a cylinder originally containing 100%  $O_2$ . These experiments revealed a time dependent relationship between  $V_T$  and  $T_i$  such that as  $T_i$  increased the  $V_T$  necessary to terminate inspiration decreased hyperbolically. From these results it was concluded that the falling threshold with time reflected the properties of the central mechanism for respiratory termination.

A model for the control of  $T_i$  and  $V_T$  was proposed. Both the depth and duration of the breath are determined at the point of inspiratory termination. During inspiration the lung volume increases at a rate dependent upon the respiratory drive. At some point in time, the volume will intersect the decaying slope of the  $V_T/T_i$  relationship. At that time, inspiration is terminated and  $V_T$  and  $T_i$  are thus defined.

Several other models elaborating upon these concepts have been proposed (58,73,77,188).

Examination of the phrenic nerve discharge reveals that it consists of four phases of activity: an augmenting, ramp-like activity during inspiration, a brief termination, a variable period of rebounding, but declining activity, and a silent expiratory phase. Conventional terminology divides the respiratory cycle into two phases, inspiration and expiration. Richter (157) has suggested that this terminology be modified to more accurately reflect the neural events occurring during the respiratory cycle as revealed in the phrenic nerve activity. Thus, it is proposed that the respiratory cycle consists of three phases: inspiration, post-inspiration or stage 1 expiration ( $E_1$ ), and stage 2 expiration ( $E_2$ ). The inspiratory phase includes the period of augmenting phrenic nerve discharge, the period of declining phrenic activity comprises the  $E_1$  phase, and the period of phrenic quiescence, the  $E_2$  phase.

In order to understand respiratory pattern generation, the following questions must be answered. What processes underlie the generation of the inspiratory "ramp"? How is inspiratory activity terminated, i.e., how is the inspiratory "off-switch" produced? What neural mechanisms account for the two stages of expiration?

After a rather abrupt onset, phrenic nerve activity progressively increases throughout inspiration. This augmenting activity results from an incrementing excitatory process as demonstrated by intracellular recordings from inspiratory bulbospinal and propriobulbar neurons. Analysis of the postsynaptic activity reveals that, during inspiration, these cells receive an augmenting pattern of excitatory postsynaptic potentials (EPSPs).

This postsynaptic activity results in an increasing depolarization and, thus, an increase in the rate of discharge of the cell (157,158).

A network of cells with collaterals may be responsible for producing the augmenting ramp-like inspiratory activity. In such a system, activation of one cell would lead to activation of other cells, which in turn would re-excite the original cells. The involvement of this type of mechanism in the genesis of the inspiratory ramp is indicated by studies involving recording from pairs of neurons within the DRG and VRG. Computation of cross-correlation histograms (CCH) of spike activities from neighboring inspiratory cells in the DRG and VRG revealed a high incidence (16/26 pairs) of correlated discharge as indicated by a sharp peak near zero lag in the CCH (84). When the microelectrodes were recording from cells on opposite sides of the medulla, only 1 of 43 pairs had a peak in the CCH indicative of a correlated discharge. In a similar study, 17% of neuron pairs had a significant peak in the CCH. The highest incidence of a positive unit-unit cross-correlation was observed in the correlations between two augmenting or two decrementing inspiratory units (85). Similar percentages of pairs showing a CCH peak were found in another investigation (100). These interactions may be due to recycling of excitation between adjacent inspiratory neurons or the existence of a common input to both cells (85).

The location of the cells responsible for generating the inspiratory ramp activity has not been determined. If, indeed, inspiratory neurons forming a recurrent excitatory loop network produce the augmenting ramp, the inspiratory bulbospinal neurons are excluded from this function (157). This is due to the fact that inspiratory bulbospinal neurons continue to discharge during the  $E_1$  phase which would tend to produce a new inspiratory

ramp of activity. Further evidence that the DRG does not constitute the ramp generator is provided by the observation that NTS lesions in chronic (23), decerebrate (156) and chloralose-urethane anesthetized (174) cats had very little effect on respiratory rhythm. Similarly, synchronous antidromic activation of inspiratory bulbospinal neurons resulted in only transient effects on the pattern of phrenic nerve discharge (83). Based on the assumption that synchronous activation of a portion of the respiratory pattern generator should lead to a phase shift or reset the rhythm, the conclusion was drawn that the bulbospinal inspiratory neurons are not responsible for the generation of respiratory timing signals. The recent observation (43) that unilateral focal cold blocks ( $20^{\circ}\text{C}$ ) in the area of the nucleus paragigantocellularis lateralis and the nucleus preolivaris in the ventrolateral rostral medulla resulted in apnea, indicates that these structures may be involved in the ramp generation.

Richter (157) has defined the properties of the ramp-generator neurons: accumulation of ramp-like excitation during inspiration and inhibition during both phases of expiration. Intracellular recordings of such interneurons revealed a steady depolarization during inspiration with an accompanying increase in discharge frequency. After inspiration, the membrane was hyperpolarized by inhibitory postsynaptic potentials (IPSPs) during  $E_1$  which gradually declined throughout  $E_2$ .

The termination of inspiratory activity occurs when a slowly increasing, centrally generated inspiratory activity (CIA) sums with the increasing afferent input from the pulmonary stretch receptors (PSR) to reach a critical threshold level (54,57,75,114). When PSR input is eliminated, the CIA activity must reach this threshold alone. Therefore, inspiration is

prolonged and the depth (tidal volume) increased. It has been proposed that the CIA is responsible for the observed increase in the excitability of the off-switch mechanism with time (54,58,74,76). The observation that changes in CIA activity by alterations in  $\text{CO}_2$  and body temperature were paralleled by changes in the off-switch excitability lends support to this conclusion (76).

Traditionally, the CIA and PSR inputs were believed to influence the off-switch via the  $R_{\text{beta}}$  cells which in turn inhibited the  $R_{\text{alpha}}$  cells (19). Recently, the role of  $R_{\text{beta}}$  neurons as interneurons receiving PSR input and inhibiting  $R_{\text{alpha}}$  neurons has been challenged by the observations that  $R_{\text{beta}}$  neurons project to the spinal cord (20) and that large bilateral lesions of the DRG, where these cells are located, has little effect on the inspiratory shortening reflex (129). Berger (20) has proposed that pump neurons in the NTS (P cells) are the neurons mediating PSR effects on respiration because inflation during either inspiration or expiration activates P cells. Likewise, the degree of expiratory prolongation produced by lung inflation during expiration correlates with the discharge rate of P cells not that of  $R_{\text{beta}}$  neurons.

The inhibition of phrenic nerve discharge coincides with an augmenting pattern of IPSPs in the bulbospinal inspiratory cells (157). The IPSP pattern parallels the spike discharge pattern of the late inspiratory neurons (57,58). These neurons are inhibited during the first half of inspiration by IPSPs, discharge in a burst of activity at the end of inspiration, and do not discharge during  $E_1$  (157). Thus, it seems possible that the late inspiratory cells may play a role in the off-switch of phrenic nerve activity since the timing of discharge is such that it would produce a sudden and massive

inhibition of neurons of the CPG. Cohen and Feldman (58) have recently challenged this conclusion based upon the observation that some of the late inspiratory neurons produced short-latency excitation of the phrenic motoneurons. This finding is inconsistent with an off-switch function for these cells. However, they concede that the late inspiratory cells recorded may be a heterogeneous population and therefore, the hypothesis that these neurons might have an off-switch function cannot be completely excluded.

Post-inspiratory activity ( $E_1$ ) is hypothesized to have a gating function in delaying the onset of expiratory activity. Intracellular recording of neurons with a post-inspiratory discharge pattern have revealed that they are inhibited during inspiration and the second phase of expiration and discharge only during the  $E_1$  phase. It seems possible that these cells may be controlled by both inspiratory and expiratory neurons and in turn, inhibit both groups, allowing a smoothing of the inspiratory/expiratory phase switch (157).

It is unlikely that the inhibition of inspiratory bulbospinal neurons which occurs during  $E_2$  is derived from the caudal NRA expiratory neurons because these neurons have no medullary collaterals (6,131). However, the group of expiratory cells in the rostral extension of the NRA, the BotC neurons, may play a role in this function. Support for this hypothesis is derived from the demonstration that these cells have inhibitory connections with inspiratory bulbospinal cells in the DRG (123).

The respiratory cycle can be viewed as being initiated by the activation of interneurons which are progressively released from an expiratory phase inhibition. This CIA is off-switched by possibly the late inspiratory neurons. The ramp generator is then gated by a powerful

inhibition and  $E_1$  occurs. The second stage of expiration occurs as expiratory neurons are released from inhibition.

### B. Afferent modulation of the CPG

There are a number of afferent feedback loops which modulate the respiratory pattern. These include chemoreceptors, both peripheral and central, and mechanoreceptors. Mechanoreceptors include the pulmonary receptors: the slowly adapting, rapidly adapting and the J receptors, and the chest wall receptors: muscle spindles and Golgi tendon organs.

The slowly adapting or pulmonary stretch receptors (PSR) are located in the smooth muscle of the trachea, main bronchi and intrapulmonary airways in the cat (168). Afferent fibers from the PSRs run in the vagus nerve and terminate within the NTS. The distribution of afferent projections of the PSRs within the NTS was studied by antidromic mapping techniques while recording within the nodose ganglion. In the cat, projections to the medial subnucleus of the NTS were demonstrated for 6/7 afferents. Two of seven units also had projections to the lateral and ventrolateral subnuclei (69). Using the technique of spike-triggered averaging, Berger and Averill (22) recently demonstrated that PSRs terminated in the medial and ventrolateral NTS and in an area just dorsolateral to the tractus solitarius. In contrast to the previous study, they failed to demonstrate any PSR with terminations in more than one subnucleus.

A similar study (4) revealed a monosynaptic connection between PSR and  $R_{\text{beta}}$  cells. Extracellular single unit spikes of PSR recorded from the nodose ganglion were used to trigger averaging of synaptic noise from inspiratory neurons. All  $R_{\text{beta}}$  neurons showed a prominent wave of synaptic depolarization that was absent from  $R_{\text{alpha}}$  neurons. The mean latency

between centrally recorded action potentials of PSR afferents and EPSPs of  $R_{\text{beta}}$  cells was 0.2 msec with vagal stimulation. This latency is consistent with that of a monosynaptic connection.

Single fiber PSRs were first recorded in cats by Adrian (1). He characterized the slowly adapting nature of the receptors and found that discharge rates were altered by changes in lung volume. Widdicombe (187) localized the slowly adapting stretch receptors to the trachea and bronchi and confirmed Adrian's observation that the PSRs were activated by a distension of the airways, not mechanical irritation within the airways.

Pulmonary stretch receptors are located within the smooth muscle of the airways (12,187). The principal stimulus appears to be changes in airway smooth muscle tension resulting from thoracic volume changes (16). Therefore, the frequency of PSR discharge correlates well with transpulmonary pressure (66).

Elevations of functional residual capacity (FRC) result in a significant increase in frequency of PSR discharge, even when the increase in FRC was maintained for one hour (139). These results indicate that even though PSRs initially adapt to a maintained volume stimulus, the frequency of discharge is still increased over control, i.e., there is not complete adaptation to a prolonged stimulus.

In addition to lung volume changes, PSRs are modulated by intrapulmonary  $\text{CO}_2$  such that increases in airway  $\text{CO}_2$  in isolated lung (61) or functionally isolated, in situ, extrapulmonary bronchi (16) result in decreased firing of PSRs. This response is believed to allow for increased tidal volumes at the same inspiratory duration in hypercapnia.

## 1. Modulation of inspiratory duration

Breuer and Hering first demonstrated that expansion of the lung reflexly inhibited inspiration (42,99). In anesthetized cats, a hyperbolic relationship between  $V_T$  and  $T_i$  exists, such that  $T_i$  decreases as  $V_T$  increases (54,192). However, in studies of conscious men (54) and anesthetized women (89), no significant changes in  $T_i$  were observed when  $V_T$  was increased by  $CO_2$  rebreathing. Only at tidal volumes greater than 2.0 times eupneic values, was  $T_i$  shortened (54). Therefore, it appears that the Breuer-Hering reflex does not seem to be involved in the control of the inspiratory off-switch mechanism in the range of eupneic tidal volumes in man.

As mentioned previously, the PRG modulates the Breuer-Hering inspiratory shortening reflex. Bilateral (115) or unilateral (75,81) lesions placed within the PRG result in an increased volume threshold for the termination of inspiration, although the time dependence is not altered.

Premature termination of  $T_i$ , elicited by stimulation of the vagus nerves (54,81) and volume inflations (54,81,190) results in a shortening of the following expiration. The relationship between  $T_i$  and subsequent expiratory duration ( $T_e$ ) is linear, such that, prolongation of  $T_i$  results in a prolongation of the subsequent  $T_e$  (56).

Pulmonary stretch receptors produce changes in the characteristics of nerve discharge as well as changes in respiratory timing. The effect of PSR to shorten  $T_i$  will necessarily decrease the duration of the burst of phrenic nerve activity. With the same rate of rise of phrenic activity, the peak amplitude of the integrated nerve activity will decrease (75). When lung inflation is withheld, phrenic nerve discharge increases at relatively the same

rate but reaches a higher peak discharge due to the increase in  $T_i$  (56). In contrast to the lack of effect of PSR on the rate of rise of phrenic nerve discharge, recurrent laryngeal nerve activity is markedly altered by lung inflation. When inflation is withheld, integrated recurrent laryngeal nerve activity increases over inflated control values from the beginning of the inspiratory phase. This result indicates that normally vagal afferent inhibition of laryngeal discharge is operative almost from the start of the inspiratory phase (56).

Afferent feedback from PSR has been demonstrated to alter the discharge of DRG and VRG cells. As mentioned previously, PSR feedback inhibits the discharge of  $R_{\alpha}$  cells and facilitates the discharge of  $R_{\beta}$  and P cells within the NTS (19,20). Inspiratory bulbospinal neurons of the VRG are virtually all inhibited by lung inflation. Of the inspiratory cells, antidromically activated from the recurrent laryngeal nerve, some are inhibited by maintained lung inflation and others show a low-frequency, long-lasting discharge throughout the expiratory pause (31). These results are consistent with the observations of inhibition of recurrent laryngeal nerve discharge by PSR afferents (56).

## 2. Modulation of expiratory duration

Inflation of the lungs during expiration results in an increase in expiratory duration. This effect is known as the Breuer-Hering expiratory lengthening reflex (42,99). In the anesthetized cat, pulses of inflation during the initial 60-80% of control expiratory time produced an increase in  $T_e$ . Inflations during the last 20-40% of normal expiration had no effect on  $T_e$  (114). This prolongation was related to both the inflation volume and the time in the expiratory phase when inflation was delivered. In general,

greater expiratory prolongation occurred when inflation volume was increased and when the volume was delivered later in the expiratory phase (114). Elevation of lung volume in dogs on cardiopulmonary bypass also resulted in an increase in  $T_e$ , indicating that changes in blood gas tensions are not responsible for this effect (17). Resistive loading of expiration in the cat (192) resulted in progressive lengthening of expiration which was abolished by vagotomy, yielding evidence that PSRs were involved. Observations in the cat with both resistive and elastic loading of expiration revealed that  $T_e$  is not simply a function of the final FRC reached. Expiratory duration was shortened more with elastic loading as compared to resistive loading at the same FRC, thus the volume profile or  $dV/dt$  also determines the degree of prolongation of expiration (116). Sustained elevation of FRC does not prolong unloaded  $T_{E}$ , but the  $V_T/T_e$  relationship is shifted upward and to the right although there is no significant change in slope (140).

The lengthening of expiration by volume loading also produces changes in the duration and depth of the following inspiration. Feldman and Gautier (81) demonstrated a linear relationship between  $T_e$  and the subsequent  $T_i$  when expiration was prolonged by vagal stimulation and lung inflation during expiration. A similar finding was reported in dogs (193). This prolongation in subsequent  $T_i$  may function to overcome the reduction in tidal volume which would normally result from increased loads or increased levels of FRC.

The prolongation of expiration by PSRs is modulated by several factors. Younes and co-workers (190) found that the duration of apnea following lung inflation is altered by the sensitivity to  $CO_2$ . When  $CO_2$  sensitivity is low, the prolongation of apnea is greater than the prolongation

seen with normal  $\text{CO}_2$  sensitivity. Lesions in the PRG also affect the Breuer-Hering expiratory lengthening reflex. Bilateral (115) PRG lesions resulted in a doubling of the gain of the expiratory lengthening reflex; thus a greater prolongation of expiration was observed for a given volume inflation during expiration. This change may be due in part to the decreased  $\text{CO}_2$  sensitivity following PRG lesions (161,166).

Based on these observations, several models have been proposed for the control of expiratory duration in cat (57), dog (194) and rabbit (63). The salient features of these models include an exponentially decaying inspiratory inhibitory and expiratory facilitatory process which prevents inspiration onset until some threshold has been reached. The level of activity from which the decay process commences at the start of expiration is set by the accumulated negative feedback from the previous inspiration, both central and vagal in origin. Inflations or vagal stimulation during expiration produce a fixed increase in the inhibitory process which then resumes its decay without a change of time constant. This results in a prolongation of expiration. Changes in gain of the reflex (due to  $\text{CO}_2$  or PRG lesions) may be accomplished either by a change in the rate of decay or threshold level.

Feldman and Cohen (79) found that expiratory neurons which commenced firing late in expiration responded to maintained expiratory inflation with a decreased rate of augmentation of activity. These neurons possibly could have been laryngeal and pharyngeal expiratory motoneurons. This is consistent with the observation of Bianchi and Barillot (31) that the firing rate of expiratory laryngeal motoneurons were depressed by maintained lung inflation.

Expiratory bulbospinal neurons located in the caudal NRA are facilitated by lung inflation, their discharge commences earlier and continues throughout the lengthened expiratory phase. The peak level of discharge increased 40-80% greater than control values (31). Peak firing rate, burst duration and number of spikes per burst were all increased in caudal NRA expiratory neurons with graded expiratory resistive loads (7). These results indicate that PSRs influence expiratory cell discharge in the NRA. Since PSRs project to the ventrolateral NTS, this effect is presumed to be mediated by NTS propriobulbar cells which project to the caudal NRA (132).

### C. Efferent outflows of the CPG

#### I. Upper airway musculature

The upper airway constitutes a major portion of total resistance to airflow and of that, nasal resistance contributes a greater portion than that of the larynx and pharynx. However, laryngeal and pharyngeal resistances are the most variable parts of that resistance (128).

The laryngeal musculature activity varies with the respiratory cycle. Two primary muscles are involved in changing glottal dimensions, the posterior cricoarytenoid (PCA) and the thyroarytenoid (TA). Activation of the PCA results in glottal abduction or tensing of the vocal cords which widens the glottal aperture. Activation of the TA results in glottal adduction which narrows the airway. The PCA and TA muscles are innervated by the recurrent laryngeal branch of the vagus nerve whose fibers originate in the ipsilateral NA (88,145).

The recurrent laryngeal (RL) nerve is activated during inspiration and its discharge characteristically begins before that of the phrenic nerve (56). This is reflected in the activity of the PCA (15,171). In eupnea the PCA is

physically active during inspiration, resulting in vocal cord abduction and a decrease in laryngeal resistance. During expiration PCA activity wanes, resulting in vocal cord adduction and a corresponding increase in laryngeal resistance (10,15,90). Similar changes in glottal dimensions during eupneic breathing in humans have recently been observed (13,72).

The increase in laryngeal resistance during expiration, which results in a retardation of expiratory airflow, at first seems counterproductive. However, this decline in PCA activity acts with the post-inspiratory discharge in the diaphragm to cause "expiratory braking" which allows expiratory airflow to proceed at a controlled rate (15,90,154). Expiratory activity in the TA, the laryngeal adductor, is a variably observed phenomenon (15,171). However, in newborn animals the TA may play an important role in the braking of expiratory airflow as diaphragm post-inspiratory activity is not present (128).

Activity of the musculature regulating upper airway resistance as well as that of the muscles governing lung volume changes is altered by PSR feedback. Withholding inflation results in an augmentation of RL nerve discharge (56) and PCA activity (181). Occlusion of the airway at end-inspiration resulted in the classical prolongation of the expiratory phase accompanied by phrenic nerve silence. This is in contrast to the response of the laryngeal nerve which showed an increase in tonic discharge during the prolonged expiratory phase (56). Lung inflation during expiration also resulted in an increase in the tonic activity of the PCA (15,171) and inspiratory laryngeal motoneuron discharge (9) during expiration. Resistive loads applied during expiration resulted in significant decreases in laryngeal aperture in three of four subjects studied which is consistent with an

increase in PCA activity (65). These authors concluded that increased laryngeal resistance during expiration would result in a higher lung volume at the time in the cycle when expiratory muscles would be activated. They hypothesized that this would leave the expiratory muscles at a longer length and, thus, at a more advantageous position on their length-tension curve resulting in a greater tension development to overcome the imposed load. In conclusion, lung volume feedback inhibits phasic PCA activity during inspiration but increases tonic activity during expiration.

Chemoreceptor afferents also modify the activity of the upper airway musculature. Hypercapnic and hypoxic stimuli produce decreases in both inspiratory and expiratory laryngeal resistance (10,11,15,90). These changes are due to an increase in inspiratory PCA activity and the appearance of PCA activity in the first portion of expiration (10,11,15). In some instances, activation of TA in response to hypercapnia has been observed (171). Corresponding changes in glottal dimensions have been observed in humans. Hypercapnia resulted in a decrease in the narrowing of the glottal aperture that normally occurred during expiration (71). These changes in PCA activity are brought about by corresponding increases in both the tonic and phasic components of RL nerve activity with hypoxic and hypercapnic stimuli (186).

The response of PCA activity to chemoreceptor activation may be modified by PSR due to the corresponding increases in tidal volume. This was investigated by observing PCA activity in response to hypercapnia and hypoxia before and after cutting of the vagus nerves below the origin of the RL nerve. Following vagotomy the response to hypoxia was altered such that PCA activity during expiration was abolished and thus expiratory laryngeal resistance was increased (11). This effect was also produced by

NaCN injection and was abolished by carotid sinus nerve section, indicating that pulmonary afferents normally inhibit the peripheral chemoreceptor effect on PCA activity. Another study in rabbits (14) determined that PSR were responsible for the activation of PCA in expiration in response to hypoxia. Sulfur dioxide inhalation, which selectively blocks PSRs in rabbits, resulted in ablation of the PCA response to hypoxia and hypercapnia. The conclusion of these two studies was that PSR and peripheral chemoreceptor stimulation affected VRG laryngeal motoneurons differently.

Activity of laryngeal musculature is also altered, as indicated by an increase in glottal aperture, in response to exercise-induced hyperpnea (71) and voluntary hyperventilation (13) in humans. These results demonstrate that a variety of inputs to the respiratory system are able to modulate upper airway resistance.

Laryngeal resistance is altered during sleep such that the transition from the awake state to slow wave sleep is accompanied by an increase in laryngeal resistance in cats (144). Laryngeal resistance increases even further during REM sleep. The increase in resistance results from a decrease in PCA activity (143) which is correlated with a decrease in VRG neuronal activity (142). This could potentially result in an occlusion of the airway during sleep. Determination of the postmortem laryngeal closing pressure has ruled out the larynx as the initial site of upper airway collapse in humans. The upper airway collapsed at pressures when the larynx was patent as revealed by endoscopic visualization (unpublished, cited in 128).

## 2. Expiratory musculature

The flow of air from the lungs during expiration is generally accepted as a passive event, with the energy necessary for the frictional work of expiration recovered from the elastic recoil of the lung and chest wall. Expiration can become an active event in situations of increased pulmonary ventilation (47,170,179), exercise (68) and elevations in end-expiratory airway pressure (35).

The internal intercostal muscles and the muscles of the anterior and lateral walls of the abdomen participate in active expiratory efforts. Expiratory muscles of the abdomen include the external and internal obliques, the rectus abdominis and the transversus abdominis as revealed by electromyographic (EMG) recordings in man (45) and dog (92).

Activity in these muscles is usually absent in the resting supine position (35,45,92) thus the conclusion was drawn that expiration is a passive event. Abdominal expiratory muscle activation is seen in man when ventilation is increased by asphyxia (45,47). However, ventilation rates of 50-160 L/min could be obtained without activation of expiratory muscles. Addition of expiratory loads (positive end-expiratory pressure) of 10 cm H<sub>2</sub>O were necessary to evoke expiratory muscle activation in all subjects (46). The depth of the following inspiration was increased in response to the load. Thus, the conclusion was drawn that, in man, expiratory loads were overcome by the greater elastic recoil pressures developed as a result of an increase in the depth of inspiration and not an increase in abdominal muscle activity (48). This concept has been challenged by the observation that in the upright position, forced expiratory maneuvers result in a decrease in abdominal volume due to activation of abdominal expiratory muscles (170).

Activation of abdominal muscles during expiration in anesthetized dogs on positive pressure ventilation was indirectly indicated by a decrease in abdominal circumference (39,94). Recordings of the EMG of the external oblique muscle in cats exposed to continuous positive airway pressure (CPAP) and positive end-expiratory pressure (PEEP) revealed that activation of expiratory muscles occurred in response to both stimuli. The mean EMG activity increase was dependent upon the amount of pressure applied, regardless of whether CPAP or PEEP was used. This indicated that the abdominal muscle activity was only dependent upon the pressure opposing expiration (37). The pattern of abdominal muscle activity changes with increasing loads. Progressive decreases of the latency of onset of the muscle activity after the start of expiration and increases in the rate of rise of activity were observed when higher expiratory loads were imposed (116).

Abdominal muscle activity can also be elicited in response to chemical stimuli. The peak integrated activity of the external oblique muscle EMG increased in response to hypoxia and hypercapnia in spontaneously breathing, anesthetized dogs. The level of activity could be increased even further by the addition of CPAP (110). However, the increase in activity could be due to changes in proprioceptive inputs due to the larger tidal volumes induced by hypoxia and hypercapnia. To rule out this possibility, the effects of progressive hyperoxic hypercapnia and normocapnic hypoxia on abdominal expiratory nerve activity were recorded in the paralyzed, anesthetized dog when mechanical ventilation was withheld (120). In this study hypercapnia and hypoxia increased the rate of rise, the mean plateau level and the rate of decline of activity of the medial branch of the cranial iliohypogastric nerve. These results indicate that chemoreceptor stimulation also modulates

the activity of the abdominal expiratory muscles.

Vagal afferents mediate the activation of abdominal muscles in response to expiratory loads. Involvement of vagal afferents was suggested by early observations that the decrease in abdominal circumference seen in response to expiratory loading was abolished by vagotomy (39,94). Cervical vagotomy abolished the appearance of external oblique EMG in response to loading of expiration (36,38). In a study designed to localize the afferents responsible for the activation of the external oblique, cutting of the vagus nerves in the abdominal cavity, close to the diaphragm did not abolish the response. A local anesthetic (Metycaine) was used to differentially block the vagus. It was observed that the abdominal muscle response to CPAP could be eliminated without affecting the inhibition of diaphragm activity that normally occurred. It was concluded from these two observations that receptors in the thorax were involved in the activation of abdominal muscles but that these receptors were not necessarily the PSRs which mediated the inhibition of the diaphragm (36). A transient activation of expiratory muscles was observed in response to a sudden opening of a tracheostomy and a consequent reduction in upper airway resistance in the cat. This response was not abolished by vagotomy. Thus, it was concluded that extrapulmonary afferents may mediate this response (154).

The increase in inspired volume in response to expiratory loading results in a greater elastic recoil pressure to overcome the expiratory load (48). Activation of abdominal muscles in response to expiratory loading decreases thoracic volume at end-expiration and forces the diaphragm higher in the thorax. These changes result in a greater resting length of the muscles of the rib cage (170) and an increase in the resting length of the

diaphragm and a decrease in its radius of curvature (67). The net effect is to increase the mechanical efficiency of the inspiratory muscles. Thus, abdominal muscle activity in response to mechanical loads may act not only to expel air from the lung but also to set inspiratory muscles at the proper length to achieve adequate ventilation in the presence of an imposed load at the lowest possible energy cost.

The external intercostal muscle fibers slope obliquely downward and forward from the upper rib to the one below. The fibers are oriented such that contraction leads to raising of the ribs and expansion of the thorax. The internal intercostal muscle fibers slope obliquely downward and backward, thus contraction leads to lowering of the ribs and a decrease in the volume of the thorax.

During quiet breathing in man, rhythmic inspiratory activity is only seen in the parasternal portion of the internal intercostals. In the lower four spaces, the internal intercostal muscles are phasically active during expiration. With active respiratory effort (voluntary or in response to carbon dioxide), phasic inspiratory activity appears in the external intercostals while expiratory related activity is present in the internal intercostals (179). In the cat such a clear distinction between internal and external intercostal activation with respiratory phase was not observed (119). Only in the intermediate thoracic region (5th through 9th ribs) was the inspiratory-external, expiratory-internal relationship present. In the cephalic spaces both muscle layers were active during inspiration and in the caudal spaces both were active during expiration. Stimulation of the external intercostal nerve resulted in antidromic activation of thoracic motoneurons which showed rhythmic depolarizations of membrane potential during

inspiration. Motoneurons which depolarized during expiration could be antidromically activated by internal intercostal nerve stimulation (169). These results indicate, that in the cat, the external intercostal muscles are inspiratory and the internals, active in expiration.

The internal intercostal muscle activity in expiration is influenced by mechanical loading. Elevation of PEEP in the cat is associated with an progressive increase in internal intercostal muscle EMG (68). Chemoreceptor activity also influences the discharge of internal intercostal muscles. Hypercapnia increases the phasic discharge of these muscles while hypocapnia which produces phrenic silence results in a tonic discharge of the internal intercostal muscles (6).

#### D. Periodic Breathing

Periodic breathing can be viewed as a control system instability. A control system is composed of a "plant", the output of which is controlled. The controlled output of the respiratory system "plant" is the supply of oxygen to and the removal of carbon dioxide from the cells of the body. The respiratory muscles which ventilate the lung, the pulmonary gas exchanger and the tissue gas exchanger constitute the "plant", the output of which is regulated by a controller, the CPG. The output of the "plant" is monitored by the controller via feedback systems including mechanoreceptors (vagal and spinal inputs) and chemoreceptors. These feedback signals are compared with a reference and the controller modifies the activity of the "plant" to correct its output. This constitutes a closed-loop system (96).

Normally, disturbances of the system result in a corrective action of the controller. When the controller over corrects for the disturbance, instability may result. Instability may be defined as a self-sustaining

oscillation in the system output. Periodic breathing, in which a self-sustaining oscillation in respiratory output is present, may thus be defined as a control system instability. The factors which can result in an instability of the control system include: an increased controller gain; an increase in feedback delay; and a reduction in system damping or a decrease in the buffer for the feedback signal (95).

#### 1. Types of periodic breathing

Periodic breathing (PB), by definition, includes only those respiratory patterns in which a predictable, self-sustaining oscillation in respiratory output is observed. Two types of PB which fulfill these criteria have been described in the literature. Cheyne-Stokes respiration (CSR), named after the two physicians who separately published observations of it, consists of regularly recurring periods of hyperpnea, alternating with periods of low or absent ventilation (152). Cluster breathing or Biot breathing, also named after the physician who described it, also consists of periods of hyperpnea interspersed with periods of central apnea. The chief difference between the two patterns is that the hyperpnea of CSR shows a gradual crescendo and decrescendo of activity, thus the description of a waxing and waning of ventilation. The ventilatory periods of Biot breathing are characterized by an abrupt onset and end of breathing. Initial observations discriminated between the two patterns by the circumstances in which they were observed: CSR was associated with congestive heart failure and Biot breathing with central nervous system damage (34). Recently, the two types of patterns have been associated with damage at different levels of the neuraxis, with CSR observed with damage to the cerebrum and Biot breathing in cases of pontine tegmentum damage (153).

An increase in circulation time (an increase in feedback delay) promotes periodic breathing as demonstrated by Guyton (97). Blood flow from the common carotid artery in the dog was diverted through a long length of tubing before being redirected into the artery prior to the carotid bifurcation. The increased delay between the lung and chemoreceptors resulted in the appearance of CSR.

An increase in controller gain and reduction of system damping could theoretically result in periodic breathing when oxygen rather than carbon dioxide is acting as the predominant drive for ventilation (52). The reasons for this are the non-linear hyperbolic ventilatory response to hypoxia as opposed to the linear ventilatory  $\text{CO}_2$  response and the relatively small stores for oxygen in the body so that small changes in oxygen balance result in larger changes in  $\text{PO}_2$ .

Periodic breathing occurs in a high percentage of preterm and full-term neonates (86) during sleep. The incidence of periodic breathing decreases over the first few months of life. All measures used indicated that infants classified as near-miss SIDS spent a greater proportion of sleep time in periodic breathing (109). Periodic breathing also is seen in normal adults during acclimatization to altitude during NREM sleep (26,185). The observation that addition of low levels of  $\text{CO}_2$  to the inspired air or restoration of normoxia (26,86) results in the reversal of periodic breathing to eupnea led to the conclusion that the development of CSR in these cases is dependent upon both hypoxia and hypocapnia. The subject's arterial  $\text{PCO}_2$  is reduced to the apneic threshold by hyperventilation in response to the hypoxia and ventilation during sleep oscillates because of the hyperbolic  $\text{PO}_2$  response curve (26).

Induction of sleep is believed to predispose to periodic breathing by virtue of the fact that the ventilatory response to  $\text{PCO}_2$  shows a modest decrease in slope and a shift of the response line to the right by about 6 torr (146) in NREM sleep. Thus, hypoxia would become a more prominent factor governing ventilation. At altitude, hypoxia, coupled with the hyperbolic ventilatory hypoxic response curve further predisposes to periodic breathing. Khoo and co-workers described a model which defined respiratory pattern stability in a variety of conditions. In this model, increased controller gain and decreased system damping resulted in controller instability and a sustained periodicity in breathing (111). This was tested experimentally by Cherniack and co-workers (50) in a cat ventilated with a servo-respirator which is controlled by the phrenic nerve activity so that tracheal pressure is held closely proportional to the moving average of the nerve activity. Increasing servo-respirator gain (greater  $V_T$  for a given level of phrenic activity) and ventilation with hypoxic gas mixtures induced CSR in all cats. These results indicate that periodic breathing can be considered as a control system instability resulting from increase controller gain, prolongation of feedback delay or decreased system damping.

## 2. Types of apnea

A key feature in both CSR and Biot breathing is the period of apnea or an abnormally prolonged expiration. The prolonged phase is the  $E_2$  phase, that when no airflow is occurring. Typically two types of apnea are distinguished: central and obstructive. Central apnea is a failure of rhythmogenesis, the airway is patent but there is no inspiratory effort. Obstructive apnea results when inspiratory effort is present but the airway is closed and therefore no airflow can occur. Prolonged expiratory apnea, a

third type of apnea recently observed in infants, consists of a prolonged active expiratory effort against a closed or partially closed glottis (173). The authors suggest that this type of apnea occurs because of a paradoxical increase in PSR stimulation with a decrease in lung volume due to instability of the alveoli.

The development of obstructive apnea is dependent upon the balance of negative pressure developed within the airway by the inspiratory muscles and the activity of muscles which maintain the patency of the airway (155). A number of theories, supported by a vast amount of literature, have been proposed to account for the development of obstructive apnea. These theories contend that a combination of factors contribute to the development of obstructive apnea. These factors include: a mechanically narrow upper airway, an excessive loss of tone in the airway dilator muscles during sleep, an instability of respiratory control causing oscillations and mismatching between diaphragm activity and upper airway dilator muscles, and an abnormal reflex/motor response causing active upper airway muscle constriction (176).

Central apnea is observed in a variety of situations. Damage to portions of the CPG can result in central apnea. The original observation of Biot breathing with its associated periods of central apnea was in a young patient with tuberculous meningitis (34). Biot breathing has also been observed in patients with damage to the tegmentum of the pons (153). A specific example of this was the Biot breathing observed in a patient with infarction of the pontine base and tegmentum below the level of the inferior colliculus (151).

These repeating cycles of central apnea are also observed in the anesthetized cat in which bilateral lesions have been placed in the NPBM (184).

Alterations in peripheral feedbacks can also result in central apnea. Removal of central chemoreceptor input by removal of the carbon dioxide load resulted in central apnea in sheep (147). Likewise, the addition of carbon dioxide to the inspired air obliterated the periods of central apnea that occurred during NREM sleep in subjects at simulated altitude (26). Similarly, removal of central chemoreceptor inputs by cooling of the intermediate area on the ventral surface of the medulla results in apnea (51,136).

Changes in mechanical afferent feedback from the airways can also give rise to central apnea. As mentioned previously, increases in pulmonary stretch receptor discharge by lung inflation or electrical stimulation of the vagi can result in apnea. Central apnea can also be elicited by stimulation of the superior laryngeal nerve (118). Superior laryngeal nerve (SLN) stimulation results in EPSPs in post-inspiratory neurons in the VRG (128). Thus the central apnea produced by SLN stimulation is due to a prolongation of the mechanical phase of expiration ( $E_1$ ).

The duration of central apnea is thus dependent upon the interaction of chemical and mechanical afferent feedback (190). Increased PSR feedback prolongs apnea while the concomitant rise in  $CO_2$  and fall in  $O_2$  facilitate the onset of the next inspiratory burst.

## CHAPTER III

### SPECIFIC AIMS

The purpose of this study was to characterize the periodic pattern, Biot breathing, with respect to each of the three components of the respiratory control system: the central pattern generator, the efferent outflows and the afferent feedbacks.

In eupnea, expiratory duration is modulated by chemoreceptor and mechanoreceptor feedback (190). The duration of apnea in Biot breathing is altered by chemoreceptor feedback (184). The first group of experiments was designed to determine whether mechanoreceptor feedback alters the duration of expiration (either within or between clusters) in Biot breathing. Positive end-expiratory pressure (PEEP) was used to increase lung volume feedback in eupnea and after induction of Biot breathing.

Phasic inspiratory activity of the recurrent laryngeal nerve is present in eupnea (56). Expiratory abdominal muscle activity is usually absent but can be recruited by expiratory loading (35). The second group of experiments was designed to determine if inspiratory activity in the recurrent laryngeal nerve is maintained and whether abdominal nerve activity is absent in Biot breathing. Expiratory loading with PEEP was performed to determine whether abdominal nerve activity could be recruited in Biot breathing.

Inspiratory and expiratory cell discharges can be recorded in the ventral respiratory group in eupnea (130). In the third group of experiments the discharge patterns of medullary respiratory cells were recorded to determine whether the apneic phase of Biot breathing is characterized by phasic inspiratory or expiratory cell activity. Alteration of the Biot pattern by PEEP was performed to determine whether expiratory cell activity was increased by expiratory loading.

## CHAPTER IV

### METHODS

#### A. Surgical procedures

For all three groups of experiments, adult mongrel cats of either sex were initially anesthetized with halothane (Fluothane, Ayerst Laboratories). The cat was restrained in a wooden box from which only the head protruded and the halothane administered by a face mask connected to a Drager-Markovet anesthesia machine. A mixture of halothane (greater than 4%, in oxygen as the carrier gas) was delivered at a flow rate of 7 L/min. Anesthetization was complete within 5-10 minutes. The cat was then removed from the box and tethered in the supine position on a surgical table. A rectal thermistor probe was inserted and rectal temperature monitored by a Yellow-Springs Instruments Telethermometer (Model 43TD). Rectal temperature was maintained at 36-38 °C by a lamp and a pad through which warm water circulated (Gorman-Rupp Industries, Model K-1-3).

A midline incision was made from the caudal border of the larynx and extended distally 3-4 cm. The trachea was exposed by blunt dissection of the sternohyoideus and sternomastoideus muscles. A transverse incision was made between two cartilaginous rings and a plastic tubing connector (1/4" diameter, Pharmaseal) was tied into the tracheal lumen with umbilical tape ligatures. At this point the anesthesia system was connected directly to the trachea and a closed, rebreathing system established. The halothane concentration was decreased (2-3%) and the carbon dioxide absorbed from

the exhaled air by a CO<sub>2</sub> absorbent (Sodasorb, W.R. Grace & Co.). An anesthesia bag from which the cat breathed was refilled with the halothane-oxygen mixture as needed.

Incisions were made bilaterally in the region of the femoral triangle and the right femoral artery and both femoral veins dissected free of the surrounding fascia. The artery and veins were cannulated with saline-filled PE-90 and PE-100 tubing and advanced into the descending aorta and vena cava, respectively. The arterial cannula was connected to a fluid-filled pressure transducer (Gould-Statham, P23Db) and arterial pressure recorded on a Grass Polygraph (Model 7). At this time the level of halothane was again adjusted to ensure a mean arterial pressure of at least 80 mm Hg while maintaining adequate depth of anesthesia.

A midline incision was made in the neck in the region of the transverse vein. The external carotid arteries were isolated just rostral to the crossing of the hypoglossal nerve and ligated with suture silk. This procedure decreased the flow of blood to the Circle of Willis thus facilitating hemostasis following the decerebration procedure. The internal carotid arteries in the cat are degenerate and therefore it was not necessary to ligate them as well.

The cat was then turned to the prone position. The head was fixed in a stereotaxic frame (Trent Wells) and midline incisions made over the top of the skull and midthoracic vertebrae. Bilateral incisions were made over the iliac crests. The temporalis muscle was then scraped away to expose the parietal bones of the skull bilaterally. The T<sub>6</sub> vertebra and iliac crests were cleared of muscle layers for the attachment of spinal clamps.

Before beginning the decerebration procedure, the stereotaxic frame was lowered so that the head of the cat was approximately level with the heart. This procedure was found to be necessary to limit the flow of air into the venous sinuses. This could result in the formation of an air embolus to which cats are very sensitive. The left parietal bone was cut using a trephine which produced a hole approximately 1.5 cm in diameter. The placement of the hole was carefully chosen to avoid piercing the superior sagittal sinus. Bone wax (Lukens) was used to seal the cut edges of the bone. The underlying dura was then cut and the parietal cortex exposed. A suction line was connected to a vacuum source capable of developing approximately 25 cm H<sub>2</sub>O negative pressure, and the cortex removed until the colliculi were visualized. A blunt spatula was inserted from the dorsal surface between the superior and inferior colliculi. Using the tentorium as a guide, the spatula was drawn down to the floor of the skull at an approximately 45° angle. The remaining cortex, diencephalon and mesencephalon rostral to the spatula were then removed. The basilar artery was clamped with a MacKenzie brain clip and the area of the Circle of Willis filled with a ball of Surgicel (oxidized regenerated cellulose). A sheet of Surgicel was placed over the cut surface of the brainstem. Following the decerebration, the cat was monitored to ensure hemostasis and the continuation of a normal respiratory pattern. The head was raised after bleeding had stopped, and the halothane continued for approximately 10 minutes at a very low level (less than 1%) and then removed. A stabilization period of approximately 30 minutes was allowed before moving the cat to another stereotaxic frame located in a large Faraday cage in the adjacent room.

The head was repositioned in a stereotaxic frame (David Kopf Instruments) and the body supported by clamps from the T<sub>6</sub> vertebra and iliac crests. This was done to minimize movement artifacts resulting from respiration. The tracheal cannula was connected to a y-tubing connector which had two side ports attached at right angles. One was connected to an air-filled pressure transducer (Gould-Statham P23Db) for the measurement of tracheal pressure. The second port was used to withdraw air for continuous measurement of CO<sub>2</sub> and O<sub>2</sub> by LB-2 and OM-11 analyzers, respectively (Beckman).

The cat was then paralyzed with an injection of gallamine triethiodide (Flaxedil, Davis-Geck) of 4 mg/kg. Gallamine triethiodide competitively blocks acetylcholine receptors at the myoneural junction. It also has a vagolytic effect such that heart rate increased from 157<sub>+7</sub> to 213<sub>+6</sub> beats per minute. An infusion of gallamine triethiodide (4 mg/kg/hr) was begun (Harvard Infusion Pump, Model 940) via the left femoral vein. Artificial ventilation was begun with a custom-made respirator which inflated the cat by generating a positive pressure in the inspiratory air line and allowing passive emptying of the lungs during expiration through a separate line. Initially, the respirator was triggered by a square wave pulse 5 volts in amplitude from an interval generator and pulse module (WP instruments, Model 830, 831) set to yield an inspiratory duration of 1.0 sec and expiratory duration of 1.5 sec for a frequency of 24/min. Tidal volume was adjusted by altering the inlet pressure until an end-tidal CO<sub>2</sub> of 4% was achieved. The peak tracheal pressure recorded during this ventilation procedure was between 6 and 8 cm H<sub>2</sub>O.

Following this, the left phrenic C<sub>5</sub> nerve rootlet was isolated via a dorsal approach. The nerve was cut distally, and the central end desheathed by carefully removing the epineureum. The nerve was then placed across a bipolar platinum electrode. In the second group of cats, the left recurrent laryngeal nerve was isolated along the dorsal aspect of the trachea, and the left cranial iliohypogastric nerve (L<sub>1</sub>) was located via a dorsal approach approximately 3-4 cm distal to its emergence from the vertebral canal. These nerves were also cut distally, the central end desheathed and laid across bipolar platinum electrodes. All nerves were immersed in pools of warm (37 °C) mineral oil in order to prevent drying.

The dorsal surface of the medulla was exposed for single cell recordings in the third group of cats. A midline incision was made through the skin, and the muscle layers overlaying the skull and first cervical vertebra were carefully separated by blunt dissection. Bleeding from the muscle layers and skin was controlled by careful use of a cautery. Retractors were inserted to widen the exposure and an occipital craniotomy was performed. Cut edges of the bone were sealed with bone wax. After the dura was cut, the exposed brainstem surface was kept moist with warm (37 °C) mineral oil.

Finally, a small hole was made in the right parietal bone for the passage of an electrode for making lesions in the pons (the electrode passed through the hole made for decerebration on the left side). The cut edges of bone were sealed with bone wax. The entire preparation for Groups I and II is shown in Figure 1. Figure 2 outlines the changes in the preparation for Group III experiments.

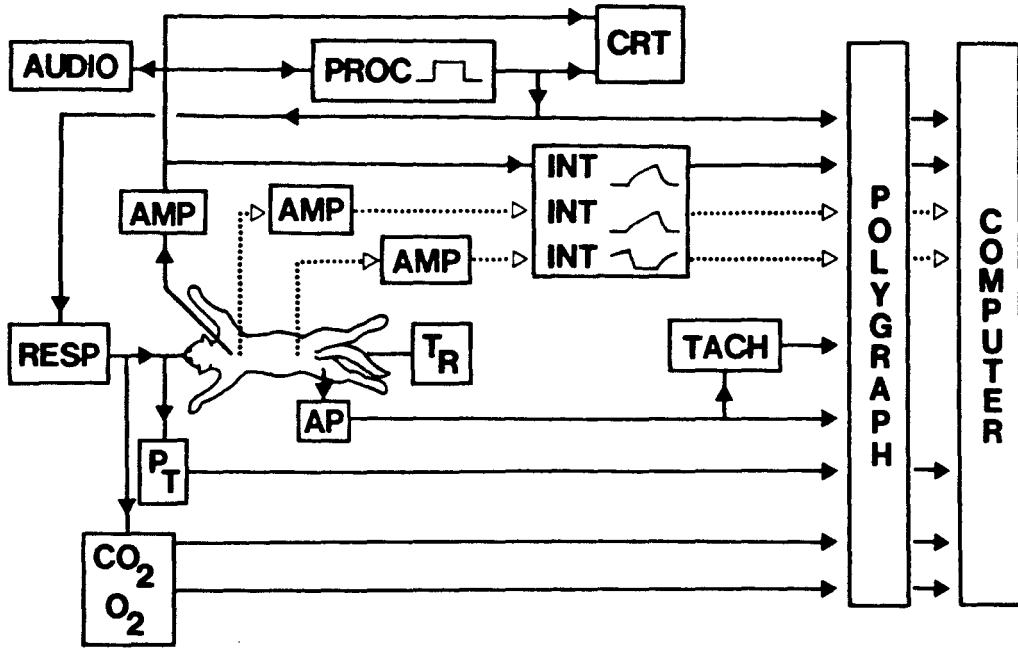
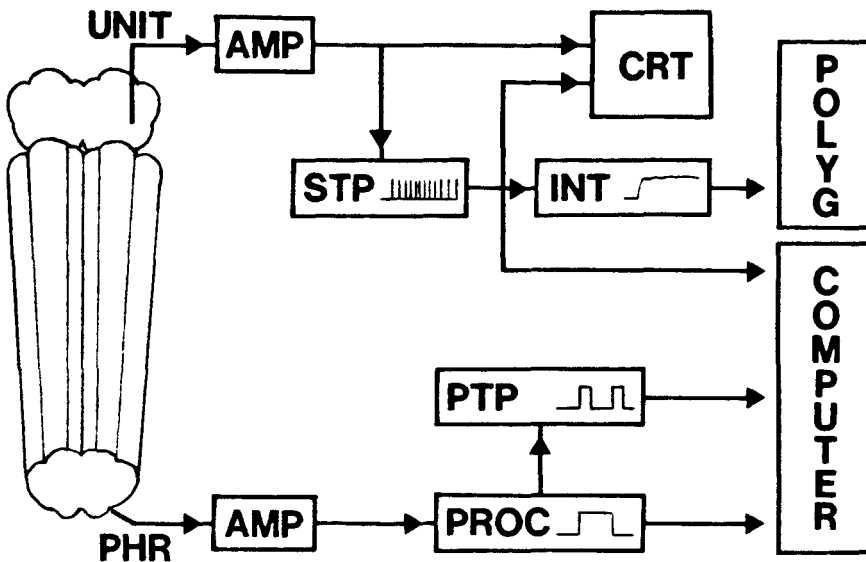
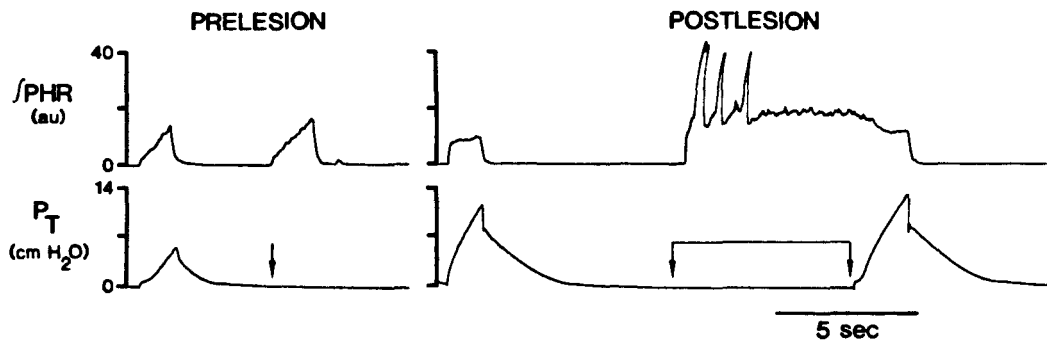


FIGURE 1. Instrumentation of the cat for groups I and II. Rectal temperature ( $T_R$ ) is monitored. Arterial pressure (AP) is displayed on the polygraph and triggers a tachograph (TACH) which quantitates heart rate. The end-tidal  $CO_2$  and  $O_2$  and tracheal pressure ( $P_T$ ) are monitored on the polygraph. Phrenic nerve activity (solid line) is amplified (AMP), rendered audible (AUDIO), processed by a custom-built circuit (PROC), integrated (INT) and displayed on an oscilloscope (CRT). The gating signal is used to drive the respirator. In group II, the dotted lines represent recurrent laryngeal and cranial iliohypogastric nerve activities which are amplified (AMP) and integrated (INT). Computer inputs for group I are I/E gate, phrenic nerve activity,  $P_T$ ,  $CO_2$  and  $O_2$ . For group II, the inputs are I/E gate, three integrated nerve activities,  $P_T$ ,  $CO_2$  and  $O_2$ .



**FIGURE 2.** Signals recorded in group III. Extracellular recordings of brainstem units (UNIT) are amplified (AMP), passed through a level detector which generates spike-triggered pulses (STP) and displayed on an oscilloscope (CRT). The STP are integrated, displayed on a polygraph (POLYG) and the CRT. Phrenic nerve activity (PHR) is amplified (AMP), processed by a custom-built circuit (PROC) to yield phrenic-triggered pulses (PTP). Computer inputs are spike-triggered pulses, phrenic-triggered pulses and the gating signal.

Following the recording of all measurements to be made during eupneic breathing, bilateral lesions of the pontine respiratory group (PRG) were made in all cats. A monopolar electrode (22 gauge, Radionics, Inc.) was inserted at an angle  $32^{\circ}$  from vertical through the holes previously cut in the parietal bone. The electrode was advanced into the PRG using stereotaxic coordinates of posterior = 3.5 mm, lateral = 4.5 mm, height = -4.0 mm (25). Current was passed through the electrode from a radiofrequency generator (Radionics, Inc.). A tip temperature of  $70^{\circ}\text{C}$  was maintained for 60 seconds. Lesion placement was evaluated physiologically, immediately after lesions were placed, by two criteria. The first was the alteration in phrenic nerve discharge that occurs with destruction of the PRG; that of increased duration and amplitude of activity. The development of apneusis when inflation was withheld for one cycle was the second criterion used to qualitatively identify an adequate lesion (Figure 3, postlesion). In some instances, the first lesion did not adequately destroy the PRG by these two criteria. In these cases, the electrode was inserted again with the angle altered to  $33^{\circ}$  and advanced 0.5 mm deeper into the pons and the lesion process was repeated. Following successful lesion placement, the inlet pressure on the respirator was increased slightly to ensure that the tracheal pressure did not limit during the prolonged inspirations. After lesion, peak tracheal pressure ranged from 8-14 cm  $\text{H}_2\text{O}$ . Periodic breathing of the cluster type (Figure 4) resulted in approximately 50% of the cats in which lesion placement was successful, as evaluated by the criteria given above.



**FIGURE 3.** Example of the no inflation test in eupnea (prelesion) and in Biot breathing (postlesion). Integrated phrenic nerve activity (PHR) and tracheal pressure ( $P_T$ ) are plotted. Arrows mark when the cycle-triggered respirator was turned off. In eupnea, PHR activity terminates even when inflation was withheld. In Biot breathing, the respirator must be turned on (second arrow) in order to terminate the apneustic breath.

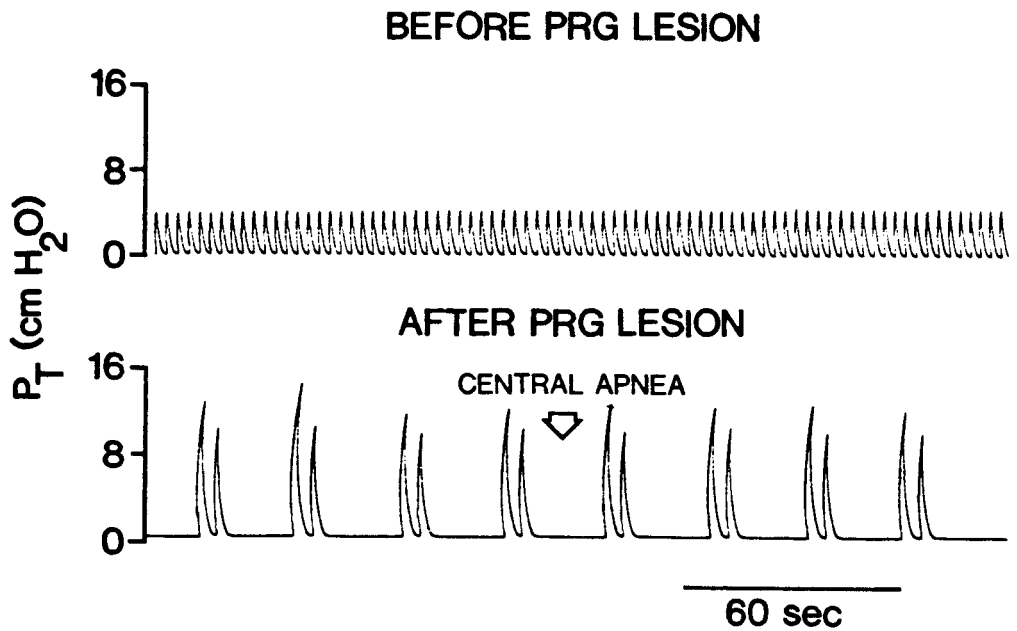


**FIGURE 4.** Example of one criterion used to assess completeness of pontine respiratory group (PRG) lesions. Tracheal pressure ( $P_T$ ) is plotted before and after lesions when the cat is ventilated by the cycle-triggered respirator. Note the increased duration and depth of inspiration following PRG lesions.

Following data collection in Biot breathing, the brainstem was removed following an overdose of sodium pentobarbital and preserved for at least one week in formalin. Following fixation in formalin, the brainstem was stripped of all meningeal tissue and blood vessels and cut into 100 micron thick slices using a vibratome. Unstained sections were mounted and observed under a microscope. The number of sections in which destruction was observed were counted and multiplied by 0.1 to yield the lesion length in millimeters. The sections representing largest lesion diameters were drawn using a camera lucida attachment.

#### B. Methods of data acquisition

As shown in Figures 1 and 2, arterial pressure and tracheal pressure were recorded by pressure transducers (Gould-Statham Model P23Db). The outputs of the transducers were calibrated in millimeters of mercury (mm Hg) by an internal calibration signal. The value of the internal calibration signal was verified with a mercury manometer periodically. Arterial pressure was thus measured in units of millimeters of mercury. Tracheal pressure was calibrated in centimeters of water (cm H<sub>2</sub>O) pressure by converting the internal calibration signal, using the relationship 1 mm Hg = 1.36 cm H<sub>2</sub>O. Both tracheal and arterial pressures were recorded on the polygraph in all experiments. The arterial pressure was used to trigger a tachograph preamplifier which allowed the recording of heart rate.

End-tidal percentages of carbon dioxide (CO<sub>2</sub>) and oxygen (O<sub>2</sub>) were measured by Beckman gas analyzers (Model LB-2 and OM-11, respectively). The gas analyzers were calibrated by passing room air (20.9% O<sub>2</sub>, 0.03% CO<sub>2</sub>) and a calibration standard gas (0% O<sub>2</sub>, 5.00% CO<sub>2</sub>) through the pick-up heads prior to each experiment. The readout of the analyzers was given in

wet gas percentages and plotted on the polygraph (Figures 1 and 2). This was converted to partial pressure in mm Hg by multiplying the barometric pressure by the wet gas percentage. The barometric pressure was determined on the day of each experiment from the reading of a barometer in the laboratory and corrected for ambient temperature and latitude.

#### 1. Nerve recordings

All nerve signals were recorded differentially with high impedance preamplifiers in series with Grass amplifiers (Models HIP511GA and P511K, respectively). A common ground electrode was placed in the right temporalis muscle. This yielded an input impedance of  $2 \times 10^{11}$  ohms. Low and high 1/2 amplitude frequency filters were set at 10 and 10K Hz. The gain of the amplifier was adjusted to yield an output signal of approximately 2 volts peak to peak. Integration of the nerve signals was performed by a bank of custom-made Paynter filters with integration time constants of 100 msec for the phrenic and recurrent laryngeal nerves and 200 msec for the cranial iliohypogastric nerve. The integrated activity of each nerve was displayed on the polygraph and quantitated in terms of peak integrated activity in arbitrary units (Figures 1 and 2).

The discharge pattern of the phrenic nerve was processed by a custom-built amplifier circuit. The phrenic signal was first amplified and a half-wave rectification performed which clipped the negative portion of the signal. An inverting amplifier and a non-inverting amplifier then produced two amplified integration signals which had very fast rise times and saturated the amplifiers. These signals were then differentiated and each of the differentiated signals fed into a Schmitt trigger which was adjusted to trigger a square wave signal whenever the signal rose above a certain level.

The output of the two Schmitt triggers marked the onset and the termination of phrenic nerve activity. A final stage of the processor initiated a positive 4 volt signal when the first Schmitt trigger fired and this signal continued until the second trigger occurred. An example of the timing of the inspiratory/expiratory gate in relation to the phrenic nerve discharge is shown in Figure 5. The output of this stage was TTL compatible and was used to trigger the respirator. The inspiratory/expiratory gating signal was further processed by a custom circuit to yield two pulses, 1 msec in duration, occurring coincident with the beginning of inspiration and expiration.

## 2. Artificial ventilation

The respirator used for ventilation in these experiments consisted of separate paths for inspiratory and expiratory airflow. Movement of air to and from the cat was regulated by solenoid valves connected to a solid-state relay. When the relay was triggered by a positive voltage signal, the inspiratory valve was opened and the expiratory valve closed. Air flowed into the lungs from a compressed air source. The pressure to which the lungs were exposed during inspiration could be altered by changing the pressure on the second stage of a gas regulator (Matheson) which was used to step the compressed air pressure down to within a physiological range. A latex glove inserted in series between the inspiratory solenoid valve and the cat served to blunt the abrupt rise in pressure when the valve opened. During a negative voltage signal, the expiratory valve opened and the lungs emptied passively. The respirator could be triggered by a square wave pulse originating from a stimulator (as described previously) or from an inspiratory/expiratory gating pulse derived from the phrenic nerve discharge

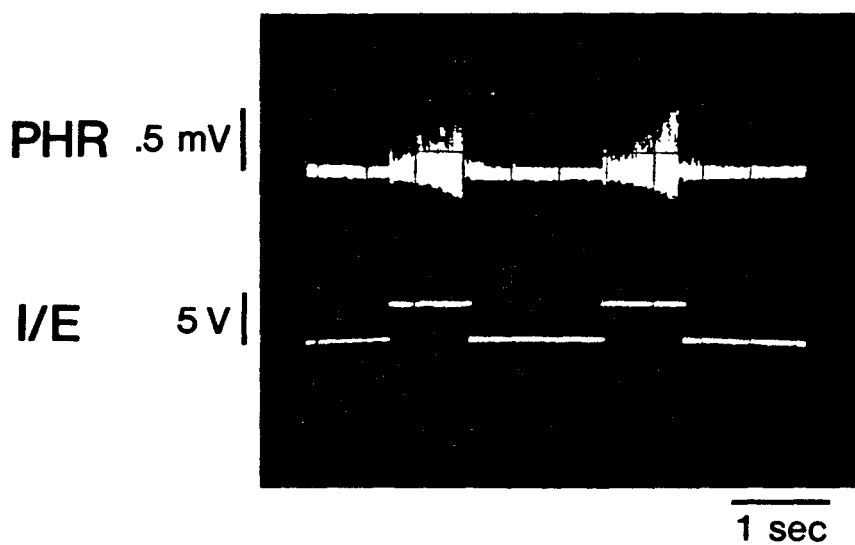
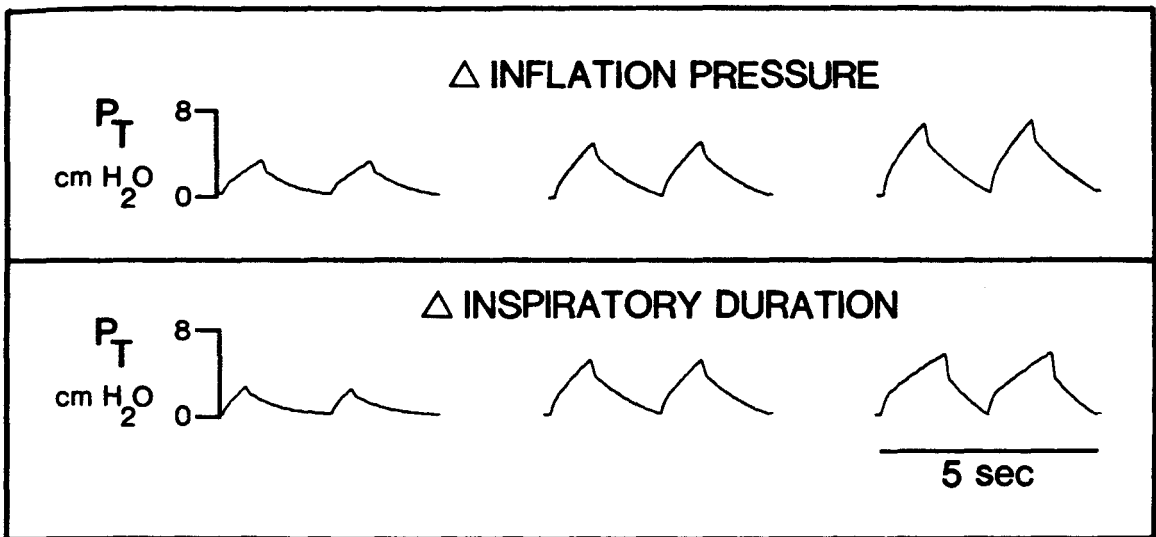


FIGURE 5. Example of oscilloscope tracing showing inspiratory expiratory gating signal (I/E) derived from phrenic nerve (PHR) activity.

(described in the following section). When the latter was the case, the respirator was defined as being cycle-triggered.

Two factors governed the peak tracheal pressure reached during inspiration. As can be seen in Figure 6, increasing the inspiratory flow rate, by increasing the inlet pressure, resulted in an increase in peak tracheal pressure. Likewise, an increase in the duration of inspiration also increased the peak tracheal pressure. The peak tracheal pressure and the total compliance of the feline respiratory system determined the volume of air delivered to the lungs during inspiration. An estimation of tidal volume was calculated by multiplying the peak tracheal pressure by the lung-thorax compliance/kg body weight of the cat. A value of 2.86 ml/cm H<sub>2</sub>O/kg body weight was used which was determined in paralyzed cats inflated from a constant pressure source (2). To determine if the tidal volumes estimated in this manner were physiologically possible, the inspiratory capacity for each animal was calculated from the relationship, inspiratory capacity=69 ml/kg body weight (2).

Several experimental maneuvers could be performed by alterations in respirator function. Positive end-expiratory pressure could be applied by plunging the expiratory air line beneath the surface of water in a beaker. The distance in centimeters that the tube was below the water surface represented the PEEP applied in cm H<sub>2</sub>O. Inflation could be withheld for a single cycle by removing the triggering signal (no inflation test). Withholding inflation in Biot breathing resulted in apneusis. In order to terminate the apneusis, it was necessary to initiate ventilation as shown in Figure 3. The respirator was activated after approximately 8 seconds of apneusis, when the phrenic nerve discharge had reached a plateau.



**FIGURE 6.** Changes in peak tracheal pressure ( $P_T$ ) from progressive increases in inflation pressure and inspiratory duration (from left to right). Note the increases in  $P_T$  as inflation pressure and inspiratory duration increase.

Therefore, in Biot breathing, the no inflation test was used to observe changes in the initial onset of nerve activity and the plateau level reached.

### 3. Extracellular recordings

Single unit activity in the brainstem was recorded extracellularly with Tungsten microelectrodes with impedances of 9-12 megohms measured at 1000 Hz (Frederick Haer). Cell activity was recorded monopolarly; referenced to the common ground electrode placed in the right temporalis muscle, by a Grass amplifier with a high impedance input (identical to those mentioned previously). The low and high 1/2 amplitude frequency filters were set at 100 and 10K Hz. The electrode was held by an electrode carrier (David Kopf Instruments) and could be advanced into the medulla by a hydraulic microdrive which was calibrated in microns. Electrode position was recorded by use of stereotaxic coordinates. The electrode was first placed at the obex, the coordinates recorded, and the location of cells recorded referenced to the obex. Following the experiment, the position of the electrode was reconfirmed by placing the electrode at the obex and again recording the coordinates. When single cells were recorded the discharge was passed through a custom built level detector which generated a 5 volt pulse of 1 msec duration whenever the activity crossed an adjustable voltage level (Figure 7) . An index of cell activity in relation to the respiratory cycle was generated by passing the pulses from the level detector through a Paynter filter and integrating the activity with a time constant of 200 milliseconds. This activity was displayed on the polygraph and was calibrated following the experiment by passing 1 millisecond pulses at known frequencies (0-200 Hz) through the Paynter filter to the polygraph (Figure 2).

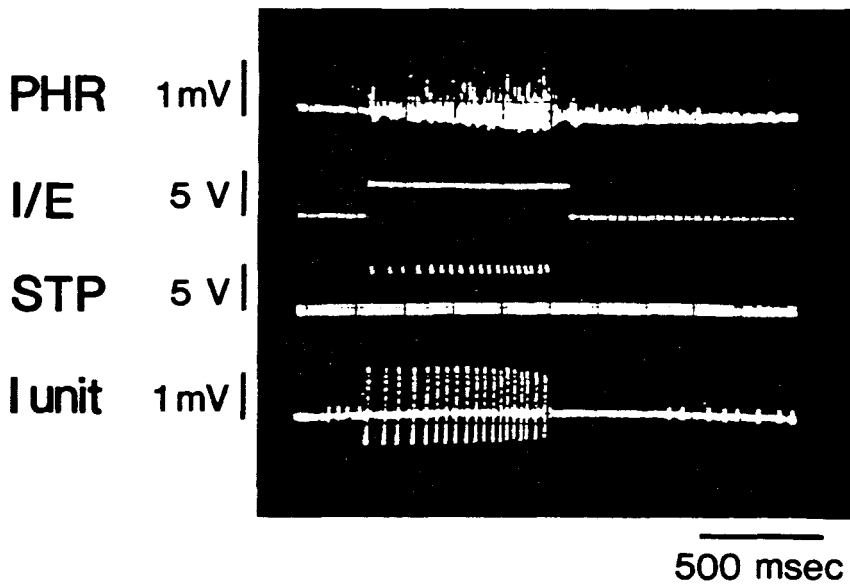


**FIGURE 7.** Example of oscilloscope tracing showing spike-triggered pulses (STP) derived from an inspiratory unit discharge (I unit). Spike-triggered pulses are 1 msec in duration.

Verification that the potentials recorded arose from cell bodies and not from axons was achieved by several methods. The electrode size was considered because lower impedance electrodes selectively record larger cell bodies while increasing the impedance of the electrodes results in a higher probability of recording axons. Cells also generate a greater current, therefore, the spike amplitude and duration are greater than those for axons. The ability to move the electrode for up to 100 microns without losing the spike discharge was another criterion used to determine that a cell body was recorded rather than an axon. Finally, the waveform of the spike was used to differentiate somas from axons, with biphasic spikes originating from somas, while axon spikes were triphasic (121).

Verification that a single cell was recorded was gained by two observations; that of a constant spike amplitude for the duration of activity and an interspike interval of no less than five milliseconds. To determine that cell discharges were indeed respiratory related two criteria were used: a constant spike amplitude throughout a respiratory phase and the retention of respiratory related activity when mechanical inflation was withheld.

#### 4. Recording of variables

As mentioned previously in the text and shown in Figures 1 and 2, the polygraph was used for recording of all integrated nerve activities, the integrated respiratory cell activities, tracheal pressure, end-tidal carbon dioxide and oxygen, heart rate and arterial pressure.

A laboratory-based computer (DEC LSI 11/23) was used for data acquisition as shown in Figures 1 and 2. The operating system used was the VENIX system (VenturCom, Inc., Cambridge, MA), a revision of UNIX (Bell Laboratories) for small machines.

All programming was done in the C language, a compiled language with fast execution speeds, making it highly useful for the collection of analog signals at very fast sample rates. Four major computer programs were utilized for data collection and calculation.

Program event.amp was designed to simultaneously sample and store data from eight analog inputs for groups I and II. The first analog to digital (A to D) channel read in the inspiratory/expiratory gate. This was used as a trigger for storage of the maximum and minimum amplitudes from the other channels as well as to measure inspiratory duration ( $T_i$ ), expiratory duration ( $T_e$ ), total cycle time ( $T_{tot}$ ) and respiratory frequency ( $f$ ). The next 6 A to D channels stored the amplitudes of integrated recurrent laryngeal, phrenic and cranial iliohypogastric nerve activities, tracheal pressure, end-tidal carbon dioxide and oxygen. The last A to D channel was used to initiate and end sampling intervals by the use of a stimulator set to deliver a constant DC input. Each channel of data was sampled every 2 msec (500 Hz) and the voltage on each channel stored. The respiratory gate was used to signal the computer to save the maximum and minimum amplitude (in volts) measured from each channel for every respiratory cycle. The amplitude of each channel was calibrated prior to data acquisition by moving the polygraph pens through full scale deflections of 0-40 relative units for integrated nerve activities and 0-16 cm H<sub>2</sub>O for tracheal pressure. The end-tidal CO<sub>2</sub> and O<sub>2</sub> channels were calibrated in mm Hg by passing room air (20.9% O<sub>2</sub>, 0.03% CO<sub>2</sub>) and a calibration gas mixture (0% O<sub>2</sub>, 5.00% CO<sub>2</sub>) through the gas analyzers.

At the end of the experiment a printout of the maximum and minimum values for each variable during each respiratory cycle sampled could be obtained along with the calibration data for each channel.

Program inttime.3ch sampled three analog channels which had inputs to separate clock boards. The clock board stored the accumulated time on each channel between samples taken by the C program which stored data. All clocks were synchronized by an external clock with a frequency of 100 KHz. Thus each analog channel of data was sampled every 10 microseconds. This program was used in the collection of data in Group III.

The three channels of information sampled were as follows (Figure 7). Idealized pulses, derived from the extracellular potentials of single units in the brainstem, were generated by a custom built level detector. Whenever the voltage from the single unit activity crossed a certain threshold, a five volt pulse, 1 millisecond in duration, was produced. The threshold level was adjustable and could be set so that only the spikes from a single cell resulted in the output of pulses. These idealized pulses were the input for the first clock board. The time between pulses was stored as the interspike interval.

On the second channel the time at which inspiration began was stored as the time at which the inspiratory/expiratory gate showed an increase in voltage (positive slope). The data gathered from this channel were used to reference the discharge of the cells recorded to the beginning of inspiration.

An electronic circuit was used to generate two five volt pulses, 1 millisecond in duration, from the inspiratory/expiratory gate (Figure 7).

These pulses occurred coincident with the beginning of inspiration and expiration, and were stored on the third channel. From these data, the durations of inspiration ( $T_i$ ) and expiration ( $T_e$ ) could be determined. A separate program was used to generate total cycle duration ( $T_{tot}$ ) and frequency ( $f$ ).

Program across was used to generate cycle-triggered histograms of unit activity in relation to the start of inspiration. Cycle-triggered histograms describe the probability of finding a cell spike in a time relationship with the onset of inspiration. Autocorrelograms, the unit activity referenced to itself, could also be constructed from this program. The lead and lag times used were 20 msec with a total of 201 bins. This yielded a resolution of 0.2 msec/bin. The purpose of computing the autocorrelogram was to confirm that data obtained was from a single cell. To do this, the bins on either side of zero, corresponding to 5 msec, were scanned for counts. The absence of any counts within these bins provided further support for the conclusion that data obtained originated from a single cell.

Onset times for each cell were determined. Cycle-triggered histograms were generated with 10 msec bin widths for each cell as referenced to phrenic nerve activity. The number of empty bins from time zero were counted and multiplied by 10 to yield onset time in msec. For expiratory cells, the duration of inspiration was subtracted from this value to yield the onset time in relation to the beginning of expiration.

Burst durations were measured from cycle-triggered histograms with 100 msec bins. The total number of bins over which the cell discharge occurred was multiplied by 100 to yield the burst duration in msec.

The number of spikes per burst was determined by counting the number of interspike intervals stored for the cycle in question and adding 1.

For plotting purposes, the cycle-triggered histograms for inspiratory cells were computed with 0.5 second bin widths, while for expiratory cells, a bin width of 1.0 second was used. A C language program (plotc) was used to plot autocorrelograms and cycle-triggered histograms by a single sheet plotter (Hewlett-Packard Model 7470A).

### C. Experimental groups

Three groups of cats were used for this study. Group I consisted of 11 cats in which the modulation of the respiratory patterns in eupnea and Biot breathing by pulmonary stretch receptors was assessed. Positive end-expiratory pressure (PEEP) was used to increase FRC and thereby, PSR discharge. Three levels of PEEP, 2, 4 and 6 cm H<sub>2</sub>O, were used. Each pressure was applied at least twice in a random sequence. The loading was performed during a single expiratory phase as well as for a series of 10 breaths during eupneic breathing. Following the induction of Biot breathing, the loads were applied for a single phase of central apnea. When possible, the pressures were applied for five clusters of breaths.

Group II consisted of 10 cats in which the activity of the efferent outflows of the respiratory system to upper airway, diaphragm and abdominal muscles were observed in cluster breathing. Recurrent laryngeal, phrenic and cranial iliohypogastric (L<sub>1</sub>) nerves were recorded during eupnea and after induction of Biot breathing. Integrated nerve activities were recorded during control (unloaded) conditions and in response to the addition of PEEP. Three levels of PEEP; 2, 4 and 6 cm H<sub>2</sub>O, were used. Each pressure was applied at least twice in a random sequence. The loading was performed during a

single expiratory phase as well as for a series of 10 breaths during eupneic breathing. Following the induction of cluster breathing, the loads were applied for a single phase of central apnea. When possible, the pressures were applied for five clusters of breaths.

In the 10 cats comprising Group III, extracellular discharges were recorded from medullary inspiratory and expiratory cells after induction of Biot breathing. Stereotaxic coordinates were used to place the electrode within the NRA (Long and Duffin, 1984). When a single respiratory related cell was encountered, the activity of the cell was recorded for at least five clusters. For inspiratory cells the response of the cell when inflation was withheld for the first breath of the cluster was recorded. The resultant apneusis was terminated by turning on the respirator, as described previously. The response of expiratory cells to loading of a single period of central apnea with PEEP of 2, 4 and 6 cm H<sub>2</sub>O was recorded and compared with the immediately preceding period of central apnea.

#### D. Statistical evaluation

All statistical comparisons involved paired data obtained from the same animal. Experiments were designed so that the response of any variable to a given perturbation was compared to the mean value from the five immediately preceding respiratory cycles. Therefore, in each series of experiments, there was a control value for each response. A correlated analysis of variance was used to compute an F-ratio for a given variable and if significant,  $p$  less than 0.05, tests for least significant differences were used to determine which pairs of mean values were significantly ( $p$  less than 0.05) different (191).

Comparisons made between values measured before and after lesion were performed by a paired Student's t-test. Differences were considered statistically significant when  $p$  was less than 0.05.

## CHAPTER V

### RESULTS

#### A. Characteristics of the Biot pattern

When bilateral radio-frequency lesions were made in the pontine respiratory group, Biot type breathing developed in 24 cats. Successful lesion placement was indicated by an increase in tidal volume and a decrease in respiratory frequency. In addition, in all cats, apneusis resulted when inflation was withheld. The 24 cats were divided into 3 groups. Group I consisted of 11 cats, while groups II and III included 10 cats each. Three cats contributed data to both groups I and II, four cats contributed data to both groups I and III.

The transition from eupnea to Biot breathing resulted in remarkable changes in the respiratory and cardiovascular variables recorded as shown in Figure 8. In eupnea, the respiratory pattern was very consistent, with regard to both frequency and volume, as indicated by the integrated phrenic nerve activity. In this example, the respirator was "cycle-triggered" such that inflation was triggered by the phrenic nerve activity. Thus, tracheal pressure ( $P_T$ ) increased during phrenic nerve activity. The tracings of end-tidal  $CO_2$  and  $O_2$  reflect the constancy of ventilation as  $P_A CO_2$  fluctuated closely about a value of 35 mm Hg and  $P_A O_2$  at 115 mm Hg. Heart rate, 225 beats/minute, showed a respiratory-related variation of less than 5 beats/minute. Arterial pressure showed a respiratory fluctuation about a mean pressure of 115 mm Hg.

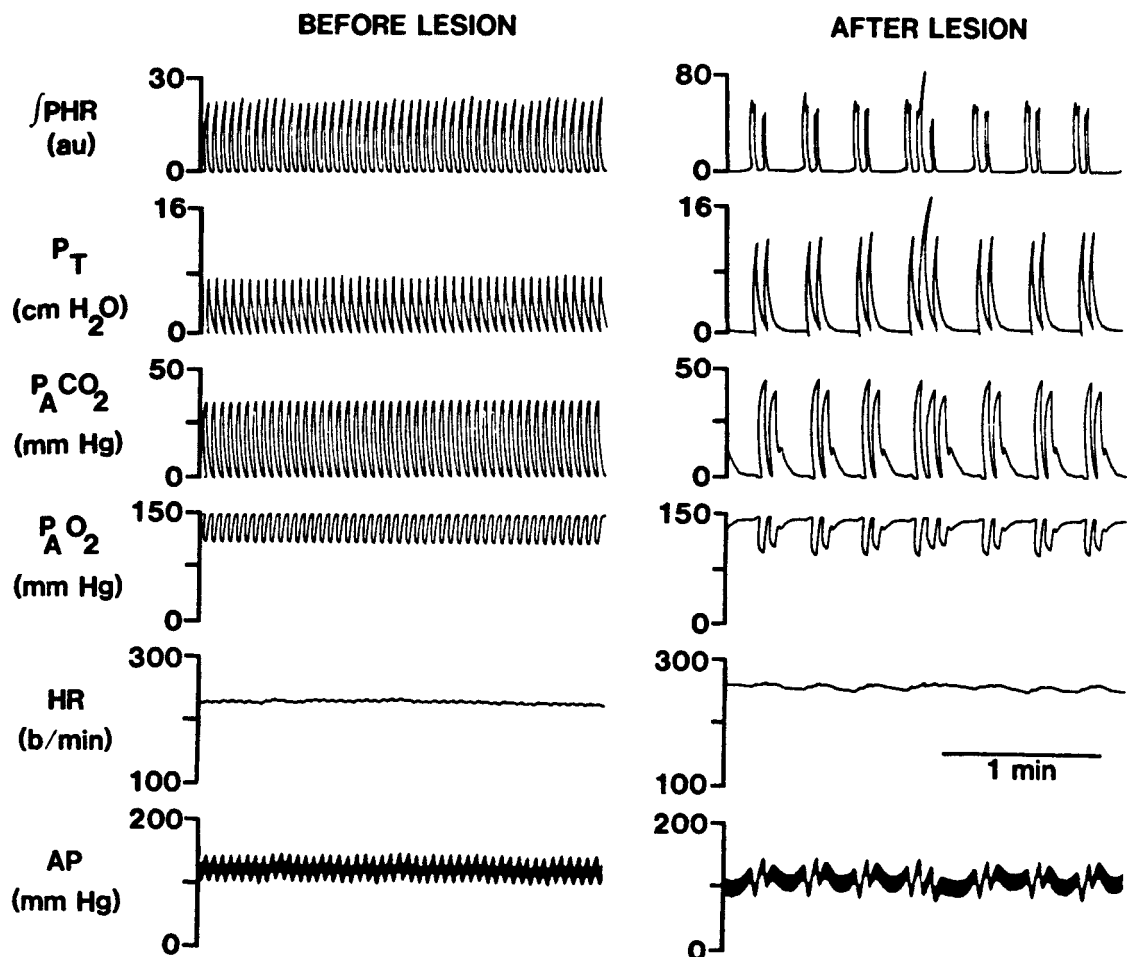


**FIGURE 8.** Example of respiratory pattern before (eupnea) and after (Biot) lesion of the PRG. Variables plotted include: integrated phrenic nerve activity (PHR) in arbitrary units (au), tracheal pressure ( $P_T$ ) in  $\text{cm H}_2\text{O}$ , alveolar carbon dioxide ( $P_{A\text{CO}_2}$ ) and oxygen ( $P_{A\text{O}_2}$ ) partial pressures in mm Hg, heart rate (HR) in beats/minute (b/min), and arterial pressure (AP) in mm Hg. The respirator is triggered from the PHR nerve activity.

Following lesion, Biot breathing, characterized by alternating ventilatory and non-ventilatory periods, developed. This pattern differed from Cheyne-Stokes breathing in that the onset and end of the ventilatory periods were abrupt and distinct rather than the gradual crescendo and decrescendo of respiratory activity seen in Cheyne-Stokes. The period of central apnea, as indicated by the absence of phrenic nerve activity, was equally distinct and predictable in both duration and occurrence. As can be seen from this example, the ventilatory clusters generally consisted of the same number of breaths. Two was the most common number of breaths per cluster, which occurred in 18 of 24 cats. In the remaining cats, 3 breaths occurred per cluster with the exception of 1 cat, in which the pattern alternated between 1 and 2 breaths/cluster. In each case, the number of breaths/cluster in a given cat was consistent from cluster to cluster, thus the onset of central apnea could be predicted.

Following PRG lesions, tidal volume increased as indicated by the increase in peak integrated phrenic nerve activity and tracheal pressure. Despite the increase in tidal volume, Biot breathing represented a hypoventilatory state, as reflected by the rise in  $P_A\text{CO}_2$  and fall in  $P_A\text{O}_2$ . During the non-ventilatory phase (central apnea) arterial oxygen fell and carbon dioxide rose, thus  $P_A\text{CO}_2$  and  $P_A\text{O}_2$  were highest and lowest, respectively, at the onset of each ventilatory cluster.

Heart rate showed a marked respiratory arrhythmia in Biot breathing, as the fluctuations in heart rate were increased to greater than 10 beats/minute about a mean of 255 beats/minute. Arterial pressure also showed an increased respiratory related fluctuation. In this example, mean arterial pressure declined slightly to 108 mm Hg.

The values measured in 18 cats for these variables in eupnea and Biot breathing are given in Table 1. Inspiratory duration was increased significantly in Biot breathing. Two expiratory durations were quantitated,  $T_{e\text{ short}}$  ( $T_{e_s}$ ) represented the duration of expiration in eupnea and the duration of expiration within the cluster in Biot breathing. The period of central apnea in Biot breathing was designated as  $T_{e\text{ long}}$  ( $T_{e_l}$ ) and had no counterpart in eupnea. The increase in  $T_{e_s}$  and the appearance of  $T_{e_l}$  in Biot breathing led to a significant increase in the duration of the respiratory cycle ( $T_{\text{tot}}$ ) and corresponding decrease in frequency. Peak integrated phrenic nerve activity was not statistically increased in Biot breathing as versus eupnea. The depth of respiration was increased significantly as seen by the increased tidal volume ( $V_T$ ). The decrease in minute ventilation in Biot breathing was accompanied by a rise in  $P_{A\text{CO}_2}$  and fall in  $P_{A\text{O}_2}$ . Despite the increased fluctuations in heart rate and arterial pressure, the mean heart rate and arterial pressure were not significantly altered by PRG lesions.

#### B. Group I-Mechanoreceptor effects on Biot breathing

The first study was designed to determine the effects of expiratory loading with positive end-expiratory pressure (PEEP) in eupnea and Biot breathing. Figure 9 shows maps of lesion sites from the 11 cats contributing data to this group. In all cases, lesions were placed in the dorsolateral tegmentum of the pons, in the region of the PRG. Lesions were  $3.2 \pm 0.2$  mm in length and as can be seen from Figure 9, ranged from 2-3 mm in diameter. The Biot patterns which occurred in each cat are also shown.

TABLE 1

Respiratory and cardiovascular variables in eupnea and Biot breathing

<u>Group</u>	<u>T<sub>i</sub> (sec)</u>	<u>T<sub>e<sub>s</sub></sub> (sec)</u>	<u>T<sub>e<sub>1</sub></sub> (sec)</u>	<u>T<sub>tot</sub> (sec)</u>	<u>f (min<sup>-1</sup>)</u>	<u>Peak PHR (au)</u>
Eupnea	1.13±0.04	1.62±0.11	-----	2.75±0.12	22.6±1.0	17±2
Biot	2.36±0.14	3.85±0.23	15.93±1.06	11.86±0.59	6.0±0.3	21±3
p	<0.001	<0.001	-----	<0.001	<0.001	0.200
<u>Group</u>	<u>V<sub>T</sub> (ml)</u>	<u>Ṡ<sub>E</sub> (ml/min)</u>	<u>P<sub>A</sub>CO<sub>2</sub> (mm Hg)</u>	<u>P<sub>A</sub>O<sub>2</sub> (mm Hg)</u>	<u>HR (min<sup>-1</sup>)</u>	<u>MAP (mm Hg)</u>
Eupnea	51±3	1143±81	33±1	114±2	220±7	120±4
Biot	103±6	599±30	48±2	95±2	229±7	121±4
p	<0.001	<0.001	<0.001	<0.001	0.228	0.762

Values expressed as Mean±S.E.M.

p values determined by Student's paired t-test.

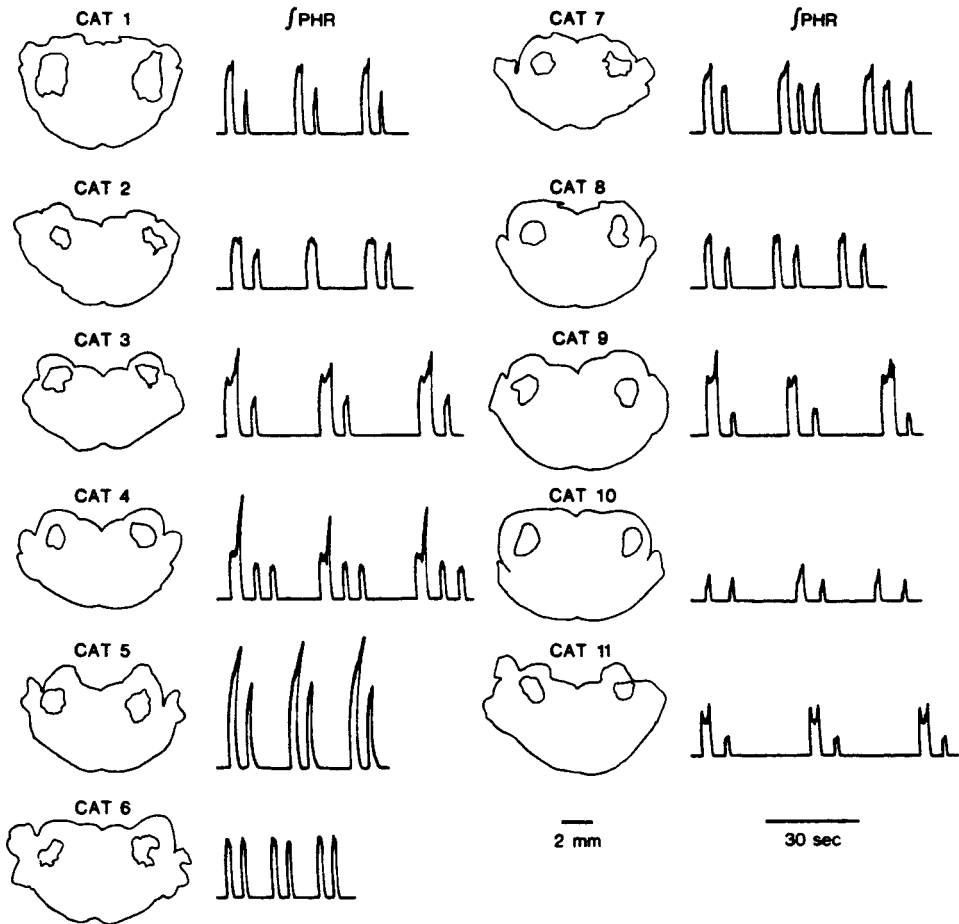


**FIGURE 9.** Tracings of tissue destruction resulting from bilateral radio frequency lesions placed within the PRG in 11 cats. The resultant integrated phrenic nerve activity (PHR) is shown for each cat.

## 1. Multiple breath responses to PEEP

Three levels of PEEP, 2, 4, and 6 cm H<sub>2</sub>O, were applied for 10 breaths in eupnea and for 5 clusters after Biot breathing developed. The effects of 2 cm H<sub>2</sub>O PEEP before lesion are shown for one cat in Figure 10. The record is broken into two panels in order to show the addition and removal of PEEP. At the arrow, PEEP was added as seen by the elevation of tracheal pressure during the expiratory phase. The addition of PEEP resulted in a slight prolongation of the initial expiratory phase. This effect persisted with maintained PEEP. There was, however, no noticeable effect on inspiratory duration. Peak phrenic nerve activity decreased for the duration of PEEP and rose to control levels when PEEP was removed. Minute ventilation was decreased resulting in a rise in P<sub>A</sub>CO<sub>2</sub> and a fall in P<sub>A</sub>O<sub>2</sub>. Heart rate and arterial pressure were not noticeably altered by the addition of PEEP.

Addition of 2 cm H<sub>2</sub>O PEEP during Biot breathing is shown in Figure 11 for the same cat. The most obvious alteration in Biot breathing was the prolongation of the phase of central apnea. The resulting decrease in respiratory frequency and minute ventilation resulted in an increase in P<sub>A</sub>CO<sub>2</sub> and fall in P<sub>A</sub>O<sub>2</sub>. The respiratory arrhythmia in heart rate as well as the fluctuations in arterial pressure became more pronounced as the respiratory frequency decreased. When PEEP was removed, a period of hyperventilation was seen during which the periodic nature of the pattern was lost. This was commonly observed and persisted for a period of time in proportion to the degree of PEEP added. This period of hyperventilation reverted to the control pattern within several minutes.

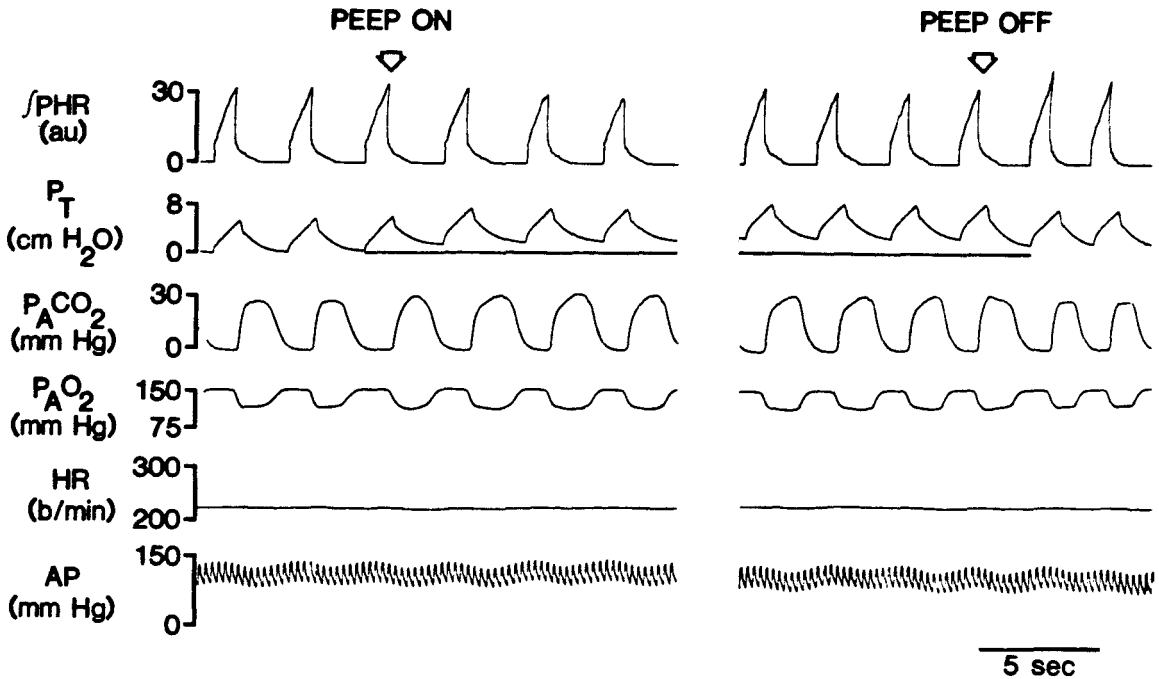


FIGURE 10. Response to application of 2 cm H<sub>2</sub>O positive end-expiratory pressure (PEEP) in eupnea for one cat. Arrows indicate where PEEP was applied (PEEP ON) and removed (PEEP OFF). Ten seconds of data were deleted between the left and right panels. Variables plotted include: integrated phrenic nerve activity (PHR), tracheal pressure (P<sub>T</sub>), alveolar carbon dioxide (P<sub>A</sub>CO<sub>2</sub>) and oxygen (P<sub>A</sub>O<sub>2</sub>) partial pressures, heart rate (HR), and arterial pressure (AP). The solid line under the P<sub>T</sub> tracing represents 0 cm H<sub>2</sub>O PEEP.

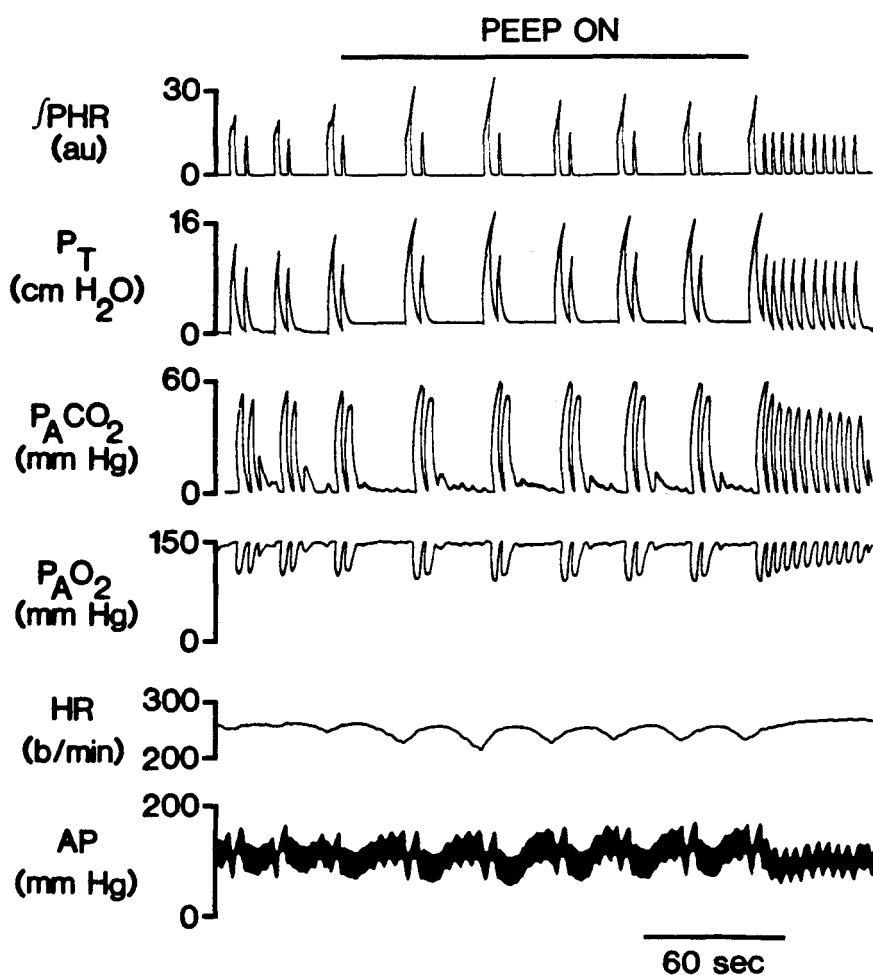
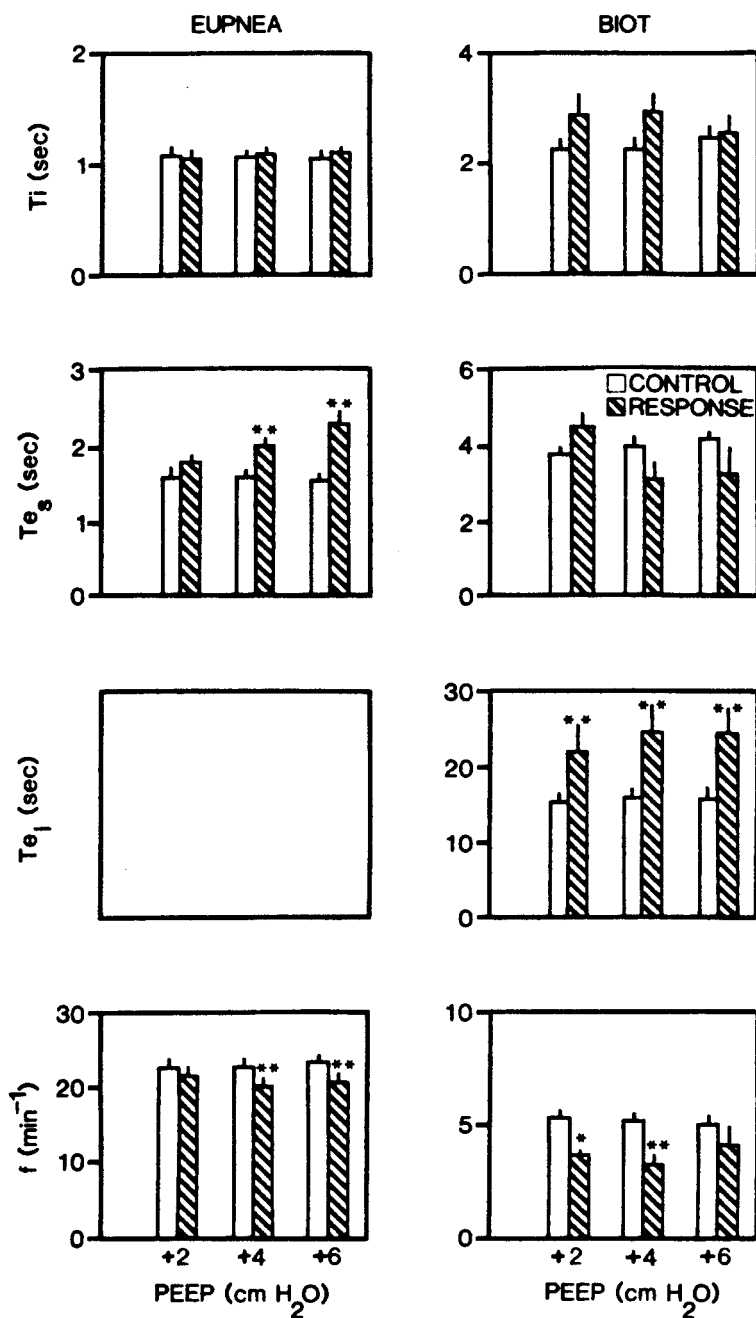


FIGURE 11. Response to application of 2 cm H<sub>2</sub>O positive end-expiratory pressure (PEEP) in Biot breathing for one cat.<sup>2</sup> Solid bar designates the period during which PEEP was applied. Variables plotted include; integrated phrenic nerve activity (PHR), tracheal pressure ( $P_T$ ), alveolar carbon dioxide ( $P_{A}CO_2$ ) and oxygen ( $P_{A}O_2$ ) partial pressures, heart rate (HR), and arterial pressure (AP).

The pooled responses of 11 cats to all three levels of PEEP, 2, 4, and 6 cm H<sub>2</sub>O, in eupnea and Biot breathing are shown in Figures 12 and 13. In eupnea, T<sub>i</sub> was not significantly altered by any level of PEEP. In contrast, T<sub>e</sub> progressively increased with higher levels of PEEP, and respiratory frequency was, therefore, reduced significantly. The change in tracheal pressure for each breath was multiplied by compliance to yield an estimation of tidal volume. A progressive decrease in minute ventilation was observed with increasing levels of PEEP due to the decrease in V<sub>T</sub> and the increase in T<sub>e<sub>1</sub></sub>. The decrease in ventilation was accompanied by a rise in P<sub>A</sub>CO<sub>2</sub> and fall in P<sub>A</sub>O<sub>2</sub>. No significant changes in heart rate or mean arterial pressure were recorded.

Following induction of Biot breathing, addition of PEEP did not result in any statistically significant increases in T<sub>i</sub>. Changes in expiratory duration within the cluster, T<sub>e<sub>s</sub></sub> were not analyzed statistically because data were not available for every cat at all pressure levels. The reason for this was that the quality of the periodic pattern was altered by PEEP. An example for one cat is shown in Figure 14. Addition of 2 cm H<sub>2</sub>O PEEP resulted in changes in the number of breaths per cluster in only 1/11 cats. With 4 and 6 cm H<sub>2</sub>O PEEP, however, the patterns, most commonly, were altered to single breaths per cluster. In 4 cats, single breaths alternated with clusters of varying number of breaths. In the majority (7/11) cats, the cluster quality of the pattern was completely eliminated with single breaths followed by periods of apnea present at 4 and 6 cm H<sub>2</sub>O PEEP.

In summary, respiratory frequency decreased progressively with higher levels of PEEP, reflecting both the increase in T<sub>e<sub>1</sub></sub> and the alteration of the pattern to one of single breaths per cluster. Minute ventilation decreased



**FIGURE 12.** Responses to application of 2, 4 and 6  $\text{cm H}_2\text{O}$  positive end-expiratory pressure (PEEP) in eupnea for 10 breaths and BiOT breathing for 5 clusters in 11 cats. Variables plotted include inspiratory duration ( $T_i$ ), the duration of expiration in eupnea or the duration of expiration within the cluster in BiOT breathing ( $T_{eS}$ ), apneic duration ( $T_{eI}$ ) and respiratory frequency ( $f$ ). (\* $p$  less than 0.05 or \*\* $p$  less than 0.01 as compared to corresponding control value).

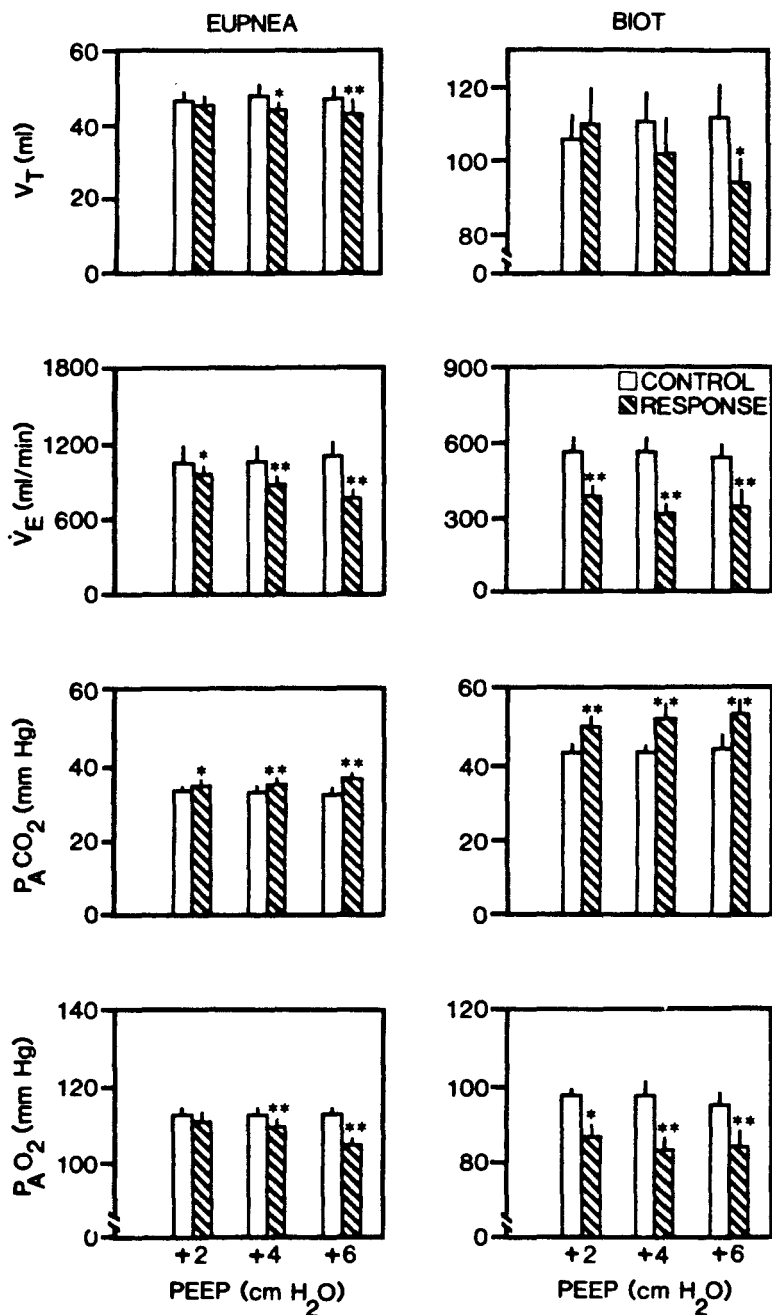
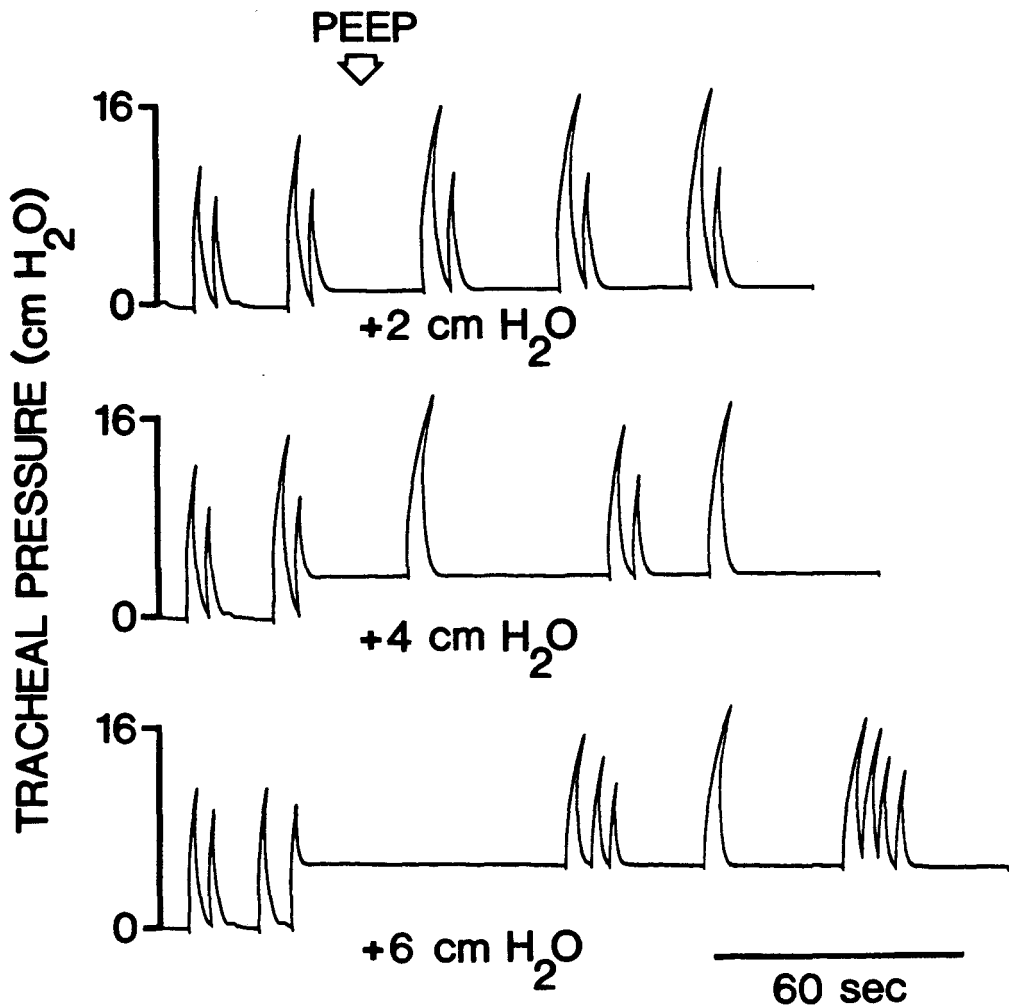


FIGURE 13. Responses to application of 2, 4 and 6 cm H<sub>2</sub>O positive end-expiratory pressure (PEEP) in eupnea for 10 breaths and Biot breathing for 5 clusters in 11 cats. Variables plotted include tidal volume ( $V_T$ ), minute ventilation ( $V_E$ ), and alveolar carbon dioxide ( $P_A CO_2$ ) and oxygen ( $P_A O_2$ ) partial pressures. (\* $p$  less than 0.05 or \*\* $p$  less than 0.01 as compared to corresponding control value).



**FIGURE 14.** Response to application of 2, 4 and 6 cm H<sub>2</sub>O positive end-expiratory pressure (PEEP) in Biot breathing for 1 cat. Respirator is cycle-triggered from the phrenic nerve, therefore, tracheal pressure reflects phrenic nerve activity.

significantly at all levels of PEEP due primarily to the decrease in frequency. This decrease in ventilation was accompanied by corresponding increases in  $P_A\text{CO}_2$  and decreases in  $P_A\text{O}_2$ . No significant changes were observed in heart rate. However, mean arterial pressure increased significantly from  $121\pm 6$  mmHg to  $131\pm 7$  mm Hg with 2 cm  $\text{H}_2\text{O}$  PEEP and from  $119\pm 5$  mm Hg to  $127\pm 8$  mm Hg at 6 cm  $\text{H}_2\text{O}$  PEEP.

## 2. Single breath responses to PEEP

In addition, PEEP was applied for a single expiratory phase in eupnea and for a single apneic phase in Biot breathing. Application of 2 cm  $\text{H}_2\text{O}$  PEEP, for a single expiration in eupnea, resulted in a prolongation of expiratory duration as seen in Figure 15. Further prolongation of  $T_{e_s}$  was seen with 4 and 6 cm  $\text{H}_2\text{O}$  PEEP. The prolongation of  $T_{e_s}$  was significantly greater with 6 cm  $\text{H}_2\text{O}$  than with either 2 or 4 cm  $\text{H}_2\text{O}$  PEEP. The increases in  $T_{e_s}$  were accompanied by increases in  $P_A\text{CO}_2$  and decreases in  $P_A\text{O}_2$  as shown in Table 2. These changes were small but highly significant.

The characteristic response to PEEP applied during a single phase of central apnea is shown in Figure 16. Application of 2 cm  $\text{H}_2\text{O}$  PEEP resulted in a prolongation of the duration of central apnea which was increased even further by addition of 4 and 6 cm  $\text{H}_2\text{O}$  PEEP.

The pooled responses of all 11 cats to applications of PEEP for a single period of central apnea are shown in Figure 15. Two cm  $\text{H}_2\text{O}$  PEEP significantly prolonged central apnea as did application of 4 and 6 cm  $\text{H}_2\text{O}$  PEEP. The duration of  $T_{e_1}$  with 6 cm  $\text{H}_2\text{O}$  PEEP was significantly greater than that in response to 2 and 4 cm  $\text{H}_2\text{O}$  PEEP.

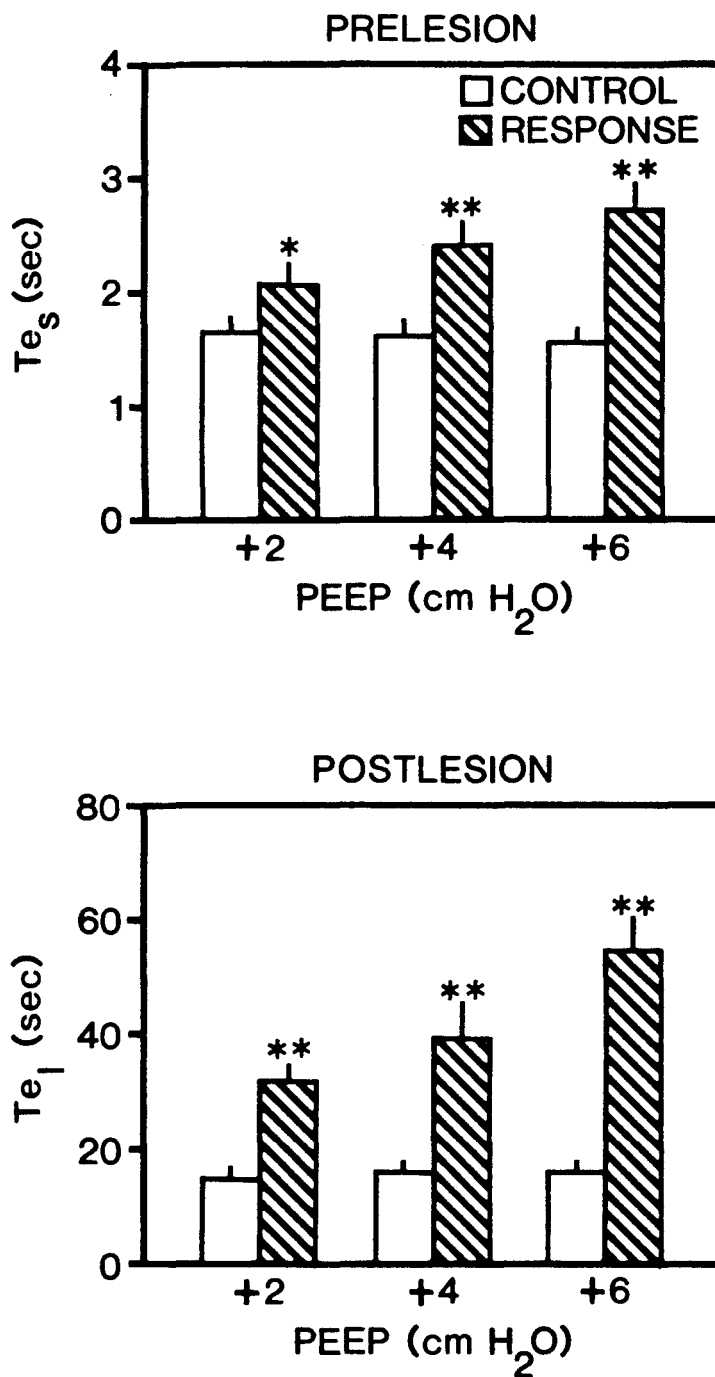


**FIGURE 15.** Response to application of 2, 4 and 6 cm H<sub>2</sub>O positive end-expiratory pressure (PEEP) for a single expiration in eupnea (prelesion) and for a single apneic period in Biot breathing (postlesion) for 11 cats. Variables plotted include: duration of expiration in eupnea ( $T_{e_s}$ ) and the duration of central apnea in Biot breathing ( $T_{e_l}$ ). (\* $p$  less than 0.05 or \*\* $p$  less than 0.01 as compared to corresponding control value).

TABLE 2

Alveolar gas tensions in response to single breath PEEP

<u>Eupnea</u>	<u>Control</u>	<u>2 cm H<sub>2</sub>O</u>	<u>Control</u>	<u>4 cm H<sub>2</sub>O</u>	<u>Control</u>	<u>6 cm H<sub>2</sub>O</u>
P <sub>A</sub> CO <sub>2</sub> (mm Hg)	32±2	33±2 <sup>*</sup>	32±2	34±2 <sup>*</sup>	31±2	35±2 <sup>*†</sup>
P <sub>A</sub> O <sub>2</sub> (mm Hg)	115±2	112±2 <sup>*</sup>	115±2	110±2 <sup>*</sup>	116±2	106±2 <sup>*†</sup>
<u>Biot</u>						
P <sub>A</sub> CO <sub>2</sub> (mm Hg)	44±2	51±3 <sup>*</sup>	44±2	53±4 <sup>*</sup>	45±3	54±3 <sup>*</sup>
P <sub>A</sub> O <sub>2</sub> (mm Hg)	98±2	87±3 <sup>*</sup>	98±2	83±4 <sup>*</sup>	95±3	84±4 <sup>*</sup>

Values expressed as Mean±S.E.M.

<sup>\*</sup>p <0.001 as compared to immediately preceding control value.<sup>†</sup>p <0.05 as compared to response at 4 cm H<sub>2</sub>O PEEP.

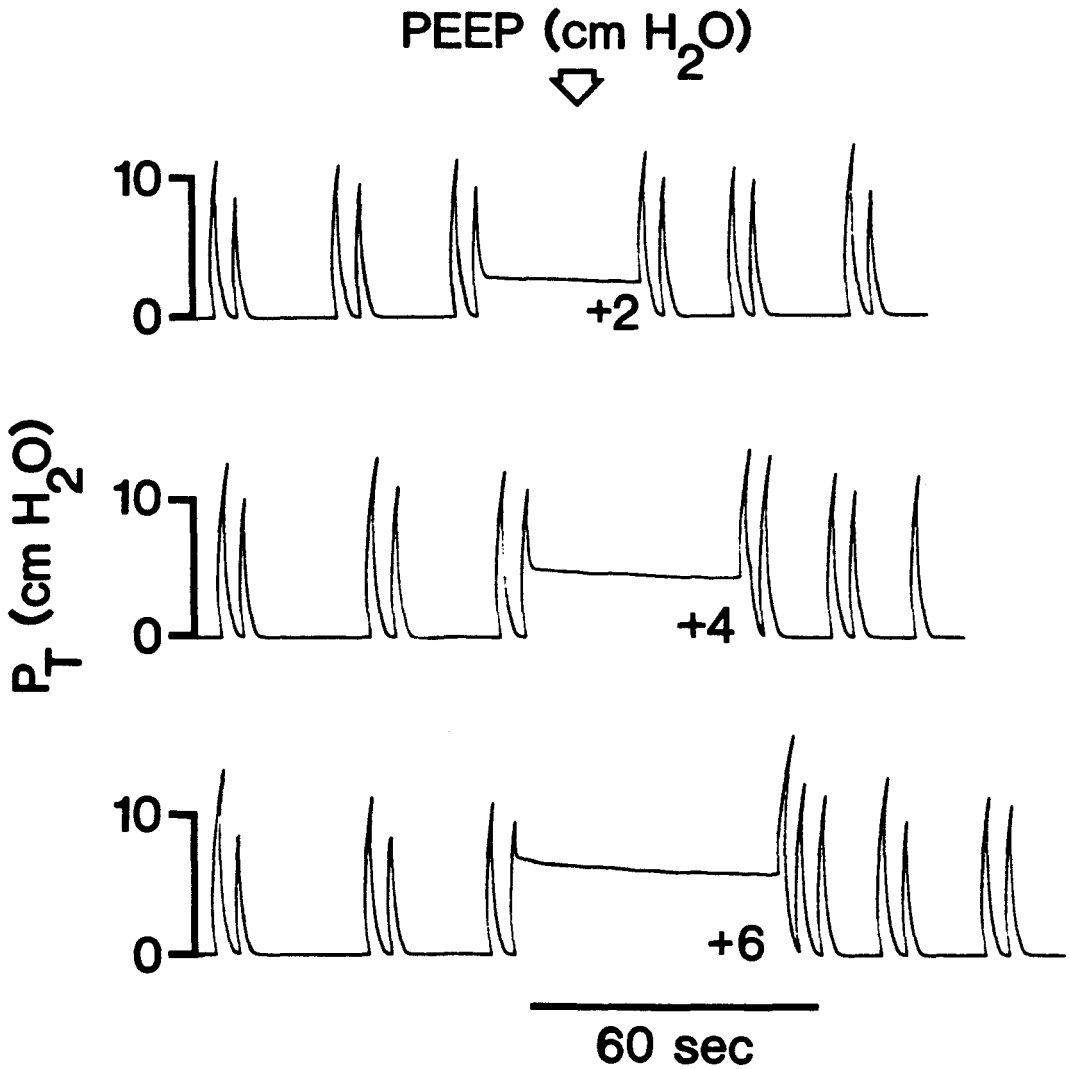


**FIGURE 16.** Response to application of 2, 4 and 6 cm H<sub>2</sub>O positive end-expiratory pressure (PEEP) for a single apneic phase in Biot breathing for 1 cat. Respirator is cycle-triggered from the phrenic nerve, therefore, tracheal pressure ( $P_T$ ) reflects phrenic nerve activity.

The relationship between  $T_e$  prolongation and the amount of PEEP applied is shown in Figure 17 . The duration of the expiration during which PEEP was applied ( $T_{e_f}$ ) was normalized to the preceding control  $T_e$  ( $T_{e_c}$ ). The normalized  $T_e$  was plotted against the level of PEEP applied. Regression analysis using the values for each individual cat revealed a significant relationship between  $T_{e_f}/T_{e_c}$  and PEEP in both eupnea and Biot breathing. The slope of the relationship was derived by regression analysis for each individual cat in eupnea and Biot breathing. A paired t-test was performed on the slopes from each cat and revealed that the mean slope of 0.13/cm H<sub>2</sub>O in eupnea was increased significantly to 0.35/cm H<sub>2</sub>O in Biot breathing. These data indicate that following PRG lesion and induction of Biot breathing, expiratory duration (central apnea) is prolonged to a greater degree by any given level of PEEP than in eupnea.

The increased expiratory load may be compensated for by an increase in inspired volume. To evaluate this mechanism as a possible compensation for the added PEEP, several indices of respiratory drive were quantitated. Peak phrenic amplitude, the duration of inspiration, the mean rate-of-rise of phrenic nerve activity (peak phrenic amplitude/ $T_i$ ), and the estimated total volume in the lung above FRC at end inspiration were measured. Linear regressions of these variables as a function of the applied PEEP were performed. No significant relationships were found between peak phrenic amplitude,  $T_i$ , or the rate of rise of phrenic nerve activity and PEEP in either eupnea or Biot breathing. However, the total volume in the lungs at the end of the first inspiration following PEEP application was significantly correlated with the level of PEEP before lesion as shown in Figure 18. Because the value of  $V_{T\text{-test}}/V_{T\text{-control}}$  was always greater than one, the

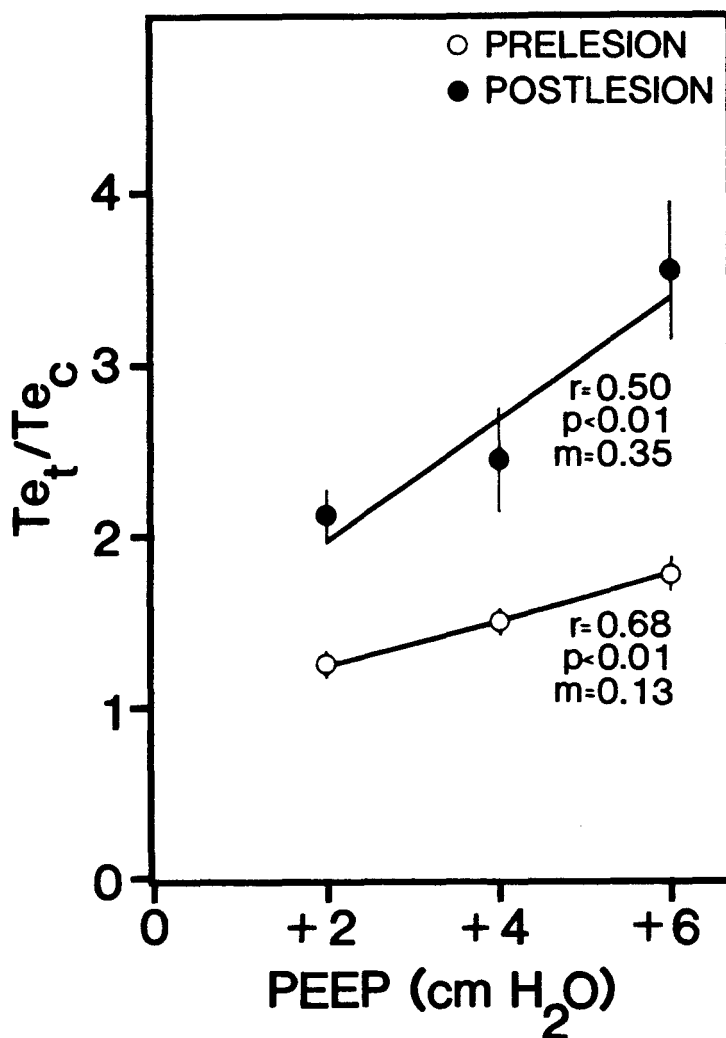
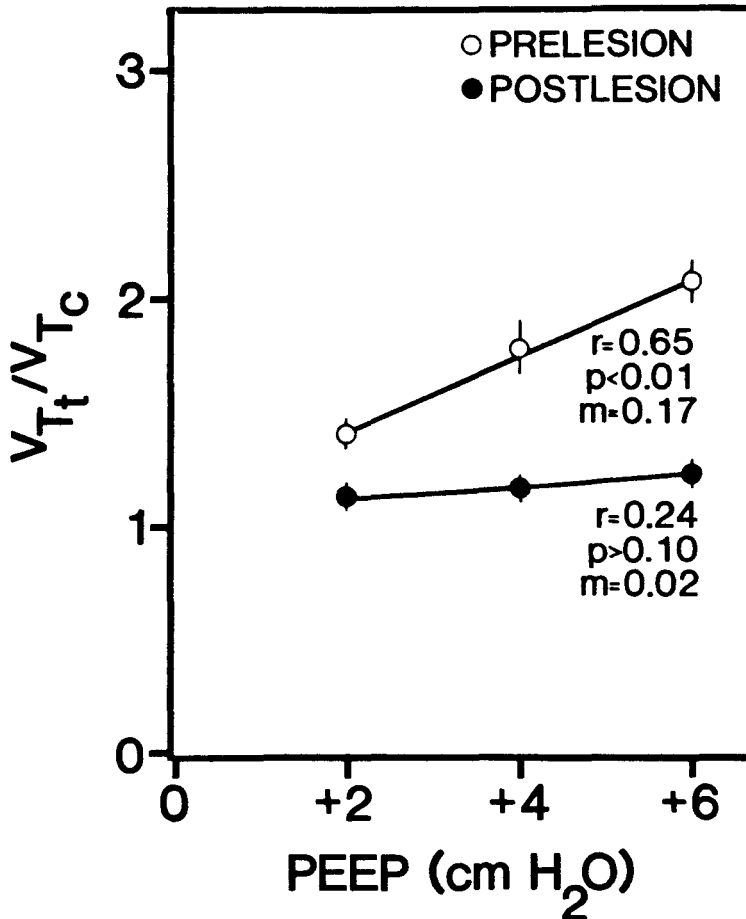


FIGURE 17. Response of expiratory duration to application of 2, 4 and 6 cm H<sub>2</sub>O positive end-expiratory pressure (PEEP) in 11 cats. The duration of expiration in response to PEEP (Te<sub>t</sub>), is normalized to the duration of the unloaded expiration (Te<sub>c</sub>) and plotted against the PEEP added for a single expiratory phase in eupnea (prelesion) and for a single apneic phase in Biot breathing (postlesion). Regression lines are plotted for both sets of data with corresponding correlation coefficient (r), level of significance for the r value (p), and slope (m) given.



**FIGURE 18.** Response of end-inspiratory lung volume to application of 2, 4 and 6  $\text{cm H}_2\text{O}$  positive end-expiratory pressure (PEEP) in 11 cats. The end-inspiratory lung volume in response to PEEP ( $V_{T_t}$ ) is normalized to the end-inspiratory lung volume in control ( $V_{T_c}$ ) and plotted against the PEEP added for a single expiratory phase in eupnea (prelesion) and for a single apneic phase in Biot breathing (postlesion). Regression lines are plotted for both sets of data with corresponding correlation coefficient ( $r$ ), level of significance for the  $r$  value ( $p$ ), and slope ( $m$ ) given.

lung volume necessary to terminate inspiration was increased in eupnea by PEEP. The positive slope indicates that a greater total lung volume was necessary to terminate inspiration as the end-expiratory lung volume increased. Following PRG lesions,  $V_T$  test/ $V_T$  control is no longer significantly correlated with the PEEP applied. This indicates that the compensatory mechanism of increasing inspired volume to overcome an expiratory load is lost after PRG lesion.

### C. Group II-Responses of upper airway and abdominal motoneurons to PEEP

The second group of experiments was designed to answer two questions. First, whether and in what pattern, outflows to the upper airway musculature and expiratory muscles were activated in Biot breathing as versus eupnea. Secondly, whether expiratory muscles were activated in response to PEEP, a possible compensatory mechanism for the increased expiratory load.

The brainstem sections of the 10 cats contributing data to this group are shown in Figure 19. The lesions were located in the dorsolateral tegmentum of the pons, in the region of the PRG. Lesions were  $3.0 \pm 0.2$  mm in length and as can be seen from Figure 19, ranged from 2-3 mm in diameter. The Biot patterns which occurred in each cat are also shown.

Indices of efferent outflows to upper airway and expiratory muscles, the recurrent laryngeal nerve (RL) and the cranial iliohypogastric nerve (CIHG), were recorded in eupnea and Biot breathing as shown in Figure 20. The tracings of RL nerve activity reveal that motoneurons innervating the laryngeal musculature were activated in phase with phrenic motoneurons both in eupnea and Biot breathing. This relationship was observed in all cats studied. Examination of the CIHG nerve activity revealed the absence of

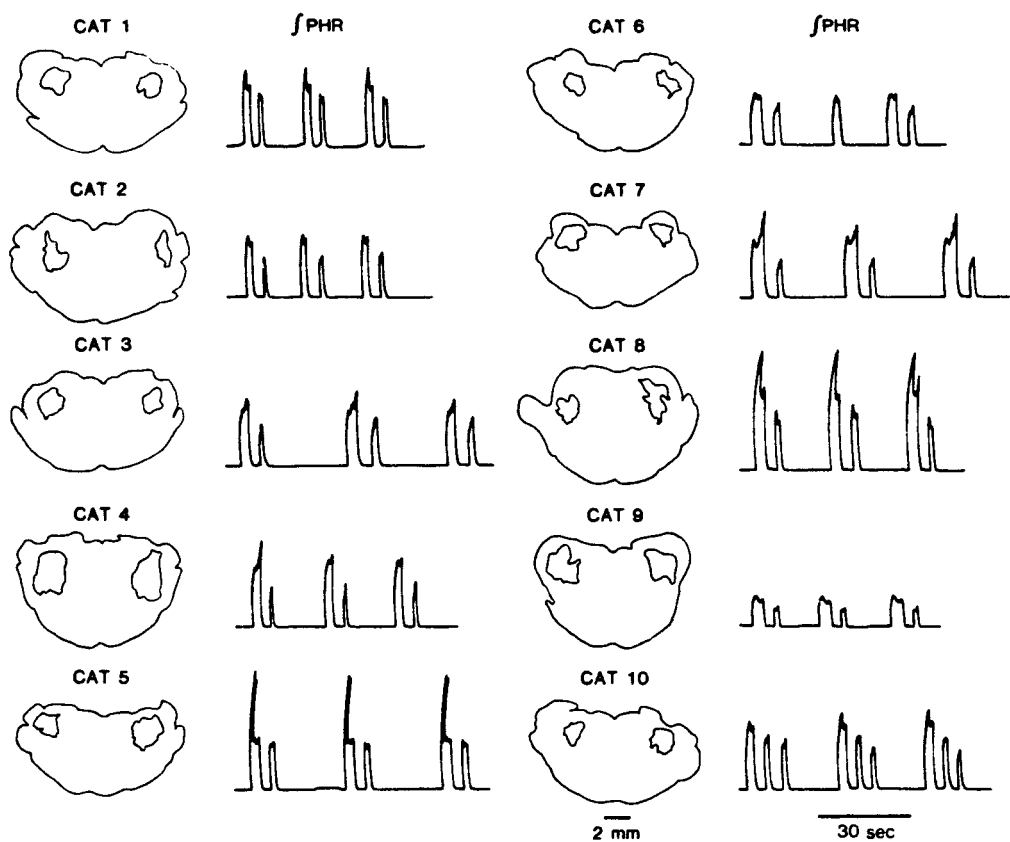


**FIGURE 19.** Tracings of tissue destruction resulting from bilateral radio frequency lesions placed within the PRG in 10 cats. The resultant integrated phrenic nerve activity (PHR) is shown for each cat.

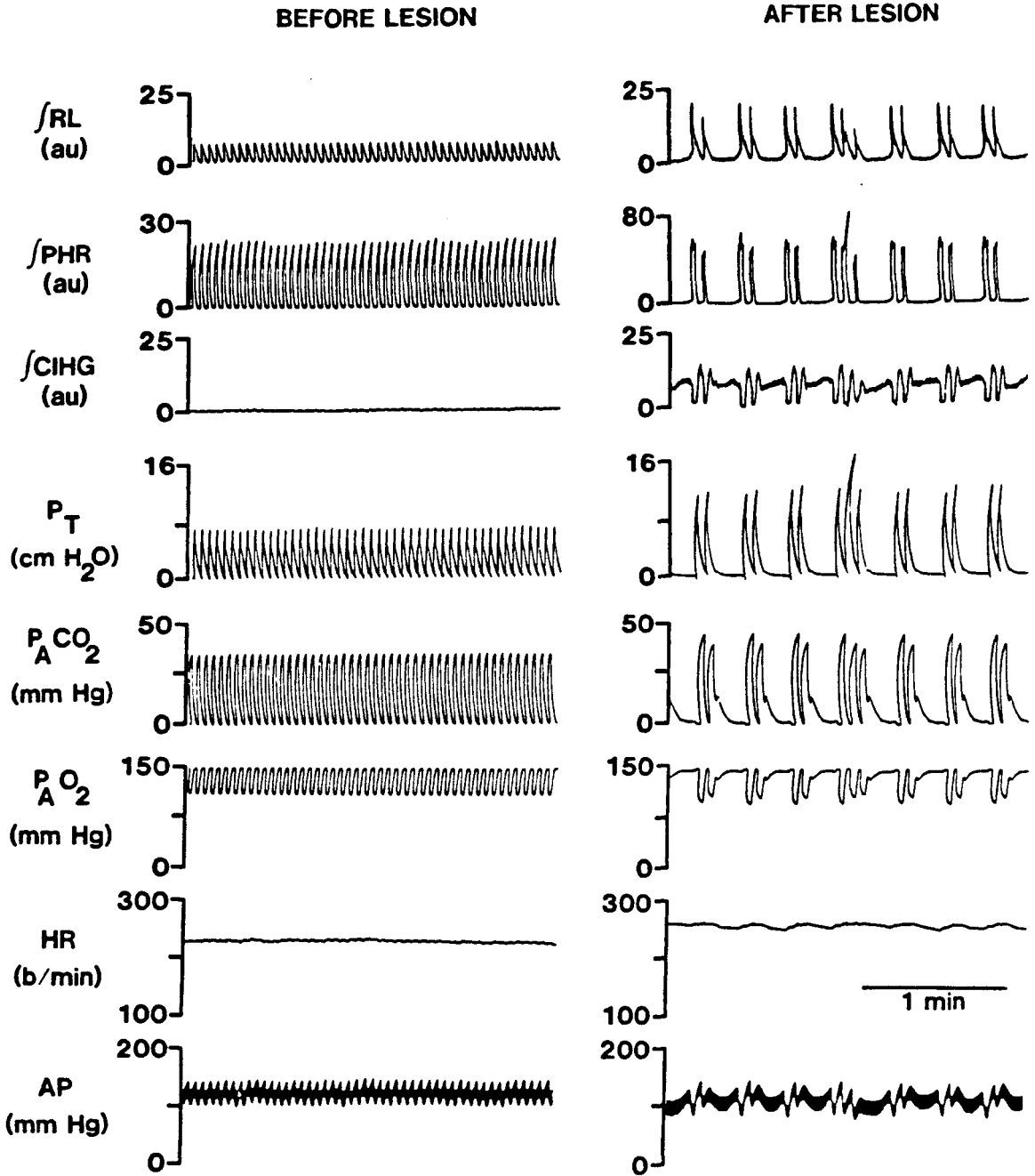


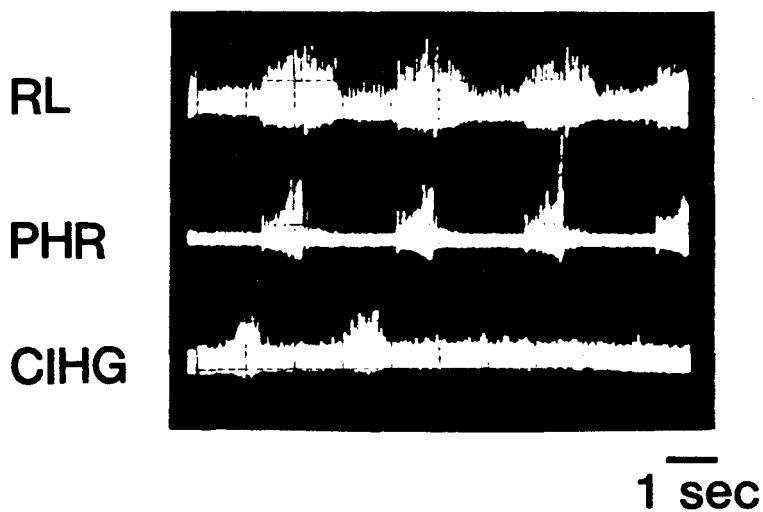
FIGURE 20. Example of respiratory pattern before (eupnea) and after (Biot) lesion of the PRG. Variables plotted include: integrated recurrent laryngeal nerve activity (RL), integrated phrenic nerve activity (PHR), integrated cranial iliohypogastric nerve activity (CIHG), tracheal pressure ( $P_T$ ), alveolar carbon dioxide ( $P_{A}CO_2$ ) and oxygen ( $P_{A}O_2$ ) partial pressures, heart rate (HR), and arterial pressure (AP).

phasic activity in eupnea in this particular case, while phasic activity appeared in Biot breathing. In eupnea, consistent phasic CIHG activity was observed in only 4/9 cats but was present in all cats in Biot breathing.

Examination of the raw activity of the RL, phrenic (PHR) and CIHG nerves revealed interesting differences between eupnea and Biot breathing (Figure 21). In eupnea, the activation of the RL nerve was coincident with that of the phrenic nerve and showed an augmenting type of pattern. A decrementing activity was present in the RL during the early portion of the expiratory phase. This occurred during the post-inspiratory discharge of the phrenic nerve. In this particular example, intermittent activation of the CIHG nerve was observed during expiration. However, it was not consistently present in any cat during eupneic breathing. Following lesion and induction of Biot breathing, phasic activity in the CIHG nerve appeared in all cats. As demonstrated in the lower portion of Figure 21, the quality of RL and phrenic nerve activities was altered by lesion placement. In all cats, the early expiratory RL activity disappeared as did the post-inspiratory activity of the phrenic nerve. Therefore, the transition from inspiration to expiration became more abrupt as the smoothing function of post-inspiratory activity appeared to be lost.

Phasic expiratory activity of the CIHG nerve could be recruited before lesion in all cats by transiently turning off the respirator and allowing the  $P_A\text{CO}_2$  to rise. The relationship between  $P_A\text{CO}_2$  and CIHG activity was quantitated by determining a threshold level of  $\text{CO}_2$  at which CIHG activity consistently appeared. Phasic activity was defined as a respiratory related oscillation of the integrated CIHG activity of greater than 5 arbitrary units. Gains of the amplifiers were maintained constant in eupnea and Biot

## PRELESION



## POSTLESION

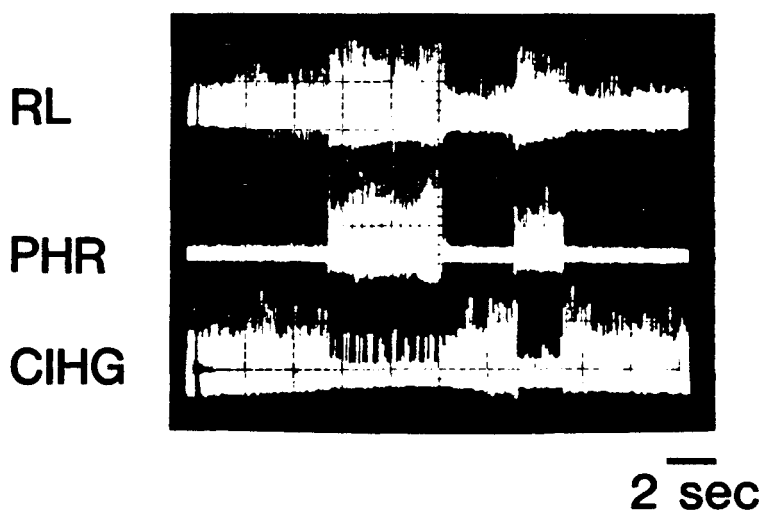


**FIGURE 21.** Oscilloscope tracings of raw activity in recurrent laryngeal (RL), phrenic (PHR), and cranial iliohypogastric (CIHG) nerves in eupnea (prelesion) and in Biot breathing (postlesion) for one cat. Note lack of post-inspiratory activity in RL and PHR nerves postlesion.

breathing for each cat. In eupnea, threshold was determined when the cat was hypoventilated by turning off the respirator. Threshold was determined in Biot breathing during the period of spontaneous hyperventilation that followed PEEP administration. The threshold (in mm Hg  $\text{CO}_2$ ) was compared with the level of  $\text{P}_A\text{CO}_2$  which the cat maintained when ventilated with the cycle-triggered respirator by a two-way analysis of variance. The threshold for appearance of phasic CIHG activity was not significantly altered following induction of Biot breathing, as shown in Table 3. The end-tidal  $\text{CO}_2$  level in eupnea was slightly but significantly lower than the threshold value. Thus, phasic CIHG activity appeared consistently in eupnea only when the end-tidal  $\text{CO}_2$  rose. As can be seen in Table 3, the end-tidal  $\text{CO}_2$  level in Biot breathing was significantly higher than the threshold at which phasic CIHG activity first appeared. These data indicated that the increase in phasic CIHG activity in Biot breathing might have been related to the increase in  $\text{P}_A\text{CO}_2$  which resulted following lesion.

The effects of PEEP on CIHG nerve activity were investigated in 7 cats in which stable recordings of CIHG activity were made in eupnea and Biot breathing. In eupneically breathing cats, application of 2, 4, and 6 cm  $\text{H}_2\text{O}$  PEEP, resulted in prolongations of  $\text{Te}_s$  as shown in Figure 22. The duration of expiration is plotted for 5 control breaths, the first expiration during which PEEP was applied and the last expiration before PEEP was removed. The duration of  $\text{Te}_s$  was significantly elevated by addition of 4 and 6 cm  $\text{H}_2\text{O}$ . When the duration of the final expiration was compared to control,  $\text{Te}_s$  was still significantly prolonged over control. This resulted in significant decreases in respiratory frequency and ventilation. Significant

TABLE 3

Carbon dioxide levels for CIHG nerve activity

Group	Threshold level (mm Hg)	Operating level (mm Hg)
Eupnea	36±2	34±1*
Biot	43±2	57±4*

Values expressed as Mean±S.E.M.

\* p &lt;0.05 as compared to corresponding threshold level value.

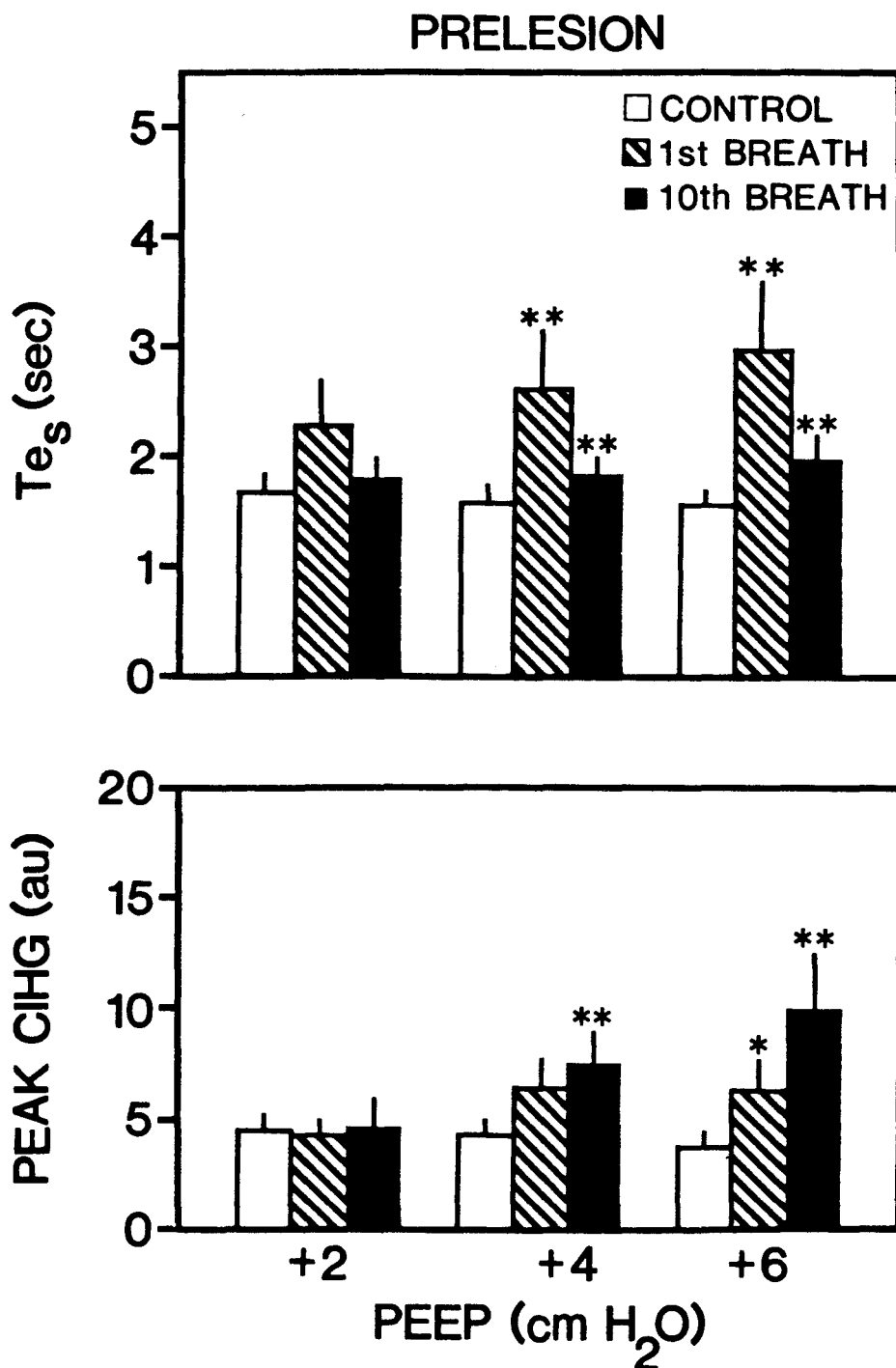


**FIGURE 22.** Expiratory duration ( $T_{e_s}$ ) and peak integrated cranial iliohypogastric nerve activity (CIHG) in response to application of 2, 4 and 6 cm H<sub>2</sub>O positive end-expiratory pressure (PEEP) in 10 cats. Responses are plotted for the first breath and tenth breath during which PEEP was applied in eupnea (prelesion). (\*p less than 0.05 or \*\*p less than 0.01 as compared to corresponding control value).

alterations in end-tidal  $\text{CO}_2$  and  $\text{O}_2$  were observed at all levels of PEEP (Table 4). Peak integrated CIHG activity increased significantly during the first loaded expiration with PEEP of 6 cm  $\text{H}_2\text{O}$ . However, when PEEP was maintained for 10 breaths, CIHG activity was significantly elevated with 4 cm  $\text{H}_2\text{O}$  PEEP as well.

The variety of patterns of expiratory nerve activity in response to addition of PEEP for a single apneic phase is shown in Figure 23. Four types of CIHG nerve responses were observed in the 7 cats in which recordings were stable at all levels of PEEP. Cat 1 typified the response seen in 4 cats in which increasing levels of PEEP resulted in an increased duration of CIHG activity throughout the prolonged apneic phase. The peak CIHG activity was observed to increase only when 6 cm  $\text{H}_2\text{O}$  PEEP was applied. In Cat 7, the application of PEEP resulted only in prolongation of the apneic phase and CIHG activity but no changes in peak frequency were observed as compared to control. In Cat 9, CIHG activity was also prolonged for the duration of the apneic phase and in all cases, peak frequency was elevated over control. The peak activity declined progressively with higher levels of PEEP. In Cat 10, there were small increases in peak frequency observed with increased levels of PEEP. Therefore, the responses of CIHG nerve activity to applied PEEP in Biot breathing cats represented a heterogeneous group.

In Biot breathing, application of PEEP resulted in immediate (first breath) prolongations of central apnea as shown in Figure 24. The duration of central apnea decreased by the 5th cluster but was still significantly elevated over control at 4 and 6 cm  $\text{H}_2\text{O}$ . In contrast to the CIHG response in eupnea, application of PEEP in Biot breathing resulted in a significant

TABLE 4

Alveolar gas tensions in response to multiple breath PEEP

<u>Eupnea</u>	<u>Control</u>	<u>2 cm H<sub>2</sub>O</u>	<u>Control</u>	<u>4 cm H<sub>2</sub>O</u>	<u>Control</u>	<u>6 cm H<sub>2</sub>O</u>
P <sub>A</sub> CO <sub>2</sub> (mm Hg)	34±1	35±1 <sup>*</sup>	34±1	37±1 <sup>*†</sup>	33±1	37±1 <sup>*†</sup>
P <sub>A</sub> O <sub>2</sub> (mm Hg)	113±1	110±2 <sup>*</sup>	113±2	108±2 <sup>*†</sup>	113±1	103±2 <sup>*†</sup>
<u>Biot</u>						
P <sub>A</sub> CO <sub>2</sub> (mm Hg)	52±2	59±3 <sup>*</sup>	54±5	67±5 <sup>*†</sup>	57±6	67±5 <sup>*†</sup>
P <sub>A</sub> O <sub>2</sub> (mm Hg)	91±3	83±3 <sup>*</sup>	90±4	74±4 <sup>*†</sup>	91±3	73±5 <sup>*†</sup>

Values expressed as Mean±S.E.M.

\* p <0.05 as compared to preceding control value.

† p <0.05 as compared to response with 2 cm H<sub>2</sub>O PEEP.

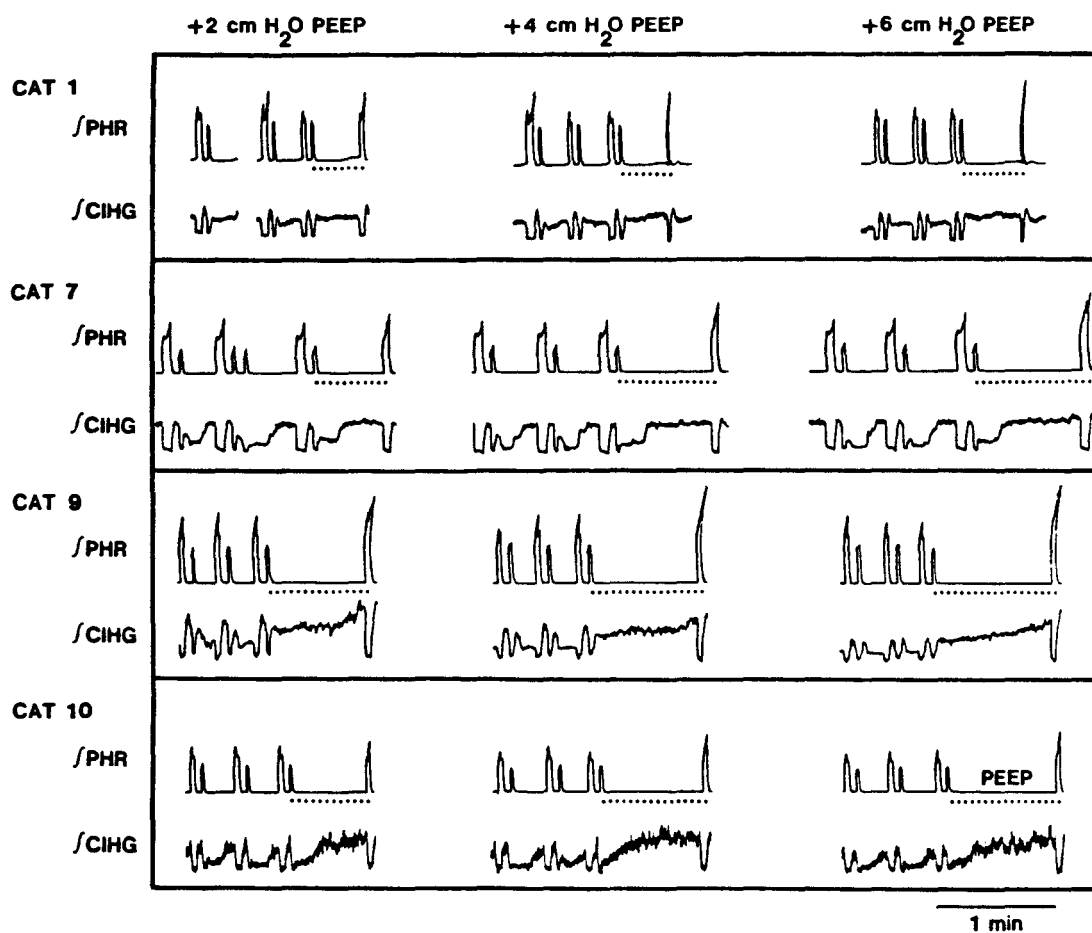


**FIGURE 23.** Examples from 4 cats of integrated phrenic (PHR) and cranial iliohypogastric (CIHG) nerve activities in response to application of 2, 4 and 6 cm H<sub>2</sub>O positive end-expiratory pressure (PEEP). Dotted lines designate apneic phase during which PEEP was applied.

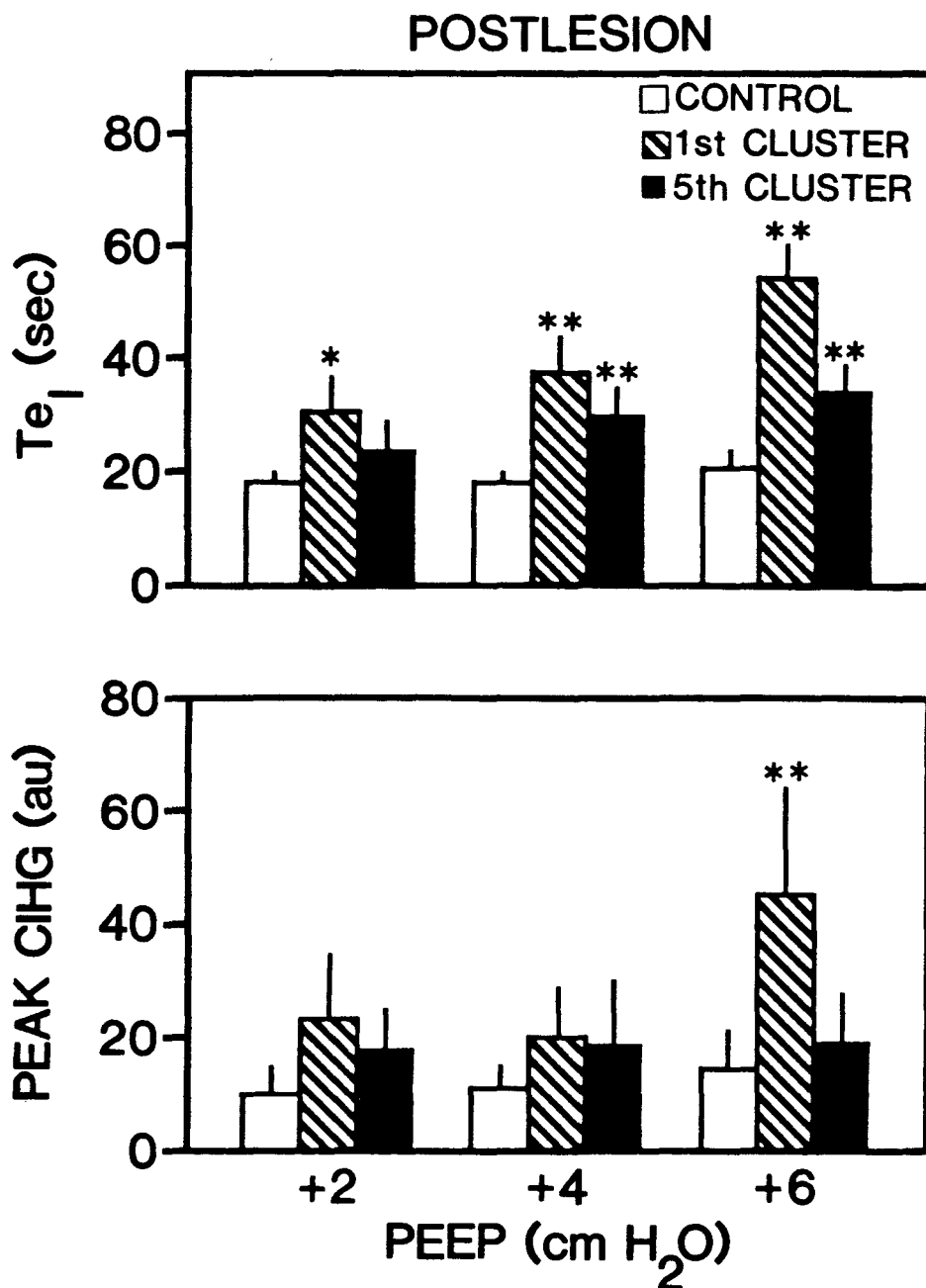


**FIGURE 24.** Duration of central apnea ( $T_{eI}$ ) and peak integrated cranial iliohypogastric nerve activity (CIHG) in response to application of 2, 4 and 6 cm H<sub>2</sub>O positive end-expiratory pressure (PEEP) in 10 cats. Responses are plotted for the first and fifth apneic phase during which PEEP was applied in Biot breathing (postlesion). (\*p less than 0.05 or \*\*p less than 0.01 as compared to corresponding control value).

increase in peak activity only at 6 cm H<sub>2</sub>O. This peak activity was not maintained so that by the 5th cluster, peak CIHG activity was not different from control at any level of PEEP. Peak CIHG activity was not consistently increased with PEEP even though P<sub>A</sub>CO<sub>2</sub> and P<sub>A</sub>O<sub>2</sub> were significantly increased and decreased, respectively (Table 4).

The relationship between peak RL and peak PHR nerve activities was assessed before and after lesion to determine whether phrenic and recurrent laryngeal nerve outputs were altered in the same direction by PEEP. The peak RL activity of the first breath following PEEP was normalized to the preceding control value and plotted against the normalized PHR activity. A regression analysis of data from 6 cats in which nerve activities were recorded pre and postlesion revealed a highly significant relationship between peak PHR activity in response to PEEP (Figure 25). There was no significant relationship between either the peak PHR activity or the peak RL activity and the PEEP applied. Thus, when peak phrenic activity was increased in response to a load, peak RL activity also increased. However, after lesion, the relationship between peak RL and peak PHR nerve activities in response to PEEP was no longer present.

#### D. Group III-Respiratory cell discharges during Biot breathing

The third group of experiments were designed to investigate the discharge patterns of medullary cells with respiratory-related activity in Biot breathing. The lesion placement and resulting Biot patterns for the 10 cats comprising this group are shown in Figure 26. Lesions were  $3.3 \pm 0.2$  mm in length and had diameters ranging from 2-3 mm.

Extracellular recordings were made of 9 inspiratory and 25 expiratory cells. Only cells which maintained their respiratory related activity when

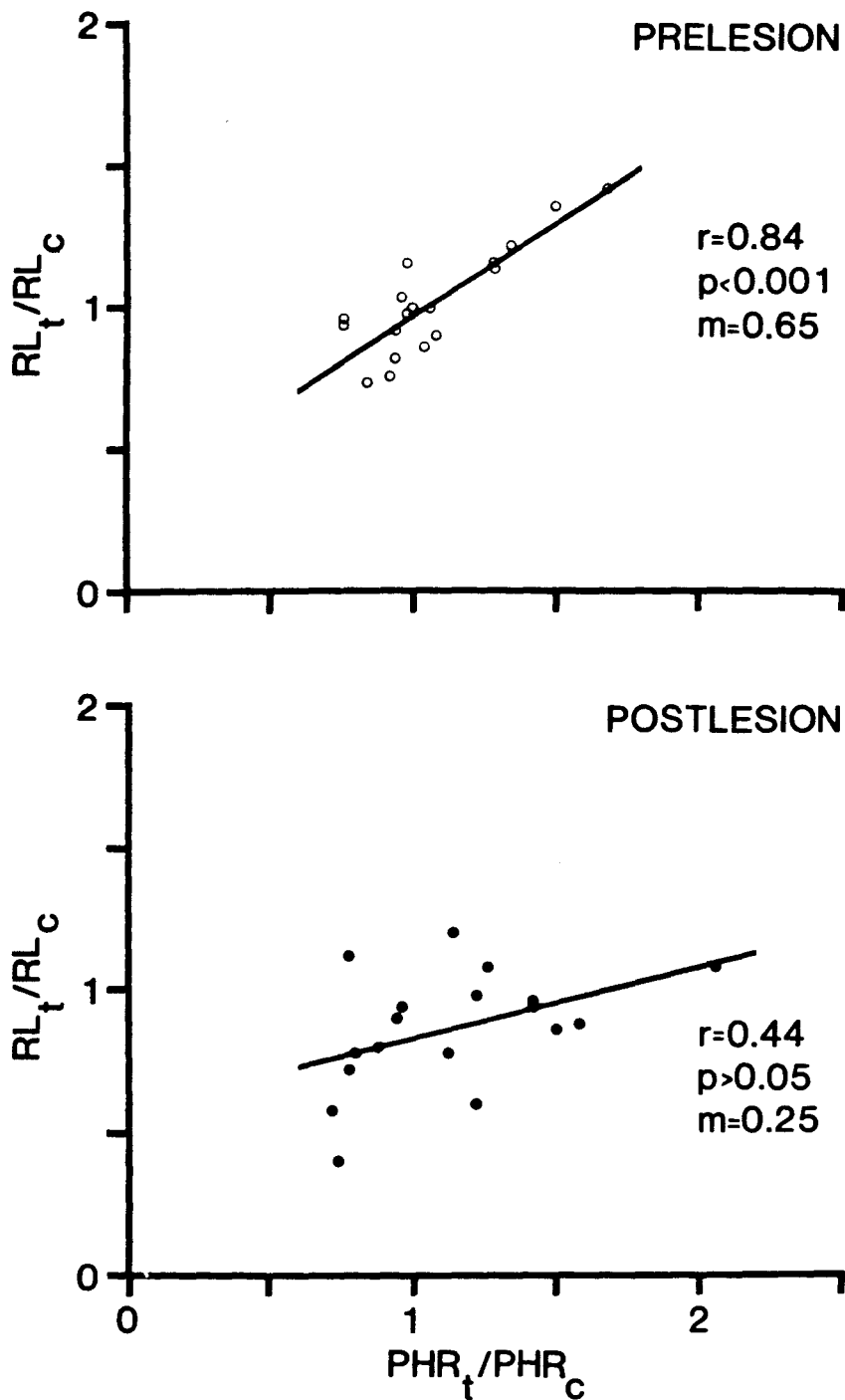


**FIGURE 25.** Peak integrated recurrent laryngeal (RL) and phrenic (PHR) nerve activities for the first breath following application of positive end-expiratory pressure (t) normalized to the preceding control (c) values are plotted in eupnea (prelesion) and Biot breathing (postlesion) for 6 cats. Regression lines are plotted for both sets of data with corresponding correlation coefficient (r), level of significance for the r value (p), and slope (m) given.

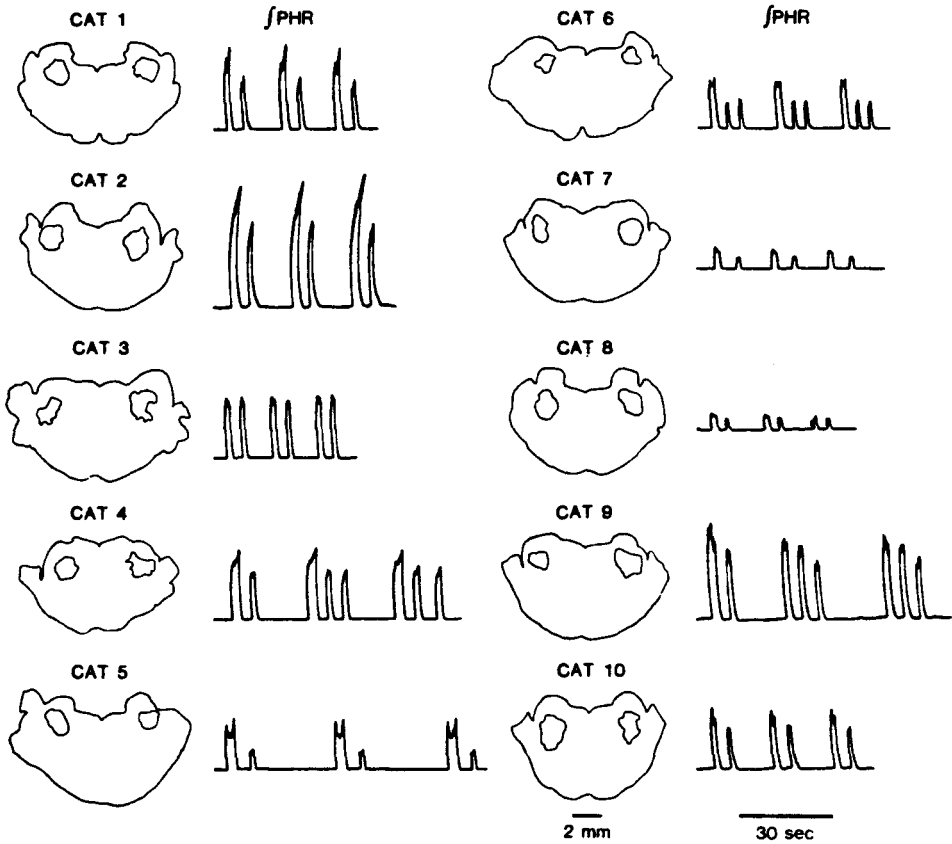


**FIGURE 26.** Tracings of tissue destruction resulting from bilateral radio frequency lesions placed within the PRG in 10 cats. The resultant integrated phrenic nerve activity (PHR) is shown for each cat.

the respirator was transiently turned off were considered to be respiratory cells. In 5/9 inspiratory cells recordings were made during Biot breathing and when inflation was withheld (no inflation test). Expiratory cells were subjected to loading with 2, 4 and 6 cm H<sub>2</sub>O PEEP. Of the 25 expiratory cells, stable recordings of responses to all three levels of PEEP were obtained in 12. Results are presented only from the 5 inspiratory and 12 expiratory cells in which complete data sets were obtained.

The locations of these cells were determined by stereotaxic coordinates and are mapped in Figure 27 in relation to the position of the obex. All cells recorded were located at the level of or caudal to the obex, 2.5-4.0 mm lateral and 2.0-4.0 mm below the dorsal surface.

#### 1. Inspiratory cell activity

The relationship between phrenic nerve activity and the discharge patterns of the 5 inspiratory cells are shown in Figure 28. In all 5 cells, the integrated inspiratory cell discharge closely resembled that of the integrated phrenic activity. One notable exception was transiently observed in the activity of cell 12 (Figure 29) when cyclic activity appeared in the integrated unit discharge during periods of phrenic quiescence. As the phrenic pattern changed spontaneously from 1 to 2 breaths/cluster, the activity of the inspiratory cell increased in frequency at a time corresponding to the second inspiration of the cluster. With this exception, no activity resembling the inspiratory burst of phrenic nerve activity was recorded in any inspiratory cell during central apnea.

The responses of 5 inspiratory cells to withholding inflation are shown in Figure 30. Cycle-triggered histograms were generated for the control and no inflation tests with 0.5 second bin widths. Time zero indicates the onset

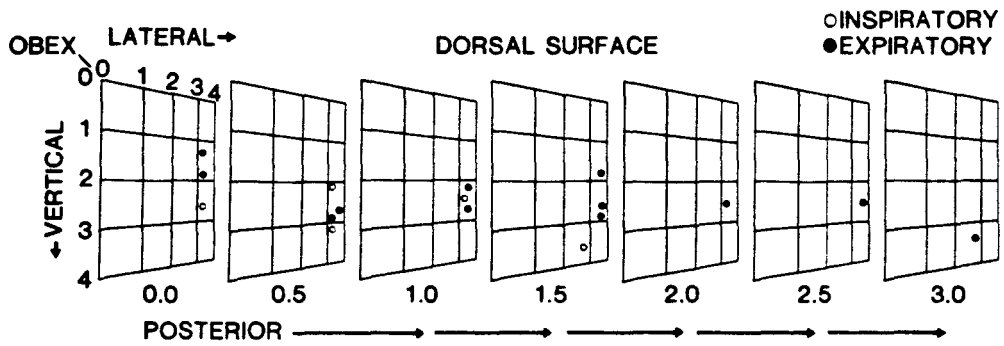


**FIGURE 27.** Location of 5 inspiratory and 12 expiratory cells recorded plotted with reference to the location of the obex. All dimensions given are in millimeters.

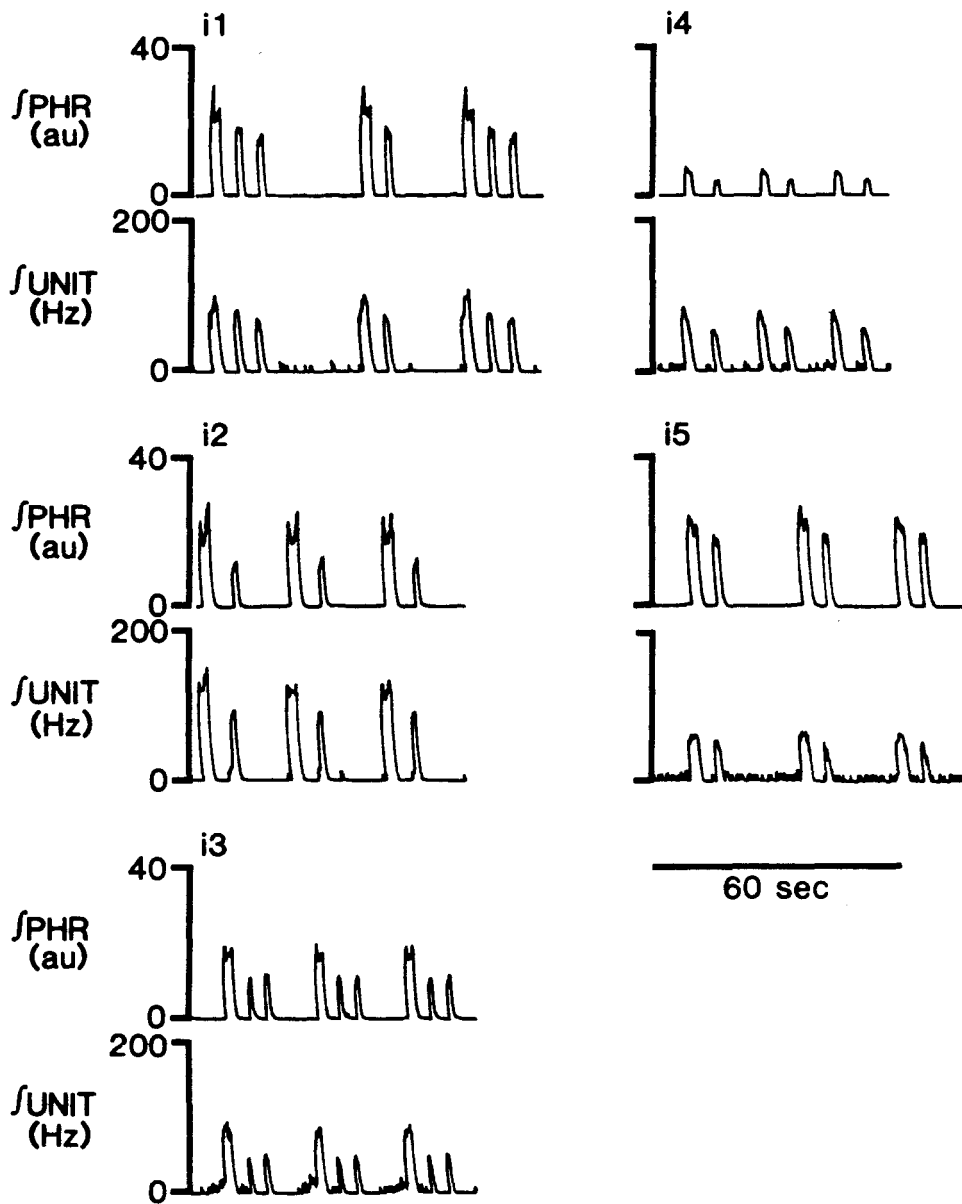


**FIGURE 28.** Illustration of integrated inspiratory cell discharge (UNIT) in spikes/second (Hz) and the corresponding integrated phrenic nerve discharge (PHR) in arbitrary units (au) for 5 inspiratory cells recorded in Biot breathing from 4 cats.

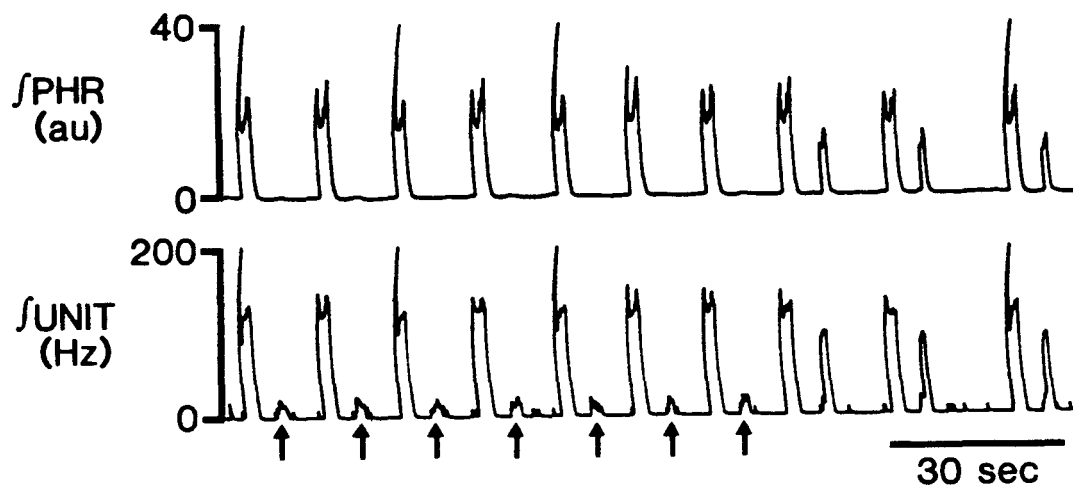


**FIGURE 29.** Illustration of integrated inspiratory cell discharge (UNIT) in spikes/second (Hz) and the corresponding integrated phrenic nerve discharge (PHR) in arbitrary units (au) for 1 inspiratory cell. The arrows mark bursts of inspiratory cell discharge for which there was no corresponding PHR discharge.

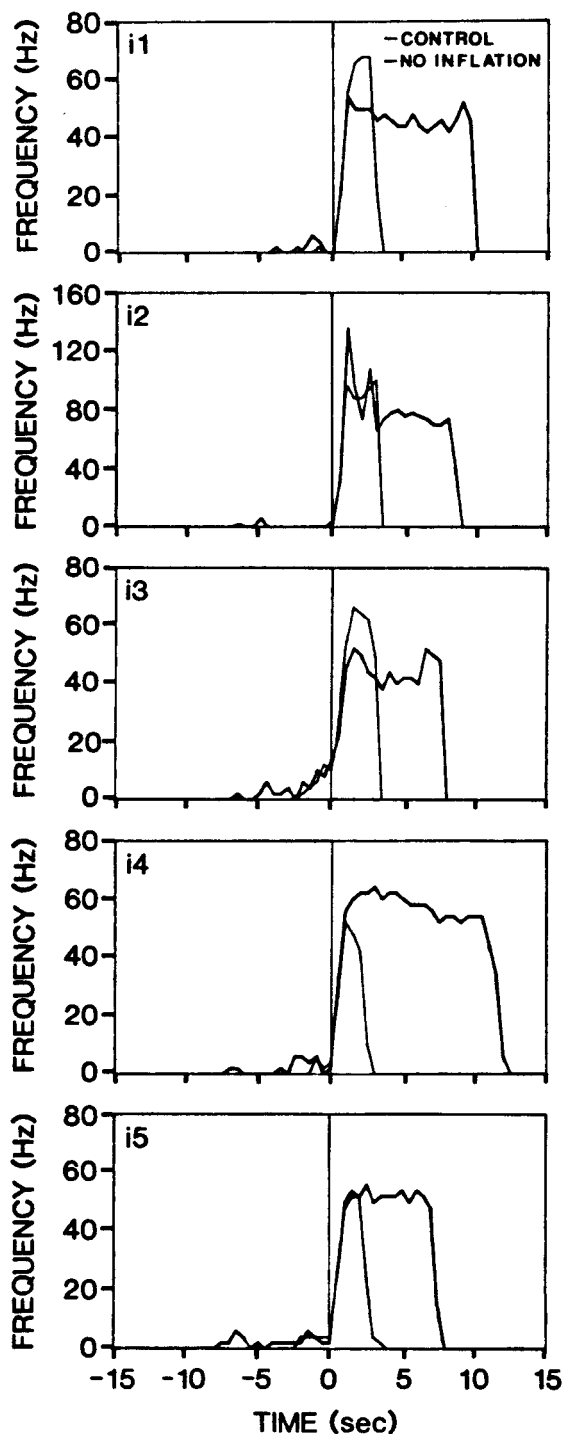


**FIGURE 30.** Cycle-triggered histograms (bin width=0.5 sec) for 5 inspiratory cells recorded in control conditions and when inflation was withheld for one cycle in Biot breathing. The apneusis which resulted from withholding inflation was terminated by turning on the respirator after 8 seconds. Unit discharge frequency is plotted as a function of time with time 0 representing the onset of inspiratory activity in the phrenic nerve.

of inspiratory activity in the phrenic nerve. All 5 cells began discharging prior to phrenic onset. With the initiation of inspiration the activity of the cell increased rapidly to a maximum and showed an equally rapid decline. When inflation was withheld (darker trace),  $T_i$  increased in length from  $2.49 \pm 0.16$  seconds to  $9.21 \pm 0.75$  seconds. The duration of the burst of inspiratory cell discharge likewise increased. However, no changes in peak discharge frequency were observed.

The characteristics of the inspiratory cell discharge are graphed in Figure 31. Withholding inflation resulted in a significant increase in the duration of the burst of inspiratory cell discharge. The number of spikes/burst also increased significantly, however, the peak discharge frequency was not altered by withholding inflation. The onset of activity in the inspiratory cells as compared to the onset of phrenic nerve activity was  $-30 \pm 10$  milliseconds in control, indicating that the rapid increase in inspiratory cell activity slightly preceded that of the phrenic. When inflation was withheld, the measured onset time was  $-40 \pm 20$  milliseconds which was not significantly different.

## 2. Expiratory cell activity

The integrated activity of the 12 expiratory cells in relation to the corresponding phrenic nerve activity is shown in Figure 32. All cells were silent during inspiration. The decline of expiratory cell activity was very rapid and occurred coincident with the start of the phrenic burst. The cells recorded showed phasic modulation with each phrenic burst such that cell activity was present during the short expirations within the cluster as well as during the phase of central apnea. In all cases, expiratory cells discharged throughout the apneic phase.

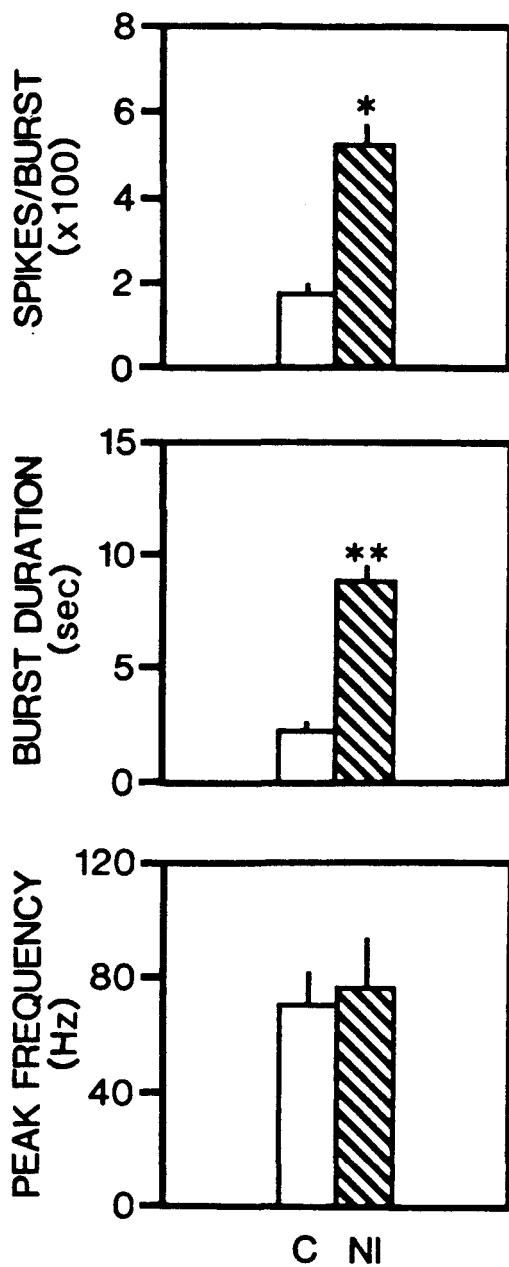


**FIGURE 31.** Responses of 5 inspiratory cells in control (C) conditions and when no inflation (NI) was given in Biot breathing. Variables plotted include: number of spikes per burst, the duration of the burst, and the peak discharge frequency. (\*p less than 0.05 or \*\*p less than 0.01 as compared to corresponding control value).

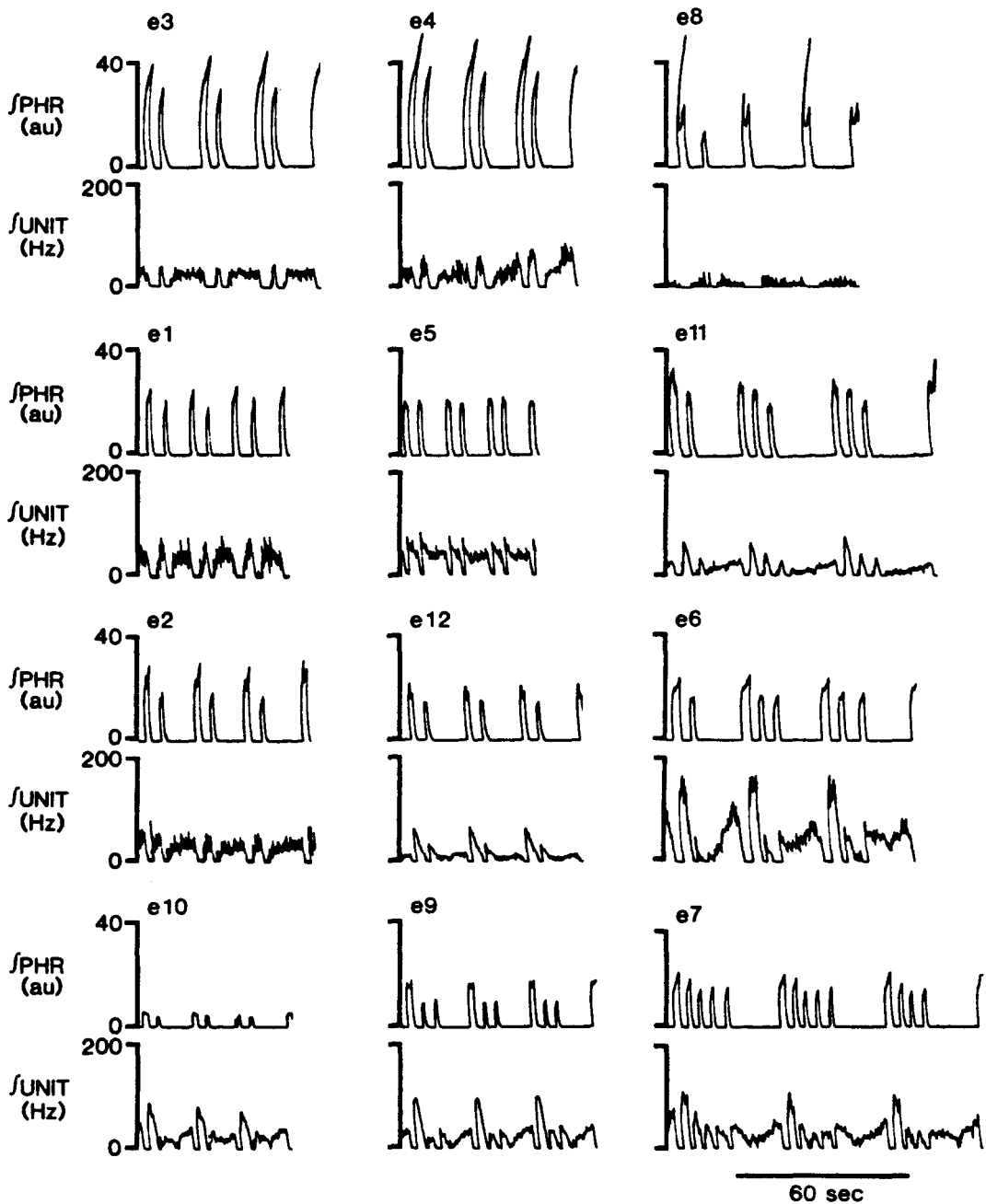
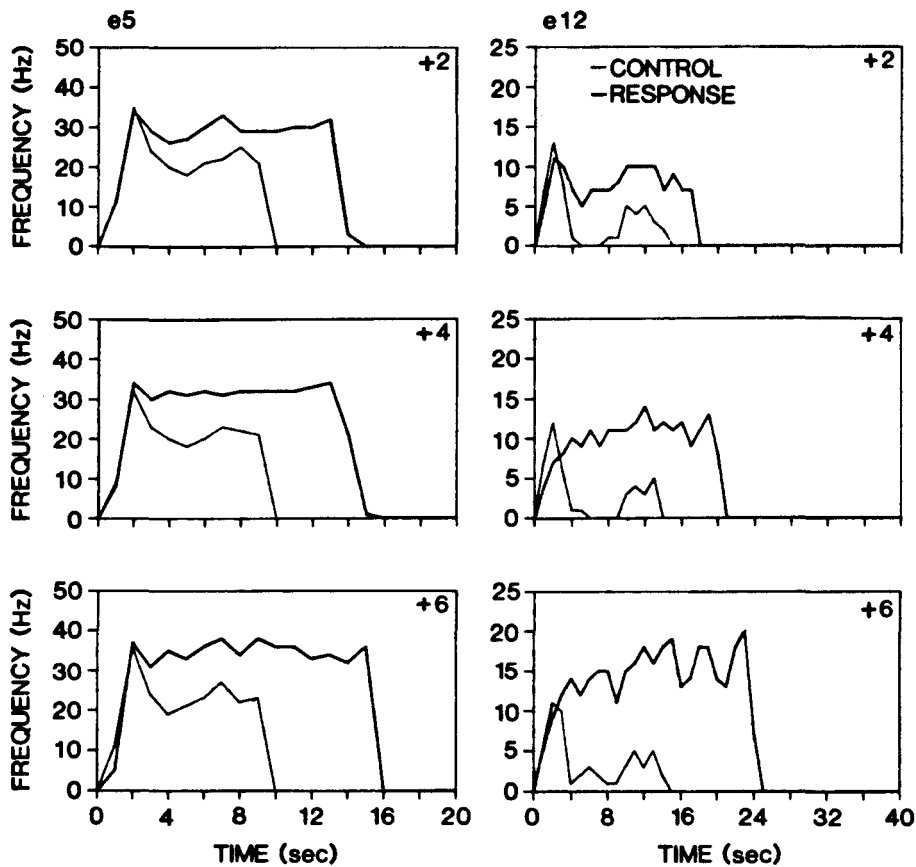


FIGURE 32. Illustration of integrated expiratory cell discharge (UNIT) in spike/second (Hz) and the corresponding integrated phrenic nerve discharge (PHR) for 12 cells recorded in Biot breathing from 8 cats.

Application of 2, 4, and 6 cm H<sub>2</sub>O PEEP resulted in prolongation of the duration of central apnea, accompanied by alterations in the discharge of the expiratory cells recorded. In 2/12 cells, the duration of the expiratory discharge was increased by PEEP but there was no significant change in the peak discharge frequency attained with addition of any level of PEEP. An example of this type of response is shown by cell e5 in Figure 33. In 3/12 cells, the duration of the expiratory burst was also increased by PEEP but peak discharge frequency was only increased by 6 cm H<sub>2</sub>O PEEP. This type of response was demonstrated by cell e12 as shown in Figure 33.

Two types of cell discharges were observed in which the peak discharge frequency did change with the addition of PEEP. In 4/12 cells, the peak discharge frequency significantly increased with the addition of greater amounts of PEEP as illustrated by cell e9 in Figure 34. In contrast to this were the 3/12 cells which showed the greatest increase in discharge frequency when 2 cm H<sub>2</sub>O PEEP was added, as illustrated by cell e8 in Figure 34. The increase in discharge frequency progressively decreased as greater degrees of PEEP were applied. Therefore, the response of expiratory cells to PEEP was similar to that of the CIHG nerves, i.e., a heterogeneous group.



**FIGURE 33.** Cycle-triggered histograms (bin width=1.0 sec) plotted for 2 expiratory cells in response to application of 2, 4 and 6 cm H<sub>2</sub>O positive end-expiratory pressure for a single apneic phase in Biot<sub>2</sub> breathing. Discharge frequency is plotted against time with time 0 representing the onset of inspiration.

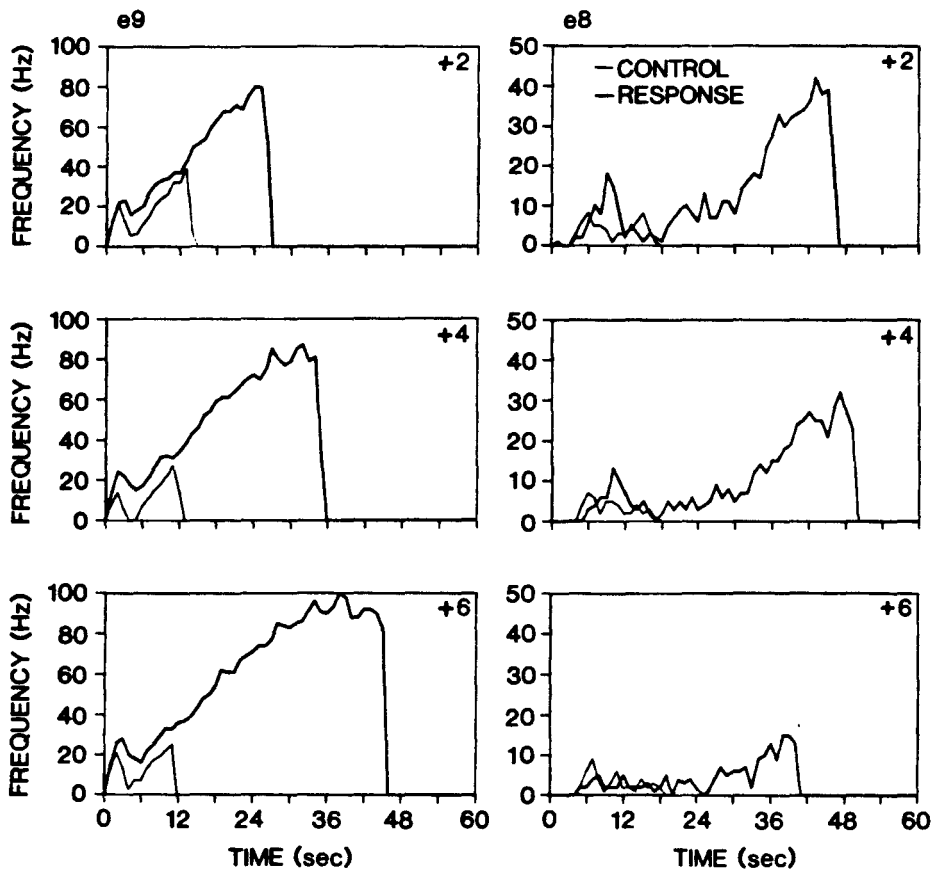


**FIGURE 34.** Cycle-triggered histograms (bin width=1.0 sec) plotted for 2 expiratory cells in response to application of 2, 4 and 6 cm H<sub>2</sub>O positive end-expiratory pressure for a single apneic phase in Biot<sup>2</sup> breathing. Discharge frequency is plotted against time with time 0 representing the onset of inspiration.

Characteristics of the expiratory cell burst in unloaded central apneas and in response to PEEP are compiled in Figure 35. The duration of the expiratory cell discharge was increased significantly over the preceding control value by all levels of PEEP. Likewise, the number of spikes/burst was increased significantly as was the the peak frequency by any level of PEEP. However, there were no significant differences between the peak frequency attained at different levels of PEEP. This occurred despite significant changes in  $T_{e1}$ ,  $P_A\text{CO}_2$  and  $P_A\text{O}_2$  with the different levels of PEEP as shown in Table 5.

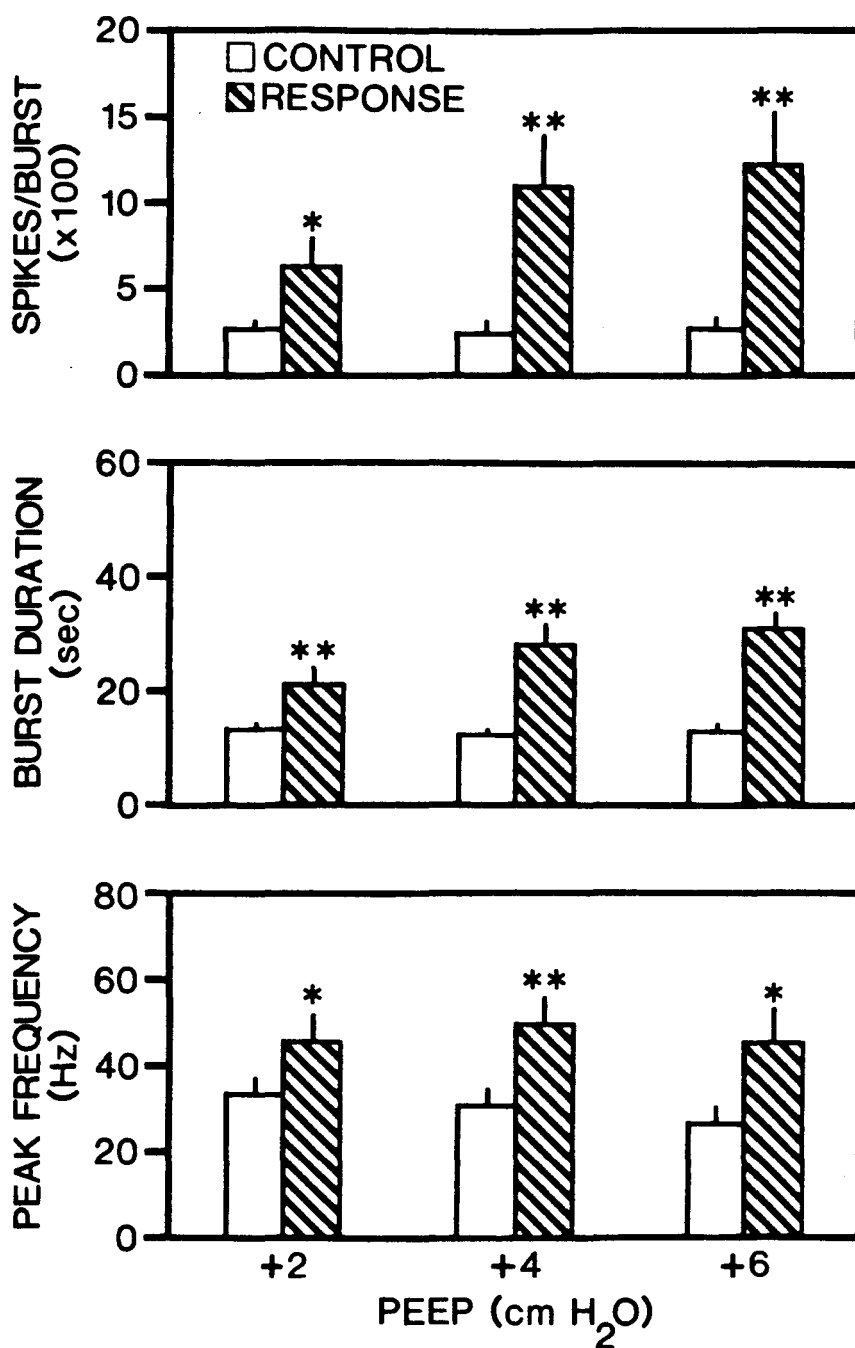


**FIGURE 35.** Responses of 12 expiratory cells in response to application of 2, 4 and 6 cm H<sub>2</sub>O positive end-expiratory pressure (PEEP) for a single apneic phase in Biot Breathing. Variables plotted include: the number of spikes per burst, the burst duration and the peak discharge frequency. (\*p less than 0.05 or \*\*p less than 0.01 as compared to corresponding control value).

TABLE 5  
Respiratory variables for expiratory cell recordings

PEEP (cm H <sub>2</sub> O)	Te <sub>1</sub> (sec)	P <sub>A</sub> CO <sub>2</sub> (mm Hg)	P <sub>A</sub> O <sub>2</sub> (mm Hg)
<u>2</u> Control	12.50±0.99	43±3	102±3
<u>2</u> Response	21.88±2.89 <sup>*</sup>	44±3	101±4
<u>4</u> Control	12.13±1.01	43±3	102±3
<u>4</u> Response	29.56±3.70 <sup>*†</sup>	46±3 <sup>*†</sup>	97±3 <sup>*†</sup>
<u>6</u> Control	12.54±0.91	44±3	102±3
<u>6</u> Response	33.98±3.25 <sup>*†</sup>	48±2 <sup>*†</sup>	94±2 <sup>*†</sup>

Values expressed as Mean S.E.M.

<sup>\*</sup>p <0.05 as compared to corresponding control value.

<sup>†</sup>p <0.05 as compared to response at 2 cm H<sub>2</sub>O PEEP.

## CHAPTER VI

### DISCUSSION

The components of the respiratory system: the central pattern generator, the efferent outflows to respiratory muscles and the chemoreceptor and mechanoreceptor afferent feedbacks, have been extensively studied in eupnea. However, eupneic breathing is not the exclusive output of the respiratory pattern generator. Sustained oscillations in respiratory output are observed in a variety of circumstances. Very few systematic studies of periodic breathing patterns have been attempted. Therefore, the present study represents a unique contribution to the literature. The periodic pattern, Biot breathing, was characterized with regards to the discharge of motoneurons innervating the diaphragm, laryngeal, and abdominal muscles and the discharges of respiratory cells in the medulla. Lung volume feedback modulation of the pattern was studied by the use of positive end-expiratory pressure (PEEP).

#### A. Characteristics of the Biot pattern

The Biot pattern consists of clusters of breaths separated by periods of central apnea, as revealed by the absence of phrenic nerve activity (Figure 8). From control systems analysis, several factors are known to predispose an otherwise stable pattern to one of periodic breathing. These include an increase in feedback delay, an increased controller gain and a reduction in system damping or a decrease in the buffer for the feedback signal (95). The factors which are crucial to the development of the Biot

pattern in the cat include the successful placement of lesions within the pontine respiratory group (PRG) and intact pulmonary stretch receptor feedback.

#### I. Factors predisposing to Biot breathing

In all cats in which Biot breathing was observed, lesions were placed within the region of the PRG (Figures 9, 19 and 26). Lesion borders indicated in these figures represent the minimum area of destruction as the tracings were made of the areas of tissue destruction in unstained sections. Actual lesion dimensions were most likely larger. In no case was Biot breathing observed when lesions were placed outside of the PRG. This supports previous conclusions that Biot breathing is dependent, in part, upon PRG destruction (184). However, some cats with bilateral PRG lesions retained a eupneic-like pattern, albeit at a slower frequency. Thus, lesion placement is but one factor in the genesis of Biot breathing in the cat.

Lesion placement within the PRG promotes the development of Biot breathing by virtue of two factors: increasing controller gain and decreasing system damping. Bilateral destruction of the PRG results in significant elevations of the end-tidal  $\text{CO}_2$  levels in the cat (166,184). Not only is resting ventilation depressed but the minute ventilation response to hypercapnia is also decreased (161,166). The resultant hypercapnia and hypoxia lead to a shift to the non-linear, hyperbolic portion of the oxygen ventilatory response curve (52). This increase in controller gain accompanied by the small oxygen stores in the body increases the potential for development of periodic breathing. This statement is supported by the observations that hypoxia can result in periodic breathing in anesthetized cats (50) and in man sleeping at altitude (26,185). Therefore, PRG lesions

can promote periodic breathing by decreasing  $\text{CO}_2$  sensitivity and shifting to the hypoxic region of the ventilatory response curve.

Intact pulmonary stretch receptor feedback is necessary for the conversion of the respiratory pattern from one characterized by apneustic breaths to one characterized by periods of apnea in the PRG lesioned cat. Withholding inflation (functional vagotomy), results in the development of apneusis which continues until terminated by lung inflation (Figure 3). The development of the apneic period is dependent upon intact volume feedback. Increasing volume feedback, by application of PEEP, produces Biot breathing in some cats in which PRG lesions alone do not result in the pattern (183). The length of apnea is determined by the interaction between chemoreceptor and pulmonary stretch receptor afferents, such that apnea is prolonged when  $\text{CO}_2$  sensitivity is low or inflation volume is high (190). Therefore, the decreased  $\text{CO}_2$  sensitivity (161,166) and the larger tidal volume resulting from PRG lesions interact to initiate a distinct period of apnea.

Decerebration and the resultant blood loss could be a factor in the genesis of Biot breathing in this model. Increased feedback delay, which would result from a lower cardiac output or hypotension, is one factor which predisposes to periodic breathing (95). Increasing feedback delay by artificially lengthening the carotid arteries (97) leads to the appearance of Cheyne-Stokes respiration. However, it is unlikely that low cardiac output or hypotension contributed to the development of periodic breathing in these cats because mean arterial pressures were greater than 90 mm Hg. Also, Biot breathing never developed in cats without PRG lesions when decerebration was successful (as judged by rapid hemostasis following decerebration). The patterns observed in this study were indistinguishable in

quality from those observed in pentobarbital anesthetized cats in which blood loss was not a consideration (184).

## 2. Biot and eupneic breathing contrasted

The Biot breathing pattern represents a significant alteration from eupnea with regards to both timing and depth (Table I). Inspiratory duration ( $T_i$ ) is significantly increased in the Biot pattern. This correlates with previous observations in which apneusis developed following PRG lesions in anesthetized, vagotomized cats (41,101,126,141,150,165,175,177,178,182) and is consistent with the concept that PRG neurons contribute an excitatory input to the postulated off-switching system (57,188).

Expiratory duration ( $T_{e_s}$ ) is also increased by PRG lesion. A linear relationship has been demonstrated between  $T_i$  and the duration of the subsequent expiration (54,56). Therefore, the lengthening of  $T_{e_s}$  may result from the increase in  $T_i$ . This would be consistent with models of the control of expiratory duration in which the accumulated negative feedback during inspiration determines the level from which an inspiratory inhibitory process decays (57,63,194).

Biot breathing is characterized by an increase in tidal volume ( $V_T$ ) as compared to control. This correlates with observations that PRG lesions increase the volume threshold for termination of inspiration (24,75,81,115). Therefore,  $V_T$  is significantly elevated and  $T_i$  increases in duration (160,165).

The peak integrated value of phrenic nerve activity is proportional to  $V_T$  (70). Tidal volume increases significantly with PRG lesions (160,165,184) but this was not reflected by an increase in peak integrated phrenic nerve activity (Table I). This may be due to a decrease in phrenic nerve viability

and/or nerve-electrode contact with time. However, the proportionality between peak phrenic nerve activity and  $V_T$  has only been demonstrated in eupnea (70). Other studies have failed to demonstrate an increase in peak integrated phrenic nerve activity following PRG lesions (24,162). Therefore, it may be possible that  $V_T$  continues to increase after phrenic nerve activity has reached a plateau in the unparalyzed, PRG lesioned animal.

Because the respirator was triggered by phrenic nerve activity, the volume required to terminate inspiration should be correlated with tracheal pressure. There are limitations to the use of tracheal pressure to measure tidal volume, however. The first is that the compliance measurement used in calculation of  $V_T$  came from cats other than those used in this study (2). Secondly, static compliance is greater than dynamic compliance as there is no resistance to airflow in the measurement of static compliance. Thirdly, compliance is a function of lung volume; at greater lung volumes compliance decreases. Calculation of inspiratory capacity for each cat revealed that the maximal  $V_T$  computed was smaller than inspiratory capacity. Therefore,  $V_T$  measurements are interpreted as directional changes only.

Despite the increases in  $V_T$  (Table 1), hypoventilation results due to the prolongation of  $T_i$ ,  $T_{e_s}$  and the appearance of  $T_{e_l}$  in Biot breathing. Thus, the  $P_{A}CO_2$  rises and  $P_{A}O_2$  falls. The rise in  $P_{A}CO_2$  results from the decreased  $CO_2$  sensitivity attributed to PRG lesions (161,166).

#### B. Respiratory responses to PEEP

Positive end-expiratory pressure decreases the rate of expiratory airflow and elevates FRC. Increases in FRC increase the discharge frequency of single PSR afferents (66,87,139). In the present study, PEEP was used to increase FRC to study PSR modulation of respiration. However,

PEEP does not affect the respiratory system solely. Clinically, PEEP is used to increase FRC, prevent the closure of atelectic alveoli and thus, improve arterial oxygenation. The improvement in  $O_2$  saturation is countered by a decrease in cardiac output which occurs with progressive increases in PEEP (62). Venous return and left ventricular function are depressed due to the increase in intrathoracic pressure (49). For this reason, low levels of PEEP (2, 4, and 6 cm  $H_2O$ ) were applied for relatively short periods of time (less than 10 minutes). No significant decreases in mean arterial pressure or increases in heart rate were observed with any level of PEEP indicating that cardiovascular influences were minimized by the low levels of PEEP.

#### 1. Multiple breath responses

Minute ventilation was significantly decreased by the addition of PEEP in both eupneic and Biot breathing (Figure 13). These results were similar to those from anesthetized cats in which PEEP of 0-15 cm  $H_2O$  (38) and expiratory threshold loads of 5 and 10 cm  $H_2O$  (87) resulted in decreased ventilation and increased  $CO_2$ . Alternately, Muza and co-workers (140) found no change in ventilation and end-tidal  $CO_2$  in response to elevation of FRC for 60 minutes.

The most distinctive alterations in respiratory variables in response to application of PEEP were increases in expiratory duration ( $Te_s$ ) in eupnea and in the duration of apnea ( $Te_l$ ) in Biot breathing (Figures 10-12). The classic explanation for this observation is that PSR discharge is increased by the elevated FRC and  $Te$  is thus prolonged due to the Breuer-Hering expiratory prolongation reflex. Both lung inflation and stimulation of vagal afferents during expiration result in expiratory prolongation due to PSR activation (81,114). Thus, the increase in  $Te_s$  in eupnea, and the increase in

$T_{e1}$  in Biot breathing in response to PEEP, probably arise from increased PSR discharge. This does not, however, rule out the possibility that extravagal afferents might elicit this response.

However, the increase in FRC results in an increase of the lung buffer for  $O_2$  and  $CO_2$ . Therefore, the time course of changes in arterial  $CO_2$  and  $O_2$  would be altered such that a longer time would elapse before  $CO_2$  rose to the threshold level to activate the next inspiration. This possibility is excluded by several lines of evidence. Prolongation of  $T_e$  occurs even when changes in arterial blood gases are prevented by cardiopulmonary bypass (17,104). If PEEP prolonged  $T_e$  simply by slowing the rate-of-rise of arterial  $CO_2$ , the  $CO_2$  levels at the end of expiration would not be different from control. However, in this study,  $T_e$  prolongation by PEEP was accompanied by significant increases in  $P_A CO_2$  and decreases in  $P_A O_2$  (Figures 12 and 13) in eupneic and Biot breathing.

End-tidal measurements of alveolar gas tensions are subject to error. If the exhaled volume is sufficiently low, the gas sampled by the analyzer will not reflect alveolar air but dead space air and the end-tidal  $CO_2$  measured will be erroneously low. However, in these studies the possibility of inaccurate  $CO_2$  measurements was minimized by increasing the inflation pressure (and thus the exhaled volume) transiently. That an accurate  $CO_2$  measurement was being made was indicated by a fall in the recorded end-tidal  $CO_2$  with this procedure. In support of the accuracy of end-tidal measurements in this study are the data reported in Figures 12 and 13. The largest increases in  $CO_2$  and decreases in  $O_2$  were observed when the decreases in  $V_T$  were largest (with 4 and 6 cm  $H_2O$  PEEP in Biot breathing). Therefore, the end-tidal  $CO_2$  increased when, if the

measurements were inaccurate, a decrease should have been observed. It would be ideal to confirm the end-tidal measurements with arterial measurements, but it is very difficult to accurately sample the arterial blood at precise times corresponding to particular phases in the Biot breathing pattern. The end-tidal  $\text{CO}_2$  values measured in response to PEEP in this study were similar in magnitude to changes in end-tidal and arterial  $\text{CO}_2$  observed with expiratory threshold loads of 10 cm  $\text{H}_2\text{O}$  in the cat (87).

Variable responses of  $V_T$  to application of PEEP in eupnea have been reported in the literature. Small increases in  $V_T$  were observed in lightly anesthetized cats in response to expiratory threshold loads of 5 and 10 cm  $\text{H}_2\text{O}$  (87). However,  $V_T$  was decreased by PEEP application of 0-15 cm  $\text{H}_2\text{O}$  in anesthetized cats (37,38). Many factors come into play in the maintenance of  $V_T$  at elevated lung volumes including the decreases in compliance and activation of expiratory muscles. The decreases in  $V_T$  observed in the present study may be due, in part, to elimination of active expiratory effort by neuromuscular blockade.

Despite the decreases in  $V_T$  with PEEP, the total end-inspiratory lung volume was increased due to the elevation of FRC. Inspiratory duration was not changed in either eupnea or Biot breathing (Figure 12). The increase in end-inspiratory lung volume would be predicted to decrease  $T_i$  by the Breuer-Hering inspiratory shortening reflex. Several possible explanations for the maintenance of  $T_i$  exist. The first is that adaptation of PSRs may occur with prolonged elevation of FRC. However, PSR discharge is significantly elevated over control values even after 60 minutes of elevated FRC (139). Secondly, the sensitivity of the inspiratory terminating reflex may be altered. An upward shift in the  $V_T/T_i$  relationship has been

demonstrated at elevated FRC, such that the volume needed to terminate inspiration at any given time is increased (64,87,140). Therefore, a greater total end-inspiratory lung volume would occur with no change in  $T_i$ , as observed in this study. A similar shift in the  $V_T/T_i$  relationship has been shown to occur in response to hypercapnia (53). The increase in total end-inspiratory lung volume may be related to the increase in alveolar  $CO_2$  observed.

In conclusion, the primary result of prolonged PEEP application is a decrease in minute ventilation with corresponding changes in  $CO_2$  and  $O_2$  (Figure 13) in both eupnea and Biot breathing. Ventilation is decreased due to decreases in both frequency and  $V_T$ . The decrease in frequency occurs primarily as a result of changes in the duration of  $T_{e_s}$  in eupnea and  $T_{e_l}$  in Biot breathing. The major differences between the response of eupneic and Biot breathing to elevated FRC are primarily quantitative. The Biot pattern is altered in quality in response to PEEP application. However, the change in pattern from multiple breaths per cluster to single breaths per cluster with higher levels of PEEP (Figure 14) is not accompanied by any significant changes in either ventilation or end-tidal  $CO_2$  and  $O_2$  as compared to the responses at lower levels of PEEP (Figure 13). Therefore, it appears that the pattern is controlled for level of ventilation and that despite changes in pattern, the same ventilation is achieved.

## 2. Habituation to PEEP

As mentioned previously, responses of minute ventilation to application of PEEP are variable in the cat. Decreases in ventilation and increases in  $CO_2$  were observed in response to PEEP of 0-15 cm  $H_2O$  (38) and expiratory threshold loads of 0-10 cm  $H_2O$  (87). However, when FRC was elevated for

60 minutes, no significant changes in ventilation and end-tidal  $\text{CO}_2$  were observed (140). It would appear that the initial reduction in ventilation diminishes as FRC elevation is maintained.

Similar changes in the respiratory response to PEEP with time were observed in the present study. The major factors reducing ventilation in eupnea and Biot breathing were the prolongation of  $T_{e_s}$  and  $T_{e_l}$ , respectively. As the duration of PEEP application is increased, the duration of  $T_{e_s}$  in eupnea and  $T_{e_l}$  in Biot breathing decrease (Figures 22 and 24). There are several possible explanations for this progressive decrease in  $T_e$  and increase in ventilation with time. The first is that there may be adaptation of PSR with time such that  $T_e$  would return to control values. As mentioned previously, evidence exists that complete adaptation of PSRs does not occur when FRC is elevated for 60 minutes (139). Therefore, the return of  $T_e$  toward control values may be due to habituation, which is defined as a gradual diminution of the response to a repeated standardized stimulus, which is independent of sensory adaptation. Habituation may occur in this situation as shown by the decreased sensitivity of the inspiratory terminating reflex when FRC is elevated (64,140). However, the habituation in this case does not allow for complete restoration of ventilation to control values as in other studies (87,140). The time of PEEP application differed markedly between the study of Muza and co-workers (140) and this study. Thus, the compensation to elevated FRC appears to be a time-dependent process. Possibly, the duration of  $T_{e_s}$  in eupnea would have returned to control values had the PEEP been maintained. However, it is unlikely that complete habituation to PEEP application would have been observed in Biot

breathing as application of 6 cm H<sub>2</sub>O PEEP resulted in severe hypercapnia and hypoxia in some cats tested.

### 3. Determination of Te by chemical and mechanical factors

There is an interaction between chemical and mechanical factors in control of Te. This is demonstrated by the increase in Te<sub>s</sub> in eupnea and Te<sub>i</sub> in Biot breathing caused by PEEP even though CO<sub>2</sub> increased and O<sub>2</sub> decreased. With application of PEEP for a single expiratory phase it was possible to evaluate the contribution of mechanical and chemical factors in the control of Te. It appears that increasing lung volume feedback resets the threshold for inspiratory initiation by chemical feedbacks. Thus, the duration of Te<sub>s</sub> in eupnea and Te<sub>i</sub> in Biot breathing increase progressively (Figure 15) while P<sub>A</sub>CO<sub>2</sub> rises and P<sub>A</sub>O<sub>2</sub> falls (Table 2). Increased chemical drive shortens the duration of Te<sub>s</sub> in eupnea (54,64,90) and Te<sub>i</sub> in Biot breathing (184). Therefore, the durations of expiration and central apnea are increased at the expense of an increased CO<sub>2</sub> and decreased O<sub>2</sub>.

This response may be due, in part, to a decrease in ventilatory response to CO<sub>2</sub> which occurs with expiratory threshold loads in the dog (105). The decreased response to hypercapnia was observed after the vagi were cut, therefore, it does not appear to be modulated by vagal afferents. The decrease in CO<sub>2</sub> sensitivity is not due to a decrease in PSR discharge frequency. Pulmonary stretch receptors have been shown to be CO<sub>2</sub> sensitive in the cat, such that with increases in airway CO<sub>2</sub> discharge frequency decreases (61). However, the discharge rate of PSR declines as airway CO<sub>2</sub> increases from 0 to 30 torr but does not significantly change over the range of 30 to 50 torr which represents the range observed here. Therefore, it appears that the increase in Te duration which occurs even

when  $\text{CO}_2$  increases results from a decreased sensitivity to  $\text{CO}_2$ , possibly mediated centrally.

The sensitivity of  $T_e$  to PSR feedback appears to be increased in Biot breathing as compared to eupnea. When the relative increase in  $T_e$  is plotted against the level of PEEP applied (Figure 17), the slope in Biot breathing is significantly greater than in eupnea, indicating that the sensitivity of the expiratory prolongation reflex is elevated in Biot breathing. Previous studies have reported similar increases in the sensitivity of the expiratory prolongation reflex following bilateral and unilateral PRG lesions (76,81,115). The prolongation of expiration is accompanied by a much greater rise in  $\text{CO}_2$  than occurs in eupnea with the same level of PEEP (Table 2). This correlates with studies indicating that  $\text{CO}_2$  sensitivity is decreased after PRG lesion (161,166).

The degree of expiratory prolongation observed is a function of two factors: the PSR discharge which inhibits the onset of inspiration and the rise in chemoreceptor feedback which promotes the onset of inspiration. Larger inspired volumes prolong expiration to a greater degree due to an increase in PSR discharge. Likewise, a decrease in  $\text{CO}_2$  sensitivity promotes a longer expiration (190). Therefore, the relatively greater prolongation of  $T_{e1}$  with the same level of PEEP results from the larger inflation volume and decreased  $\text{CO}_2$  sensitivity occurring in Biot breathing.

The interaction between chemical and mechanical factors in the control of  $T_{e_s}$  in eupnea and  $T_{e1}$  in Biot breathing is shown in Figure 36. Time zero indicates the beginning of expiration. Chemoreceptor feedback gradually rises ( $\text{CO}_2$  increases,  $\text{O}_2$  decreases) and when a threshold is crossed, expiration is terminated. Elevation of FRC by PEEP results in a

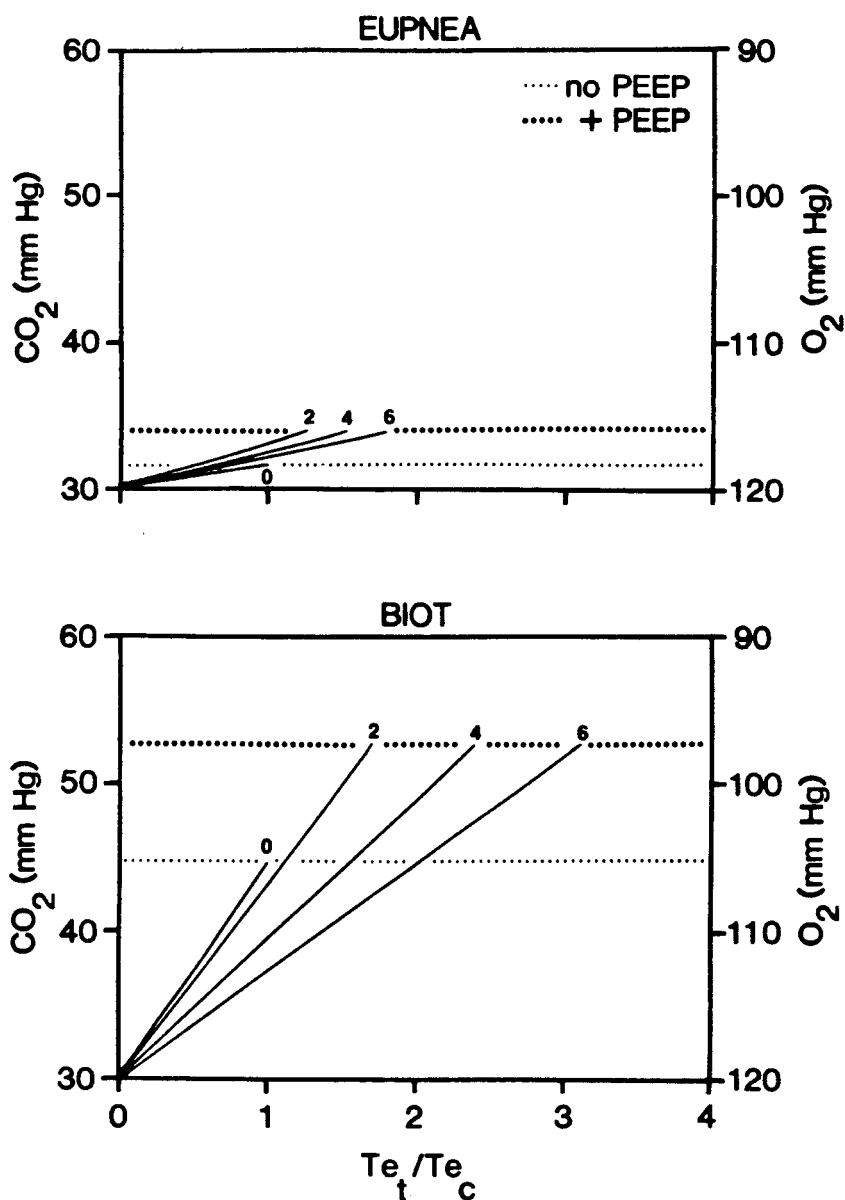


FIGURE 36. Chemical feedbacks ( $\text{CO}_2$  and  $\text{O}_2$ ) plotted against the duration of expiration with PEEP added normalized to the duration of expiration with no PEEP ( $T_{e_t}/T_{e_c}$ ) in eupnea and Biot breathing. The small numbers indicate the level of PEEP added in  $\text{cm H}_2\text{O}$ . As PEEP is increased  $T_e$  is prolonged with an increase in the chemical feedback (heavier dotted line) in eupnea and Biot breathing. Data taken from Figure 17.

decreased rate-of-rise of chemoreceptor feedback which will prolong expiration. However, the threshold at which expiration is terminated is elevated in both eupnea and Biot breathing by the application of PEEP. Therefore, arterial  $O_2$  has to fall to a lower level to stimulate the onset of the next inspiration. The decreased sensitivity to  $CO_2$  resulting from PRG lesion, is shown by the greater chemoreceptor feedback threshold in unloaded Biot breathing as compared to eupnea. The greater elevation of the chemoreceptor feedback threshold in Biot breathing with PEEP is reflective of the greater inspired volumes as compared to eupnea. Thus, the duration of expiration is determined by the interaction of inspiration inhibitory factors (PSRs) and inspiration excitatory factors (hypoxia and hypercapnia). The observation that the chemical threshold for initiation of inspiration is elevated in both eupnea and Biot breathing indicates that the inspiratory inhibitory effect of PSR input resets the threshold for initiation of inspiration by chemical feedback. When lung volume feedback is decreased, the chemical threshold for inspiratory initiation is suddenly lowered. This accounts for the appearance of eupneic breathing when PEEP is removed (Figure 11).

The total end-inspiratory lung volume of the first breath following PEEP application is an indicator of the chemical drive at which expiration is terminated (190). Obviously, the chemical drive at the end of a PEEP prolonged expiration is increased, especially with the higher levels of PEEP in eupnea (Figure 18). Thus, it appears that respiratory drive was increased following the prolonged expiration, which is in agreement with other studies (37,87). However, in Biot breathing, end-inspiratory lung volume was no longer increased with higher levels of PEEP. The lack of increase in

respiratory drive despite large increases in  $\text{CO}_2$  and decreases in  $\text{O}_2$  may be due to PSR overriding chemoreceptor inputs. This may explain, in part, the inability of Biot breathing cats to withstand prolonged elevations of PEEP.

### C. Activities of upper airway and abdominal nerves

The discharge patterns of nerves supplying the upper airway and abdominal musculature have been described in eupnea. The recurrent laryngeal (RL) nerve innervates the laryngeal muscles which regulate laryngeal resistance and thus airflow. The cranial iliohypogastric (CIHG) nerve innervates the muscles of the abdominal wall and thus, is activated during active expiratory efforts. However, the activity patterns of these efferent outflows of the respiratory system have not been recorded in Biot breathing.

#### I. Abdominal nerve activity patterns

Biot breathing is characterized by phasic expiratory nerve activity (Figures 21 and 23). This activity is generally absent in eupnea. The presence of phasic CIHG activity after PRG lesion compares with the release of phasic expiratory activity in the internal intercostals and abdominal muscles by cooling in the area of the retrofacial nucleus (44). Pitts and co-workers identified a region in the ventrolateral pons in which lesions resulted in the production of apneusis in the vagal cold-blocked cat (150). They postulated that interruption of a pathway from the PRG to the medullary respiratory centers was responsible for this effect. Similarly, lesions in the ventrolateral pons lateral to the superior olivary nucleus produced apneusis (141). The areas of these lesions roughly correspond to the areas of cooling. Thus, lesions in areas which result in respiratory patterns resembling those that result from PRG destruction are also involved

in the release of expiratory activity.

It is possible that these two observations are correlated. One explanation for these observations is that both PRG lesion and retrofacial area cooling interrupt a ponto-medullary pathway at two different points along its course. However, relatively few connections have been shown between pontine and NTS respiratory neurons (32,33) by antidromic activation. A more probable explanation is that both insults interrupt the central chemoreceptor function. Cooling of the intermediate area on the ventral surface of the medulla results in phrenic apnea (51). A cooling probe placed in the retrofacial area, very near to the ventral surface also produces phrenic apnea and in addition, releases expiratory muscle activity (44). Lesion destruction of the PRG results in a decreased  $\text{CO}_2$  sensitivity (161,166) and increases in  $\text{CO}_2$  are known to increase the discharge of expiratory bulbospinal cells (5,138) and expiratory abdominal nerves (120). Therefore, the appearance of expiratory nerve activity in Biot breathing is more likely due to the decrease in  $\text{CO}_2$  sensitivity and concomitant increase in  $P_A\text{CO}_2$  which occurs as a result of PRG lesion. It is less likely that the release of expiratory nerve activity is due to disinhibition resulting from the interruption of a pontomedullary pathway by which PRG neurons would normally inhibit rhythmic excitation of expiratory NRA cells.

Abdominal nerve activity in Biot breathing is characterized by an initial augmenting phase followed by a plateau that is maintained during the apneic phase (Figure 23). In eupneic breathing the duration of expiration is shorter such that external oblique muscle EMG shows only the augmenting phase (116) while longer  $T_e$  results in the expression of the plateau phase (120). The augmenting phase occurs early in expiration when contraction of

the abdominal muscles would accelerate the emptying of the lungs, whereas the plateau phase occurs later in expiration when airflow is no longer occurring (189). The plateau phase is thus thought to function in maintaining the diaphragm and rib cage muscles at optimal lengths to facilitate the next inspiratory effort (67,120). The plateau phase may also be related to the maintenance of venous return as hemorrhage in the dog leads to appearance of the plateau phase of abdominal muscle contraction when respiratory movements are eliminated by hyperventilation to apnea (189).

Elevations in PEEP progressively increase FRC. If the diaphragm is to be maintained at its initial operating length, the plateau level of abdominal muscle activity might be expected to increase. In eupnea, peak CIHG activity increases with the application of PEEP (Figure 22). However, in Biot breathing the response to PEEP is variable from cat to cat. In some cases, PEEP increased the plateau level (Figure 23, Cats 1,9,10) while in others, the plateau level was not altered by the application of PEEP (Cat 7). When the responses of all cats were pooled, peak activity of CIHG increased only with 6 cm H<sub>2</sub>O PEEP on the first cluster. This activity was not maintained so that by the fifth cluster of PEEP application, CIHG activity was not significantly elevated with any level of PEEP (Figure 24). Chemical stimuli recruit abdominal muscle activity (90,120) and mechanical loading also increases abdominal muscle activity (37,116). Augmentation of the peak external oblique muscle activity response to hypercapnia is observed when CPAP of 8 cm H<sub>2</sub>O is added, such that the muscle activity is increased even further (110). Therefore, in Biot breathing with PEEP added, a great increase in CIHG activity would be expected due to the mechanical loading and corresponding load-induced hypercapnia. This type of augmentation was

observed in this study in eupneic breathing. Peak CIHG activity was not significantly increased with 4 cm H<sub>2</sub>O until the tenth breath of PEEP application (Figure 22) when CO<sub>2</sub> was elevated significantly (Table 3). However, a similar augmentation in CIHG nerve activity was not observed in Biot breathing. The increase in CIHG activity that was observed with 6 cm H<sub>2</sub>O PEEP in Biot breathing was not maintained by the fifth cluster (Figure 24) despite a dramatic increase in CO<sub>2</sub> (Table 3). Thus, it would appear that after PRG lesion, chemical, as well as mechanical, augmentation of CIHG nerve activity is eliminated. The failure to maintain CIHG activity is not related to an increase in MAP, which would inhibit CIHG activity (189) because there were no significant changes in MAP with any level of PEEP.

The afferent pathway for the recruitment of abdominal muscle activity with mechanical loading is the vagus (37,110). However, extra-vagal fibers may also play a role in the recruitment of abdominal muscle activity as vagotomy does not abolish the transient inhibition of abdominal activity associated with a sudden decrease in airway resistance (154). This extra-vagal pathway may be through intercostal or abdominal muscle spindles which would act to augment alpha motoneuron discharge (154). Increases in FRC would increase the resting lengths of the abdominal muscles which would, by the myotatic reflex, augment abdominal nerve activity. Dorsal root rhizotomy (T<sub>8</sub>-L<sub>3</sub>) abolishes the increase in external oblique muscle EMG activity observed in response to CPAP in the cat (36). Cutting the CIHG nerve for recording would have removed muscle spindle information from that one dorsal root. However, it appears unlikely that this factor explains the lack of recruitment of CIHG nerve fibers in response to PEEP as CIHG activity was observed to increase in some cats.

## 2. Recurrent laryngeal nerve activity patterns

When the respiratory pattern is altered from eupnea to apneusis by cooling the rostral pons in vagotomized, decerebrated cats, the RL nerve shows an apneustic discharge pattern, similar to that of the phrenic nerve (163,164). Thus, when PRG inputs are eliminated, the RL still retains its inspiratory activity. Therefore, it is not unexpected that in Biot breathing, phasic activation of the RL would persist as in eupnea (Figure 20). However, the patterns of phrenic and RL nerve discharges were markedly altered by the transition to Biot breathing as noted in the results. The disappearance of the expiratory-related activity in the RL following PRG lesion has been noted previously (163). This occurred concomitant with the disappearance of the post-inspiratory activity in the phrenic nerve activity (Figure 21). The post-inspiratory phase of declining phrenic activity and RL activation smooths the transition between inspiration and expiration, regulating the emptying of air from the lungs and acting as an expiratory airflow braking mechanism (15). The apparent absence of the post-inspiratory phase following PRG lesions has important implications not only in regards to the regulation of expiratory airflow. This observation also lends credence to the concept that the PRG constitutes an integral part of the central pattern generator for respiration. Thus, the role of the PRG in rhythm generation may be underestimated as hypothesized by St. John (162).

The first breath responses to PEEP of the phrenic and RL nerve amplitudes were normalized to the preceding control values and a regression analysis performed to determine if an increase in PHR activity was correlated with an increase in RL nerve activity. In eupnea, there was a significant relationship between the two and the slope was positive,

indicating that an increase in phrenic nerve amplitude on the first inspiration following PEEP was accompanied by an increase in RL activity. However, following PRG lesion, in Biot breathing, the regression analysis revealed that this relationship no longer persisted (Figure 25). Parallel increases in RL and phrenic nerve activity have been demonstrated in the pentobarbital anesthetized dog in response to both hypercapnic and hypoxic stimuli (186). However, in that study the responses were measured when steady state conditions were reached, whereas the results reported here were transient, first breath responses. Analyzing the breath-to-breath responses to a transient increase in inspired  $\text{CO}_2$ , Haxhiu and co-workers (98) found proportional increases in the EMG of the posterior cricoarytenoid muscle and diaphragm in conscious cats. Because the application of PEEP was associated with increases in  $\text{P}_A\text{CO}_2$  and decreases in  $\text{P}_A\text{O}_2$  it would be expected that directionally similar changes in RL and phrenic nerve activity would occur as seen before lesion. The lack of relationship between the discharges of the two nerves in response to PEEP after lesion is thus unexpected because the chemical changes associated with PEEP were much more dramatic than in eupnea (Table 3).

That this response is lost after PRG lesion implies a role for the PRG in matching the outputs of the upper airway and diaphragm muscles in response to a chemoreceptor stimulus. This matching has important implications for facilitating an increase in inspiratory airflow. The mechanism whereby PRG lesion might alter the linking between inspiratory outflows of the DRG and VRG is unknown but may be related to the decrease in  $\text{CO}_2$  sensitivity associated with PRG lesion (161,166). Projections from PRG neurons to the VRG have been identified by

antidromic activation but whether these connections play a role in the linking of phrenic and RL nerve activities is uncertain (33).

#### D. Discharges of respiratory cells in Biot breathing

This study represents the first recordings of respiratory cell activities in Biot breathing. This was not a trivial accomplishment insofar as the spontaneous respiratory frequencies were very low and volume inflations of the lung were large, resulting in movement of the brainstem.

##### I. Inspiratory cell discharges

The inspiratory cells recorded typically showed discharge patterns which closely followed that of the phrenic nerve. Inspiratory cells were located from 3-4 mm lateral to the midline, 2-4 mm below the dorsal surface and 0-2 mm caudal to the obex (Figure 27). These coordinates approximate the location of the NRA (125). At the level of the obex, in the cat, there is an area of intermixing of inspiratory and expiratory cells which are located in the rostral and caudal portions of the NRA, respectively (130). The expiratory cells recorded in this study were typical of NRA expiratory cells in patterns of discharge (see next section) but not of NA laryngeal motoneurons (30,131). The inspiratory cells recorded were frequently encountered in the same electrode penetration as an expiratory cell which was characterized as a NRA cell. Therefore, it seems likely that these cells were NRA inspiratory cells.

The onset of inspiratory cell discharges usually precede the initiation of phrenic nerve activity by 30 msec. The cells rapidly attain their peak discharge rate followed by an abrupt termination of activity. (Figure 28). The patterns of phrenic nerve discharge and inspiratory cell activity closely parallel each other which is similar to the observation of Merrill (131) who

found that NRA inspiratory cell discharge mirrored the development of tension in the diaphragm. The cells recorded here correspond with the "late-inspiratory" cells identified by Merrill (131), all of which were antidromically activated from the cervical cord and had demonstrable arborizations within the phrenic nucleus and thoracic cord. Therefore, it seems likely that the inspiratory cells recorded in this study might have been cells which activate phrenic and intercostal motoneurons. This conclusion is supported, in part, by the observation that when inflation was withheld and apneusis developed, apneustic discharge patterns were observed for all cells (Figure 30), although apneustic discharge also develops in the RL nerve (163,164). The formation of this discharge pattern when inflation was withheld indicates that the cells were indeed respiratory cells, and that they received central inspiratory activity (CIA). The lack of significant increases in the peak discharge frequency is surprising, since withholding inflation in the PRG lesioned cat results in an apneustic breath, the amplitude of which is greater than the non-apneustic control (75,81). These results correlate, however, with observations in Dial anesthetized and encephale isole (decorticate) cats in which no increase in discharge frequency of VRG inspiratory cells was observed in response to airway occlusion in eupnea (31). Within an individual cat, the discharge of each inspiratory cell responded to the no inflation test in the same direction as did the phrenic nerve discharge. The directions of response were different between cats, therefore no significant changes in discharge frequency were observed (Figure 31).

Perhaps the most intriguing finding concerning inspiratory cells is the activity of cell i2 (Figure 29). This cell illustrates a two discharges/cluster

pattern while the phrenic nerve discharges once per cluster. As the phrenic nerve pattern spontaneously shifts to two/cluster, it can be seen that the second burst of cell activity corresponds with the second breath of the cluster. As the activity of the phrenic nerve appears in that second breath, the activity of the inspiratory cell increases, indicating that either it is facilitated by PSR feedback or that the increase in CIA which results in the second phrenic burst facilitates this cell. The latter explanation is more likely as there is no phasic PSR feedback during apnea when the cell was spontaneously active. The importance of this observation is that phrenic apnea does not necessarily imply absence of central inspiratory activity. Thus, researchers who define phrenic silence as the lack of respiratory oscillator activity may be in error (91). It is tempting, also, to conclude that the "central apnea" observed in Biot breathing is not necessarily a complete absence of inspiratory activity, but that this activity may simply not reach a critical threshold level to drive the phrenic motoneuron pool. It is unjustified to base a conclusion on a single observation and further experiments are warranted. However, this presents an intriguing addition to our concept of pattern generation.

## 2. Expiratory cell discharges

The expiratory cells recorded were located from 3-4 mm lateral, 1-4 mm below the dorsal surface and 0-3 mm caudal to the obex (Figure 27). These coordinates are consistent with the location of the NRA cell column of the VRG (125). It is unlikely that these cells were located in the NTS not only because of their deep locations, but because the NTS is noted for its paucity of expiratory cells (20,74). These cells were not NA laryngeal motoneurons as demonstrated by their firing patterns (Figure 32). Expiratory

laryngeal motoneurons discharge at the onset of expiration, reach peak frequency early and cease firing early in expiration (30,31). In addition, the absence of early expiratory activity in the RL nerve in Biot breathing while CIHG nerve activity was present (Figure 21) lends further support to the conclusion that the expiratory cells were not laryngeal motoneurons.

These cells have the characteristic discharge of NRA expiratory cells which show an incrementing discharge in expiration (30). These cells show a low initial rate which gradually increases to a plateau or peak late in expiration (131). Discharge of the NRA expiratory cells is inhibited during inspiration, as demonstrated by chloride reversal of IPSPs (158). This inhibition is believed to be derived from early burst NRA inspiratory neurons (131,132). Expiratory cells recorded in this study showed this type of discharge pattern (Figure 32). Cell discharge frequency reached a plateau during central apnea which was consistent with that of NRA expiratory cells (131). A similar plateau phase is observed in the discharge of the external oblique muscle EMG when the expiratory phase is sufficiently long (120) while only the incrementing phase is seen when  $T_e$  is short (116).

These cells might activate abdominal motoneurons as 98% of NRA expiratory cells were found to be antidromically activated from the contralateral spinal cord (130,131). Axons from these cells terminate from the  $T_1$ - $L_3$  levels (82,131) and have been shown to monosynaptically activate thoracic expiratory motoneurons (113). Further support for this conclusion is drawn from observing that the discharge patterns of CIHG motoneurons (Figure 23) and the expiratory cells recorded (Figure 32) are very similar. Both discharge patterns include: an abrupt onset of activity coincident with the termination of inspiration; a plateau phase; and an equally abrupt

termination of activity when the next inspiratory phase begins.

The demonstration that NRA expiratory cells fire throughout the protracted phase of central apnea does not imply that these cells are the source of inspiratory inhibition and the resultant apnea. Evidence suggests that NRA expiratory cells do not inhibit inspiratory premotor cells because no intramedullary axon collaterals have been demonstrated for these cells (6,130,131). The source of inspiratory inhibition, according to current models of pattern generation, is most likely the late peak expiratory cells of the Botzinger complex (BotC) which have inhibitory connections with the DRG (108,123,132). However, this does not eliminate inhibition at the level of the phrenic motor nucleus. Active expiratory phase inhibition of phrenic motoneurons does exist, as demonstrated by chloride reversal of the expiratory hyperpolarization (21). Injection of HRP into caudal regions of the NRA where expiratory activity is recorded, results in an equal density labeling in the phrenic motor nucleus and thoracic ventral horn (82). Although spike-triggered averaging of synaptic noise revealed monosynaptic inhibition of phrenic motoneurons from expiratory cells in the BotC, no inhibition could be demonstrated from the caudal NRA (134).

Expiratory NRA bulbospinal cells are facilitated by maintained lung inflations (31). Expiratory resistive loads increase the firing rate, burst duration and number of spikes per burst of NRA expiratory cells (7). These cells have also been shown to be responsive to CO<sub>2</sub> with hypercapnia increasing the peak discharge frequency (5,138). The results shown in these studies are in agreement with those of the present study (Figure 35). However, the facilitation of expiratory cells is inconsistent with the observation that PEEP did not significantly alter the peak discharge

frequency of the CIHG nerve (Figure 24). Several explanations are possible. The cell discharges were recorded for one apneic phase in response to PEEP while the nerves were followed for 5 phases. Application of PEEP resulted in a significant increase in the peak discharge frequency of the CIHG nerve only at 6 cm H<sub>2</sub>O (Figure 24). Therefore, the cats used for the recording of cell discharges may have been more sensitive to the level of PEEP applied. Using  $T_{e1}$  prolongation as an index of sensitivity to PEEP, it can be seen that the prolongation was greater in the cats in which CIHG activity was recorded (compare Figure 24 and Table 5). Therefore, it cannot be argued that expiratory cell discharge reached a higher frequency with PEEP while that of the CIHG nerve did not simply because of a greater prolongation of  $T_{e1}$ . If the cell discharges were followed for more than one apneic phase, it is possible that peak frequency would decline such that it would no longer be significantly elevated as with the CIHG nerve activity at 6 cm H<sub>2</sub>O. However, the discharge frequency of the cells does not increase progressively with increases in load as was found for NRA expiratory cells with resistive loading (7).

Neurograms represent the summed activities of individual nerve fibers. The heterogeneity of responses of CIHG activity in response to PEEP would suggest that the balance of activity of all the nerve fibers determines the compound nerve activity recorded. Thus, CIHG activity increased in some cats in response to PEEP while in others, it did not. The net effect was that no significant increases occurred. The fact that cell discharge showed a significant increase may simply be due to the random sampling of cells and recording from more cells which showed an increase in discharge in response to PEEP. Also, NRA expiratory cells are active even when there is

no demonstrable abdominal muscle activity (44). Therefore, expiratory cell activity does not necessarily imply expiratory muscle activity and indicates that a critical mass of cells must be activated before muscle activity is observed. For this reason, total nerve activity remains the better indicator of actual muscle activity. Therefore, the net result is that, in spite of an increase in expiratory cell discharge in response to PEEP, the Biot breathing cat is compromised in the ability to respond to the imposed load.

#### E. Summary

Sustained oscillations in the output of a controlled system can result from: an increase in controller gain, decreased damping of the feedback signal and an increase in feedback delay. A sustained oscillation in the output of the respiratory controller, Biot breathing, has been described in the present study. The placement of lesions within the pontine respiratory group leads to Biot breathing by a decrease in the sensitivity to  $\text{CO}_2$  and an increase in  $V_T$ .

The decrease in  $\text{CO}_2$  sensitivity leads to an increase in  $P_a\text{CO}_2$  and decrease in  $P_a\text{O}_2$ . As a result, the respiratory controller is shifted to operating on the non-linear, hyperbolic portion of the hypoxic ventilatory response curve. Thus, controller gain is increased and there is decreased damping of the feedback signal, due to the lower stores for oxygen in the body. This contributes to instability and an oscillation of the respiratory output.

The duration of expiration is dependent upon the chemical drive, which promotes initiation of inspiration, and the volume feedback from the lung, which delays the initiation of inspiration. In Biot breathing, long periods of apnea result from the decrease in  $\text{CO}_2$  sensitivity and the high level of lung

volume feedback. Therefore, PRG lesions promote Biot breathing due to a decreased  $\text{CO}_2$  sensitivity and an increased  $V_T$ .

The controller output appears to oscillate around a chemical threshold. When the chemoreceptor feedback exceeds this threshold, a ventilatory period is initiated during which the chemoreceptor feedback is driven below threshold, due to the increase in controller gain. An apneic period ensues, the duration of which is determined by the rise in chemoreceptor feedback and the decline in lung volume feedback from the ventilatory period. When the chemoreceptor feedback exceeds threshold, a ventilatory period is initiated and the cycle repeats.

Biot breathing is unlike eupnea, in that, only the duration of expiration is altered by changes in chemo- and mechanoreceptor feedbacks. A previous study revealed that only the duration of  $T_{e1}$  is consistently altered in response to hypercapnic, hypoxic and hyperoxic stimuli (184). In this study, only the duration of  $T_{e1}$  was consistently altered by PEEP, which increases PSR feedback. Therefore, it appears that either these feedbacks are, in some way, gated off during the ventilatory phase or that the sensitivity to these feedbacks is too low, such that larger changes in feedback must occur in order to elicit changes in the respiratory output. The interaction between chemo- and mechanoreceptor feedbacks is such that mechanoreceptor feedback resets the threshold for termination of apnea by chemoreceptor input. Therefore, PEEP application results in hypoventilation and an increase in chemoreceptor feedback.

Efferent outflows of the respiratory controller are also altered in Biot breathing. The loss of post-inspiratory activity in the recurrent laryngeal nerve activity implies possible changes in the braking of expiratory airflow.

The loss of directional matching of recurrent laryngeal and phrenic nerve activities during inspiration would necessarily alter the generation of a smooth inspiratory airflow. The PRG also appears to be involved in the "setting" of the diaphragm and rib cage muscles at the optimal length for inspiration in the face of an expiratory load. In Biot breathing, a loss of mechanoreceptor initiated and chemoreceptor sustained abdominal nerve activity was observed. Therefore, a role for the PRG in every phase of the respiratory cycle seems indicated. The PRG appears to function in the smoothing of both inspiratory and expiratory airflows and in the stabilization of thoracic volume during the non-ventilatory portion of expiration.

Recording of respiratory related cells in the brainstem has revealed that "central apnea" may not be truly "central" in origin. The absence of phrenic nerve activity does not necessarily imply the lack of cyclic inspiratory activity in the brainstem. This activity may fail to reach a critical threshold level to activate phrenic motoneurons or may be actively inhibited. Therefore, the involvement of the PRG in modulating this brainstem inspiratory activity is an intriguing area for further study.

A great deal of attention has been focused in the past few years on the topic of respiratory rhythm generation. Though the subject of intense investigation, the location of the rhythm generator remains unknown. Obviously, from the results of this study, PRG destruction leaves the rhythm generator intact, as a rhythmic respiratory output is still produced. However, the function of the respiratory controller is to provide adequate ventilation, which is the product of both frequency and volume. Therefore, the respiratory controller is a pattern generator, not simply a rhythm generator, and adjusts both frequency and volume in order to provide

ventilation. From the changes which result in both the timing and depth of respiratory output in response to PRG lesion, it is evident that the PRG is an integral part of the central pattern generator for respiratory output.

## CHAPTER VII

### CONCLUSIONS

1. Biot breathing may result following placement of lesions in the pontine respiratory group (PRG) in cats with intact lung volume feedback. The distinctive feature of Biot breathing is the long period of central apnea that separates ventilatory clusters. Therefore, the PRG constitutes an integral part of the respiratory rhythm generator.
2. The duration of central apnea in Biot breathing is prolonged by increased lung volume feedback. This feedback appears to alter the threshold for the termination of apnea by chemoreceptor feedback.
3. Phasic activity of the cranial iliohypogastric nerve consistently appears in Biot breathing. This activity persists throughout the apneic phase. Increased expiratory nerve activity is not maintained in response to increased lung volume feedback in Biot breathing. Therefore, it is concluded that the PRG participates in active expiratory discharges elicited by increased lung volume feedback during eupnea.
4. The post-inspiratory discharge of the recurrent laryngeal nerve is absent in Biot breathing as are the parallel changes in phrenic and recurrent laryngeal nerve activities in response to alteration of lung volume feedback. Therefore, in eupnea, the PRG appears to function in coordinating the transitions between inspiratory and expiratory phases.

5. The phase of central apnea is characterized by maintained discharge of expiratory cells and absence of phasic inspiratory cell discharge. That is, expiratory cell discharges were never observed to terminate prior to the completion of the long apneic pause. It is possible that inspiratory activity may be inhibited by expiratory cell discharge during the apneic phase, although the specific details of this inhibition are not known.
6. The PRG is an integral component of the respiratory pattern generator for eupneic breathing. Destruction of this locus predisposes to the production of a periodic pattern, Biot breathing. Contrasting Biot breathing with eupnea reveals that the PRG normally participates in: determining the threshold for chemoreceptor mediated initiation of inspiration by lung volume feedback, eliciting active expiratory discharges in response to increased lung volume feedback, and the smoothing of the transitions between inspiratory and expiratory phases.

## CHAPTER VIII

### REFERENCES

1. Adrian, E.D. Afferent impulses in the vagus and their effect on respiration. J. Physiol. (London) 33: 332-358, 1933.
2. Agostoni, E., F.F. Thimm and W.O. Fenn. Comparative features of the mechanics of breathing. J. Appl. Physiol. 14: 679-683, 1959.
3. Archard, O. and V.M. Bucher. Courants d'action bulbaires a rythme respiratoire. Helv. Physiol. Acta 12: 265-283, 1954.
4. Backman, S.B., C. Anders, D. Ballantyne, N. Rohrig, H. Camerer, S. Mifflin, D. Jordan, H. Dickhaus, K.M. Spyer and D.W. Richter. Evidence for a monosynaptic connection between slowly adapting pulmonary stretch receptor afferents and inspiratory beta neurones. Pflugers Arch. 402: 129-136, 1984.
5. Bainton, C.R. and P.A. Kirkwood. The effect of carbon dioxide on the tonic and the rhythmic discharges of expiratory bulbospinal neurones. J. Physiol. (London) 296: 291-314, 1979.
6. Bainton, C.R., P.A. Kirkwood and T.A. Sears. On the transmission of the stimulating effects of carbon dioxide to the muscles of respiration. J. Physiol. (London) 280: 249-272, 1978.
7. Baker, J.P., Jr., D.T. Frazier, M. Hanley and F.W. Zechman, Jr. Behavior of expiratory neurons in response to mechanical and chemical loading. Respir. Physiol. 36: 337-351, 1979.
8. Baker, T.L., A. Netick and W.C. Dement. Sleep-related apneic and apneustic breathing following pneumotoxic lesion and vagotomy. Respir. Physiol. 46: 271-294, 1981.
9. Barillot, J.C. and M. Dussardier. Modalites de decharge des motoneurones larynges inspiratoires dans diverses conditions experimentales. J. Physiol. (Paris) 66: 593-629, 1973.
10. Bartlett, D., Jr. Effects of hypercapnia and hypoxia on laryngeal resistance to airflow. Respir. Physiol. 37: 293-302, 1979.
11. Bartlett, D., Jr. Effects of vagal afferents on laryngeal responses to hypercapnia and hypoxia. Respir. Physiol. 42: 189-198, 1980.
12. Bartlett, D., Jr., P. Jeffery, G. Sant'Ambrogio and J.C.M. Wise. Location of stretch receptors in the trachea and bronchi of the dog. J. Physiol. (London) 258: 409-420, 1976.

13. Bartlett, D., Jr. and S.L. Knuth. Human vocal cord movements during voluntary hyperventilation. Respir. Physiol. 58: 289-294, 1984.
14. Bartlett, D., Jr., S.L. Knuth and K.V. Knuth. Effects of pulmonary stretch receptor blockade on laryngeal responses to hypercapnia and hypoxia. Respir. Physiol. 45: 67-77, 1981.
15. Bartlett, D., Jr., J.E. Remmers and H. Gautier. Laryngeal regulation of respiratory airflow. Respir. Physiol. 18: 194-204, 1973.
16. Bartlett, D., Jr. and G. Sant'Ambrogio. Effects of local and systemic hypercapnia on the discharge of stretch receptors in the airways of the dog. Respir. Physiol. 26: 91-99, 1976.
17. Bartoli, A., E. Bystrzycka, A. Guz, S.K. Jain, M.I.M. Noble and D. Trenchard. Studies of the pulmonary vagal control of central respiratory rhythm in the absence of breathing movements. J. Physiol. (London) 230: 449-465, 1973.
18. Baumgarten, R. von, A. von Baumgarten and K.-P. Schaefer. Beitrag zur lokalisationsfrage bulboreticularer respiratorischer neurone der katze. Pflugers Archiv. 264: 217-227, 1957.
19. Baumgarten, R. von and E. Kanzow. The interaction of two types of inspiratory neurons in the region of the tractus solitarius of the cat. Arch. Ital. Biol. 96: 361-373, 1958.
20. Berger, A.J. Dorsal respiratory group neurons in the medulla of cat: spinal projections, responses to lung inflation and superior laryngeal nerve stimulation. Brain Res. 135: 231-254, 1977.
21. Berger, A.J. Phrenic motoneurons in the cat: subpopulations and nature of respiratory drive potentials. J. Neurophysiol. 42: 76-90, 1979.
22. Berger, A.J. and D.B. Averill. Projection of single pulmonary stretch receptors to solitary tract region. J. Neurophysiol. 49: 819-830, 1983.
23. Berger, A.J. and K.A. Cooney. Ventilatory effects of kainic acid injection of the ventrolateral solitary nucleus. J. Appl. Physiol. 52: 131-140, 1982.
24. Berger, A.J., D.A. Herbert and R.A. Mitchell. Properties of apneusis produced by reversible cold block of the rostral pons. Respir. Physiol. 33: 323-337, 1978.
25. Berman, A.L. The brainstem of the cat. Madison: University of Wisconsin Press, 1968.

26. Berssenbrugge, A., J. Dempsey, C. Iber, J. Skatrud and P. Wilson. Mechanisms of hypoxia-induced periodic breathing during sleep in humans. J. Physiol. (London) 343: 507-524, 1983.
27. Bertrand, F. and A. Hugelin. Respiratory synchronizing function of the nucleus parabrachialis medialis: pneumotaxic mechanisms. J. Neurophysiol. 34: 189-207, 1971.
28. Bertrand, F., A. Hugelin and J.F. Vibert. A stereologic model of pneumotaxic oscillator based on spatial and temporal distributions of neuronal bursts. J. Neurophysiol. 37: 91-107, 1974.
29. Bianchi, A.L. Localisation et etude des neurones respiratoires bulbaires. J. Physiol. (Paris) 63: 5-40, 1971.
30. Bianchi, A.L. Modalites de decharge et proprietes anatomo-fonctionnelles des neurones respiratoires bulbaires. J. Physiol. Paris 64: 555-587, 1974.
31. Bianchi, A.L. and J.C. Barillot. Activity of medullary respiratory neurones during reflexes from the lungs in cats. Respir. Physiol. 25: 335-352, 1975.
32. Bianchi, A.L. and W.M. St.John. Pontile axonal projections of medullary respiratory neurons. Respir. Physiol. 45: 167-183, 1981.
33. Bianchi, A.L. and W.M. St.John. Medullary axonal projections of respiratory neurons of pontile pneumotaxic center. Respir. Physiol. 48: 357-373, 1982.
34. Biot, M.C. Contribution a l'etude du phenomene respiratoire de Cheyne-Stokes. Lyon Medicale 23: 561-567, 1876.
35. Bishop, B. Abdominal muscle and diaphragm activities and cavity pressures in pressure breathing. J. Appl. Physiol. 18: 37-42, 1963.
36. Bishop, B. Reflex control of abdominal muscles during positive-pressure breathing. J. Appl. Physiol. 19: 224-232, 1964.
37. Bishop, B. Diaphragm and abdominal muscle responses to elevated airway pressures in the cat. J. Appl. Physiol. 22: 959-965, 1967.
38. Bishop, B. and H. Bachofen. Vagal control of ventilation and respiratory muscles during elevated pressures in the cat. J. Appl. Physiol. 32: 103-112, 1972.
39. Bjurstedt, H. Influence of the abdominal muscle tone on the circulatory response to positive pressure breathing in anesthetized dogs. Acta Physiol. Scand. 29: 145-162, 1953.

40. Boyd, T.E. and C.A. Maaske. Vagal inhibition of inspiration, and accompanying changes of respiratory rhythm. J. Neurophysiol. 2: 533-542, 1939.
41. Breckenridge, C.G. and H.E. Hoff. Pontine and medullary regulation of respiration in the cat. Am. J. Physiol. 160: 385-394, 1950.
42. Breuer, J. Self-steering of respiration through the nervus vagus (Engl. trans.). In: Breathing: Hering-Breuer Centenary Symposium, ed. R. Porter, London: Churchill, 1970, pp. 359-364.
43. Budzinska, K., C. von Euler, F.F. Kao, T. Pantaleo and Y. Yamamoto. Effects of graded focal cold block in rostral areas of the medulla. Acta Physiol. Scand. 124: 329-340, 1985.
44. Budzinska, K., C. von Euler, F.F. Kao, T. Pantaleo and Y. Yamamoto. Release of expiratory muscle activity by graded focal cold block in the medulla. Acta Physiol. Scand. 124: 341-351, 1985.
45. Campbell, E.J.M. An electromyographic study of the role of the abdominal muscles in breathing. J. Physiol. (London) 117: 222-233, 1952.
46. Campbell, E.J.M. The effects of increased resistance to expiration on the respiratory behaviour of the abdominal muscles and intra-abdominal pressure. J. Physiol. (London) 136: 556-562, 1957.
47. Campbell, E.J.M. and J.H. Green. The variations in intra-abdominal pressure and the activity of the abdominal muscles during breathing. J. Physiol. (London) 122: 282-290, 1953.
48. Campbell, E.J.M., J.B.L. Howell and B.W. Peckett. The pressure-volume relationships of the thorax of anaesthetized human subjects; a comparison of the effects of expiratory resistance and positive pressure inflation. J. Physiol. (London) 136: 563-568, 1957.
49. Cassidy, S.S. and J.H. Mitchell. Effects of positive pressure breathing on right and left ventricular preload and afterload. Fed. Proc. 40: 2178-2181, 1981.
50. Cherniack, N.S., C. von Euler, I. Homma and F.F. Kao. Experimentally induced Cheyne-Stokes breathing. Respir. Physiol. 37: 185-200, 1979.
51. Cherniack, N.S., C. von Euler, I. Homma and F.F. Kao. Graded changes in central chemoceptor input by local temperature changes on the ventral surface of medulla. J. Physiol. (London) 287: 191-211, 1979.

52. Cherniack, N.S. and G.S. Longobardo. Cheyne-Stokes breathing: an instability in physiologic control. N. Eng. J. Med. 288: 952-957, 1973.
53. Clanton, T.L. and W.T. Lipscomb. Effects of hypercapnia on Breuer-Hering threshold for inspiratory termination. J. Appl. Physiol. 57: 1211-1221, 1984.
54. Clark, F.J. and C. von Euler. On the regulation of the depth and rate of breathing. J. Physiol. (London) 222: 267-295, 1972.
55. Cohen, M.I. Switching of the respiratory phases and evoked phrenic responses produced by rostral pontine electrical stimulation. J. Physiol. (London) 217: 133-158, 1971.
56. Cohen, M.I. Phrenic and recurrent laryngeal discharge patterns and the Hering-Breuer reflex. Am. J. Physiol. 228: 1489-1496, 1975.
57. Cohen, M.I. and J.L. Feldman. Models of respiratory phase-switching. Fed. Proc. 36: 2367-2374, 1977.
58. Cohen, M.I. and J.L. Feldman. Discharge properties of dorsal medullary inspiratory neurons: relation to pulmonary afferent and phrenic efferent discharge. J. Neurophysiol. 51: 753-776, 1984.
59. Cohen, M.I. and A. Hugelin. Suprapontine reticular control of intrinsic respiratory mechanisms. Arch. Ital. Biol. 103: 317-334, 1965.
60. Cohen, M.I. and S.C. Wang. Respiratory neuronal activity in pons of cat. J. Neurophysiol. 22: 33-50, 1959.
61. Coleridge, H.M., J.C.G. Coleridge and R.B. Banzett. Effect of CO<sub>2</sub> on afferent vagal endings in the canine lung. Respir. Physiol. 34: 135-151, 1978.
62. Cournand, A., H.I. Motley, L. Werko and D.W. Richards, Jr. Physiological studies of the effects of intermittent positive pressure breathing on cardiac output in man. Am. J. Physiol. 152: 162-174, 1948.
63. D'Angelo, E. Verification of a model for the mechanisms controlling expiratory duration in rabbits under various conditions. Respir. Physiol. 59: 239-264, 1985.
64. D'Angelo, E. and E. Agostoni. Tonic vagal influences on inspiratory duration. Respir. Physiol. 24: 287-302, 1975.
65. Daubenspeck, J.A. and D. Bartlett, Jr. Expiratory pattern and laryngeal responses to single-breath expiratory resistance loads. Respir. Physiol. 54: 307-316, 1983.

66. Davenport, P.W., D.T. Frazier and F.W. Zechman, Jr. The effect of the resistive loading of inspiration and expiration on pulmonary stretch receptor discharge. Respir. Physiol. 43: 299-314, 1981.
67. DiMarco, A.F., M.S. DiMarco, K.P. Strohl and M.D. Altose. Effects of expiratory threshold loading on thoracoabdominal motion in cats. Respir. Physiol. 57: 247-257, 1984.
68. DiMarco, A.F., J.R. Romaniuk, C. von Euler and Y. Yamamoto. Immediate changes in ventilation and respiratory pattern associated with onset and cessation of locomotion in the cat. J. Physiol. (London) 343: 1-16, 1983.
69. Donoghue, S., M. Garcia, D. Jordan and K.M. Spyer. The brain-stem projections of pulmonary stretch afferent neurones in cats and rabbits. J. Physiol. (London) 322: 352-364, 1982.
70. Eldridge, F.L. Relationship between phrenic nerve activity and ventilation. Am. J. Physiol. 221: 535-543, 1971.
71. England, S.J. and D. Bartlett, Jr. Changes in respiratory movements of the human vocal cords during hyperpnea. J. Appl. Physiol. 52: 780-785, 1982.
72. England, S.J., D. Bartlett, Jr. and J.A. Daubenspeck. Influence of human vocal cord movements on airflow and resistance during eupnea. J. Appl. Physiol. 52: 773-779, 1982.
73. Euler, C. von. On the origin and pattern control of breathing rhythmicity in mammals. In: Neural origin of rhythmic movements, Cambridge: Cambridge Univ. Press, 1983, pp. 469-485.
74. Euler, C. von, J.N. Hayward, I. Marttila and R.J. Wyman. Respiratory neurons of the ventrolateral nucleus of the solitary tract of the cat: vagal input, spinal connections and morphological identification. Brain Res. 61: 1-22, 1973.
75. Euler, C. von, I. Marttila, J.E. Remmers and T. Trippenbach. Effects of lesions in the parabrachial nucleus on the mechanism for central and reflex termination of inspiration in the cat. Acta Physiol. Scand. 96: 324-337, 1976.
76. Euler, C. von and T. Trippenbach. Excitability changes of the inspiratory 'off-switch' mechanism tested by electrical stimulation in nucleus parabrachialis in the cat. Acta Physiol. Scand. 97: 175-188, 1976.
77. Feldman, J.L. A network model for control of inspiratory cutoff by the pneumotaxic center with supportive experimental data in cats. Biol. Cybernetics 21: 131-138, 1976.

78. Feldman, J.L. Neurophysiology of breathing in mammals. In: Handbook of Physiology, Washington, D.C.: Am. Physiol. Soc., in press.
79. Feldman, J.L. and M.I. Cohen. Relation between expiratory duration and rostral medullary expiratory neuronal discharge. Brain Res. 141: 172-178, 1978.
80. Feldman, J.L., M.I. Cohen and P. Wolotsky. Powerful inhibition of pontine respiratory neurons by pulmonary afferent activity. Brain Res. 104: 341-346, 1976.
81. Feldman, J.L. and H. Gautier. Interaction of pulmonary afferents and pneumotaxic center in control of respiratory pattern in cats. J. Neurophysiol. 39: 31-44, 1976.
82. Feldman, J.L., A.D. Loewy and D.F. Speck. Projections from the ventral respiratory group to phrenic and intercostal motoneurons in the cat: an autoradiographic study. J. Neurosci. 5: 1993-2000, 1985.
83. Feldman, J.L., D.R. McCrimmon and D.F. Speck. Effect of synchronous activation of medullary inspiratory bulbo-spinal neurones on phrenic nerve discharge in cat. J. Physiol. (London) 347: 241-254, 1984.
84. Feldman, J.L., D. Sommer and M.I. Cohen. Short time scale correlations between discharges of medullary respiratory neurons. J. Neurophysiol. 43: 1284-1295, 1980.
85. Feldman, J.L. and D.F. Speck. Interactions among inspiratory neurons in dorsal and ventral respiratory groups in cat medulla. J. Neurophysiol. 49: 472-490, 1983.
86. Fenner, A., U. Schalk, H. Hoenicke, A. Wendenburg and T. Roehling. Periodic breathing in premature and neonatal babies: incidence, breathing pattern, respiratory gas tensions, response to changes in composition of ambient air. Ped. Res. 7: 174-183, 1973.
87. Finkler, J. and S. Iscoe. Control of breathing at elevated lung volumes in anesthetized cats. J. Appl. Physiol. 56: 839-844, 1984.
88. Gacek, R.R. and M.J. Lyon. Fiber components of the recurrent laryngeal nerve in the cat. Ann. Otol. 85: 460-471, 1976.
89. Gautier, H., M. Bonora and J.H. Gaudy. Breuer-Hering inflation reflex and breathing pattern in anesthetized humans and cats. J. Appl. Physiol. 51: 1162-1168, 1981.

90. Gautier, H., J.E. Remmers and D. Bartlett, Jr. Control of the duration of expiration. Respir. Physiol. 18: 205-221, 1973.
91. Gebber, G.L. Central oscillators responsible for sympathetic nerve discharge. Am. J. Physiol. 239: H143-H155, 1980.
92. Gesell, R. Individuality of breathing. Am. J. Physiol. 115: 168-180, 1936.
93. Gesell, R., J. Bricker and C. Magee. Structural and functional organization of the central mechanism controlling breathing. Am. J. Physiol. 117: 423-452, 1936.
94. Gesell, R. and C. Moyer. The dual excitatory action of the vagal stretch reflex. Am. J. Physiol. 131: 674-680, 1941.
95. Grodins, F.S. Control theory and biological systems. New York: Columbia University Press, 1963.
96. Grodins, F.S. Models. In: Lung Biology in Health and Disease: Regulation of Breathing, ed. T. Hornbein, New York: Marcel Dekker, Inc., 1981, pp. 1313-1351.
97. Guyton, A.C., J.W. Crowell and J.W. Moore. Basic oscillating mechanism of Cheyne-Stokes breathing. Am. J. Physiol. 187: 395-398, 1956.
98. Haxhiu, M.A., E. van Lunteren, J. Mitra and N.S. Cherniack. Responses to chemical stimulation of upper airway muscles and diaphragm in awake cats. J. Appl. Physiol. 56: 397-403, 1984.
99. Hering, E. Self-steering of respiration through the nervus vagus (Engl. trans.). In: Breathing: Hering-Breuer Centenary Symposium, ed. R. Porter, London: Churchill, 1970, pp. 365-394.
100. Hilaire, G., R. Monteau and A.L. Bianchi. A cross-correlation study of interactions among respiratory neurons of dorsal, ventral and retrofacial groups in cat medulla. Brain Res. 302: 19-31, 1984.
101. Hoff, H.E. and C.G. Breckenridge. The medullary origin of respiratory periodicity in the dog. Am. J. Physiol. 158: 157-172, 1949.
102. Hugelin, A. Anatomical organization of bulbopontine respiratory oscillators. Fed. Proc. 36: 2390-2394, 1977.
103. Hugelin, A. and M.I. Cohen. The reticular activating system and respiratory regulation in the cat. Ann. N.Y. Acad. Sci. 109: 586-603, 1963.

104. Jammes, Y., P.T.P. Bye, R.L. Pardy, C. Katsardis, S. Esau and C. Roussos. Expiratory threshold load under extracorporeal circulation: effects of vagal afferents. J. Appl. Physiol. 55: 307-315, 1983.
105. Jammes, Y., P.T.P. Bye, R.L. Pardy and C. Roussos. Vagal feedback with expiratory threshold load under extracorporeal circulation. J. Appl. Physiol. 55: 316-322, 1983.
106. Kalia, M. Neuroanatomical organization of the respiratory centers. Fed. Proc. 36: 2405-2411, 1977.
107. Kalia, M. Anatomical organization of central respiratory neurons. Ann. Rev. Physiol. 43: 105-120, 1981.
108. Kalia, M., J.L. Feldman and M.I. Cohen. Afferent projections to the inspiratory neuronal region of the ventrolateral nucleus of the tractus solitarius in the cat. Brain Res. 171: 135-141, 1979.
109. Kelley, D.H. and D.C. Shannon. Periodic breathing in infants with near-miss sudden infant death syndrome. Pediatrics 63: 355-360, 1979.
110. Kelsen, S.G., M.D. Altose and N.S. Cherniack. Interaction of lung volume and chemical drive on respiratory muscle EMG and respiratory timing. J. Appl. Physiol. 42: 287-294, 1977.
111. Khoo, M.C.K., R.E. Kronauer, K.P. Strohl and A.R. Slutsky. Factors inducing periodic breathing in humans: a general model. J. Appl. Physiol. 53: 644-659, 1982.
112. King, G.W. Topology of ascending brainstem projections to nucleus parabrachialis in the cat. J. Comp. Neurol. 191: 615-638, 1980.
113. Kirkwood, P.A. and T.A. Sears. Monosynaptic excitation of thoracic expiratory motoneurons from lateral respiratory neurones in the medulla of the cat. J. Physiol. (London) 234: 87P-88P, 1973.
114. Knox, C.K. Characteristics of inflation and deflation reflexes during expiration in the cat. J. Neurophysiol. 36: 284-295, 1973.
115. Knox, C.K. and G.W. King. Changes in the Breuer-Hering reflexes following rostral pontine lesion. Respir. Physiol. 28: 189-206, 1976.
116. Koehler, R.C. and B. Bishop. Expiratory duration and abdominal muscle responses to elastic and resistive loading. J. Appl. Physiol. 46: 730-737, 1979.
117. Larrabee, M.G. and R. Hodes. Cyclic changes in the respiratory centers, revealed by the effects of afferent impulses. Am. J. Physiol. 155: 147-164, 1948.

118. Lawson, E.E. Prolonged central respiratory inhibition following reflex-induced apnea. J. Appl. Physiol. 50: 874-879, 1981.
119. Le Bars, P. and B. Duron. Are the external and internal intercostal muscles synergist or antagonist in the cat? Neurosci. Lett. 51: 383-386, 1984.
120. Ledlie, J.F., A.I. Pack and A.P. Fishman. Effects of hypercapnia and hypoxia on abdominal expiratory nerve activity. J. Appl. Physiol. 55: 1614-1622, 1983.
121. Lemon, R. Methods for neuronal recording in conscious animals. New York: Wiley and Sons, 1984.
122. Lipski, J., L. Kubin and J. Jodkowski. Synaptic action of R<sub>beta</sub> neurons on phrenic motoneurons studied with spike-triggered averaging. Brain Res. 288: 105-118, 1983.
123. Lipski, J. and E.G. Merrill. Electrophysiological demonstration of the projection from expiratory neurones in rostral medulla to contralateral dorsal respiratory group. Brain Res. 197: 521-524, 1980.
124. Loewy, A.D. and H. Burton. Nuclei of the solitary tract: efferent projections to the lower brain stem and spinal cord of the cat. J. Comp. Neurol. 181: 421-450, 1978.
125. Long, S.E. and J. Duffin. The medullary neurons: a review. Can. J. Physiol. Pharmacol. 62: 161-182, 1984.
126. Lumsden, T. Observations on the respiratory centres in the cat. J. Physiol. (London) 57: 153-160, 1923.
127. Marckwald, M. Die athembewegungen und deren innervation beim kaninchen. Z. Biol. 23: 149-283, 1887.
128. Mathew, O.P. and J.E. Remmers. Respiratory function of the upper airway. In: Lung Biology in Health and Disease: Sleep and Breathing, eds. N.A. Saunders and C.E. Sullivan, New York: Marcel Dekker, Inc., 1984, pp. 163-200.
129. McCrimmon, D.R., D.F. Speck and J.L. Feldman. Role of the dorsal respiratory group (DRG) in processing vagal and superior laryngeal nerve afferents in cat. Soc. Neurosci. Abs. 10: 707, 1984.
130. Merrill, E.G. The lateral respiratory neurones of the medulla: their associations with nucleus ambiguus, nucleus retroambiguus, the spinal accessory nucleus and the spinal cord. Brain Res. 24: 11-28, 1970.

131. Merrill, E.G. Finding a respiratory function for the medullary respiratory neurons. In: Essays on the Nervous System, eds. R. Bellairs and E.G. Gray, Oxford: Clarendon Press, 1974, pp. 451-486.
132. Merrill, E.G. Where are the real respiratory neurons? Fed. Proc. 40: 2389-2394, 1981.
133. Merrill, E.G. Network properties of respiratory neurones. In: Proceedings of the international symposium: central neural production of periodic respiratory movements, eds. J.L. Feldman and A.J. Berger, Chicago: Northwestern Univ., 1982, pp. 54-55.
134. Merrill, E.G. and L. Fedorko. Monosynaptic inhibition of phrenic motoneurons: a long descending projection from Botzinger neurons. J. Neurosci. 4: 2350-2353, 1984.
135. Merrill, E.G., J. Lipski, L. Kubin and L. Fedorko. Origin of the expiratory inhibition of nucleus tractus solitarius inspiratory neurones. Brain Res. 263: 43-50, 1983.
136. Millhorn, D.E., F.L. Eldridge and T.G. Waldrop. Effects of medullary area I<sub>s</sub> cooling on respiratory response to chemoreceptor inputs. Respir. Physiol. 49: 23-39, 1982.
137. Mitchell, R.A. and A.J. Berger. Neural regulation of respiration. In: Lung Biology in Health and Disease: Regulation of Breathing, ed. T. Hornbein, New York: Marcel Dekker, Inc., 1981, pp. 541-620.
138. Mitchell, R.A. and D.A. Herbert. The effect of carbon dioxide on the membrane potential of medullary respiratory neurons. Brain Res. 75: 345-349, 1974.
139. Muza, S.R. and D.T. Frazier. Response of pulmonary stretch receptors to shifts of functional residual capacity. Respir. Physiol. 52: 371-386, 1983.
140. Muza, S.R., L.-Y. Lee, C.P. Pan, F.W. Zechman and D.T. Frazier. Respiratory volume-timing relationship during sustained elevation of functional residual capacity. Respir. Physiol. 58: 77-86, 1984.
141. Ngai, S.H. and S.C. Wang. Organization of central respiratory mechanisms in the brain stem of the cat: localization by stimulation and destruction. Am. J. Physiol. 190: 343-349, 1957.
142. Orem, J. Medullary respiratory neuron activity: relationship to tonic and phasic REM sleep. J. Appl. Physiol. 48: 54-65, 1980.
143. Orem, J. and R. Lydic. Upper airway function during sleep and wakefulness: experimental studies on normal and anesthetized cats. Sleep 1: 49-68, 1978.

144. Orem, J., A. Netick and W.C. Dement. Increased upper airway resistance to breathing during sleep in the cat. Electroencephal. Clin. Neurophysiol. 43: 14-22, 1977.
145. Pasaro, R., S. Gonzalez-Baron and J.M. Delgado-Garcia. Differential localization of laryngeal motoneurons within the nucleus ambiguus of the cat. Neurosci. Lett. Suppl. 10: S373-S374, 1982.
146. Phillipson, E.A. Control of breathing during sleep. Am. Rev. Respir. Dis. 118: 909-939, 1978.
147. Phillipson, E.A., J. Duffin and J.D. Cooper. Critical dependence of respiratory rhythmicity on metabolic CO<sub>2</sub> load. J. Appl. Physiol. 50: 45-54, 1981.
148. Pitts, R.F., H.W. Magoun and S.W. Ranson. Localization of the medullary respiratory centers in the cat. Am. J. Physiol. 126: 673-688, 1939.
149. Pitts, R.F., H.W. Magoun and S.W. Ranson. Interrelations of the respiratory centers in the cat. Am. J. Physiol. 126: 689-707, 1939.
150. Pitts, R.F., H.W. Magoun and S.W. Ranson. The origin of respiratory rhythmicity. Am. J. Physiol. 127: 654-670, 1939.
151. Plum, F. and E.C. Alvord, Jr. Apneustic breathing in man. Archiv. Neurol. 10: 101-112, 1964.
152. Plum, F. and R.J. Leigh. Abnormalities of central mechanisms. In: Lung Biology in Health and Disease: Regulation of Breathing, ed. T. Hornbein, New York: Marcel Dekker, Inc., 1981, pp. 989-1067.
153. Plum, F. and J.B. Posner. The Diagnosis of Stupor and Coma. Philadelphia: F.A. Davis Co., 1980.
154. Remmers, J.E. and D. Bartlett, Jr. Reflex control of expiratory airflow and duration. J. Appl. Physiol. 42: 80-87, 1977.
155. Remmers, J.E., W.J. de Groot, E.K. Sauerland and A.M. Anch. Pathogenesis of airway occlusion during sleep. J. Appl. Physiol. 44: 931-938, 1978.
156. Richardson, C.A. and R.A. Mitchell. Power spectral analysis of inspiratory nerve activity in the decerebrate cat. Brain Res. 233: 317-336, 1982.
157. Richter, D.W. Generation and maintenance of the respiratory rhythm. J. Exp. Biol. 100: 93-107, 1982.

158. Richter, D.W., H. Camerer, M. Meesmann and N. Rohrig. Studies on the synaptic interconnection between bulbar respiratory neurones of cats. Pflugers Arch. 380: 245-257, 1979.
159. Rikard-Bell, G.C., E.K. Bystrzycka and B.S. Nail. Brainstem projections to the phrenic nucleus: a HRP study in the cat. Brain Res. Bull. 12: 469-477, 1984.
160. St.John, W.M. Respiratory tidal volume responses of cats with chronic pneumotoxic center lesions. Respir. Physiol. 16: 92-108, 1972.
161. St.John, W.M. Differing responses to hypercapnia and hypoxia following pneumotoxic center ablation. Respir. Physiol. 23: 1-9, 1975.
162. St.John, W.M. Maintenance of respiratory modulation by pneumotoxic mechanisms in deep anesthesia. Exp. Neurol. 87: 382-386, 1985.
163. St.John, W.M., D. Bartlett, Jr., K.V. Knuth and J.-C. Hwang. Brain stem genesis of automatic ventilatory patterns independent of spinal mechanisms. J. Appl. Physiol. 51: 204-210, 1981.
164. St.John, W.M., T.A. Bledsoe, and H.W. Sokol. Identification of medullary loci critical for neurogenesis of gasping. J. Appl. Physiol. 56: 1008-1019, 1984.
165. St.John, W.M., R.L. Glasser and R.A. King. Apneustic breathing after vagotomy in cats with chronic pneumotoxic center lesions. Respir. Physiol. 12: 239-250, 1971.
166. St.John, W.M. and S.C. Wang. Integration of chemoreceptor stimuli by caudal pontile and rostral medullary sites. J. Appl. Physiol. 41: 612-622, 1976.
167. Salmoiraghi, G.C. and B.D. Burns. Notes on mechanism of rhythmic respiration. J. Neurophysiol. 23: 14-26, 1960.
168. Sant'Ambrogio, G. Information arising from the tracheobronchial tree of mammals. Physiol. Rev. 62: 531-569, 1982.
169. Sears, T.A. The slow potentials of thoracic respiratory motoneurons and their relation to breathing. J. Physiol. (London) 175: 404-424, 1964.
170. Sharp, J.T., N.B. Goldberg, W.S. Druz and J. Danon. Relative contributions of rib cage and abdomen to breathing in normal subjects. J. Appl. Physiol. 39: 608-618, 1975.

171. Sherrey, J.H. and D. Megirian. Analysis of the respiratory role of intrinsic laryngeal motoneurons of cat. Exp. Neurol. 49: 456-465, 1975.
172. Sieck, G.C. and R.M. Harper. Pneumotaxic area neuronal discharge during sleep-waking states in the cat. Exp. Neurol. 67: 79-102, 1980.
173. Southall, D.P., D.G., Talbert, P. Johnson, C.J. Morley, S. Salmons, J. Miller and P.J. Helms. Prolonged expiratory apnoea: a disorder resulting in episodes of severe arterial hypoxaemia in infants and young children. Lancet 2: 572-577, 1985.
174. Speck, D.F. and J.L. Feldman. The effects of microstimulation and microlesions in the ventral and dorsal respiratory groups in medulla of cat. J. Neurosci. 2: 744-757, 1982.
175. Stella, G. On the mechanism of production, and the physiological significance of "apneusis". J. Physiol. (London) 93: 10-23, 1938.
176. Sullivan, C.E., F.G. Issa, M. Berthon-Jones and N.A. Saunders. Pathophysiology of sleep apnea. In: Lung Biology in Health and Disease: Sleep and Breathing, ed. N.A. Saunders and C.E. Sullivan, New York: Marcel Dekker, Inc., 1984, pp. 299-363.
177. Tang, P.C. Localization of the pneumotaxic center in the cat. Am. J. Physiol. 172: 645-652, 1953.
178. Tang, P.C. Brain stem control of respiratory depth and rate in the cat. Respir. Physiol. 3: 349-366, 1967.
179. Taylor, A. The contribution of the intercostal muscles to the effort of respiration in man. J. Physiol. (London) 151: 390-402, 1960.
180. Torvik, A. The spinal projection from the nucleus of the solitary tract. An experimental study in the cat. J. Anat. 91: 314-322, 1957.
181. Van Lunteren, E., K.P. Strohl, D.M. Parker, E.N. Bruce, W.B. Van de Graaff and N.S. Cherniack. Phasic volume-related feedback on upper airway muscle activity. J. Appl. Physiol. 56: 730-736, 1984.
182. Wang, S.C., S.H. Ngai and M.J. Frumin. Organization of central respiratory mechanisms in the brain stem of the cat: genesis of normal respiratory rhythmicity. Am. J. Physiol. 190: 333-342, 1957.

183. Webber, C.L., Jr. and L.M. Oyer. Afferent influences on respiratory instability and periodic breathing in the cat. In: Proceedings of the international symposium: central neural production of periodic respiratory movements, eds. J.L. Feldman and A.J. Berger, Chicago: Northwestern Univ., 1982, pp. 117-118.
184. Webber, C.L., Jr. and D.F. Speck. Experimental biot periodic breathing in cats: effect of changes in  $PI_{O_2}$  and  $PI_{CO_2}$ . Respir. Physiol. 40: 321-344, 1981.
185. Weil, J.V., M.H. Kryger and C.H. Scoggin. Sleep and breathing at high altitude. In: Sleep Apnea Syndromes, eds. C. Guilleminault and W.C. Dement, New York: Alan R. Liss, Inc., 1978, pp. 119-136.
186. Weiner, D., J. Mitra, J. Salamone, and N.S. Cherniack. Effect of chemical stimuli on nerves supplying upper airway muscles. J. Appl. Physiol. 52: 530-536, 1982.
187. Widdicombe, J.G. Receptors in the trachea and bronchi of the cat. J. Physiol. (London) 123: 71-104, 1954.
188. Wyman, R.J. Neural generation of the breathing rhythm. Ann. Rev. Physiol. 39: 417-448, 1977.
189. Youmans, W.B., D.T. Tjioe and E.Y. Tong. Control of involuntary activity of abdominal muscles. Am. J. Phys. Med. 53: 57-74, 1974.
190. Younes, M., P. Vaillancourt and J. Milic-Emili. Interaction between chemical factors and duration of apnea following lung inflation. J. Appl. Physiol. 36: 190-201, 1974.
191. Zar, J.H. Biostatistical analysis. Englewood Cliffs: Prentice-Hall, Inc., 1984.
192. Zechman, F.W., D.T. Frazier and D.A. Lally. Respiratory volume-time relationships during resistive loading in the cat. J. Appl. Physiol. 40: 177-183, 1976.
193. Zuperku, E.J. and F.A. Hopp. On the relation between expiratory duration and subsequent inspiratory duration. J. Appl. Physiol. 58: 419-430, 1985.
194. Zuperku, E.J., F.A. Hopp and J.P. Kampine. Central integration of pulmonary stretch receptor input in the control of expiration. J. Appl. Physiol. 52: 1296-1315, 1982.

## APPROVAL SHEET

The dissertation submitted by Linda Mae Oyer has been read and approved by the following committee:

Charles L. Webber, Jr., Ph.D., Director  
Associate Professor, Physiology  
Loyola, Stritch School of Medicine

Robert D. Wurster, Ph.D.  
Professor, Physiology  
Loyola, Stritch School of Medicine

John T. Sharp, M.D.  
Professor, Medicine and Physiology  
Loyola, Stritch School of Medicine

Melvin Lopata, M.D.  
Associate Professor, Medicine  
University of Illinois College of Medicine at Chicago

Walter M. St. John, Ph.D.  
Professor, Physiology  
Dartmouth Medical School, Hanover, New Hampshire

The final copies have been examined by the director of the dissertation and the signature which appears below verifies the fact that any necessary changes have been incorporated and that the dissertation is now given final approval by the Committee with reference to content and form.

The dissertation is therefore accepted in partial fulfillment of the requirements for the degree of Doctor of Philosophy.

Jan. 30, 1986

Date

Charles L. Webber Jr.

Director's Signature